EFFECT OF CO_2 ON THE PHASE BEHAVIOR OF NORMAL PARAFFINS

By

JURIS VAIROGS

Bachelor of Science
University of Nebraska
Lincoln, Nebraska
1958

Master of Science
Oklahoma State University
Stillwater, Oklahoma
1966

Submitted to the Faculty of the
Graduate College of the
Oklahoma State University
in partial fulfillment of
the requirements for
the Degree of
DOCTOR OF PHILOSOPHY
August, 1969

EFFECT OF CO_2 ON THE PHASE BEHAVIOR OF NORMAL PARAFFINS

Thesis Approved:

Wayne C. Edmister
Thesis Adviser

Robert L. Robinson, Jr.

Robert D. Freeman

R. N. Maddox

D. D. Burham
Dean of the Graduate College

PREFACE

Vapor-liquid equilibrium K-values were obtained experimentally for a laboratory prepared mixture of the normal paraffins, methane, ethane, propane, pentane, hexane and decane. Isotherms of 150°F and 250°F were determined from pressures near 100 psia up to the single phase pressure. Two different amounts of carbon dioxide were added to the base system and the isotherms repeated. The purpose of this investigation was the development of certain equipment and methods for obtaining K-values for components of complex hydrocarbon systems. A K-value correlation was also developed.

I am deeply indebted to Professor W. C. Edmister for suggesting the problem of this thesis and for the aid and inspiration supplied by him during the period of preparation. I sincerely appreciate the encouragement and help received from the staff of the School of Chemical Engineering, particularly Dr. K. C. Chao and Dr. R. L. Robinson, Jr. as well as my fellow students.

The financial assistance of the American Petroleum Institute is gratefully acknowledged. Phillips Petroleum Company donated the hydrocarbons. The assistance and cooperation of the Cities Service Oil Company, the Continental Oil Company and the Pan American Oil Company is appreciated.

The greatest expression of my gratitude goes to members of my family whose constant encouragement made this study possible.

TABLE OF CONTENTS

LIST OF TABLES

LIST OF FIGURES

CHAPTER I

INTRODUCTION

The distribution of a component in a system composed of a vapor and a liquid phase is expressed as the K-value. The K-value of a component is defined as the mole fraction of that component in the vapor phase, y_i, divided by the mole fraction of that component in the liquid phase, x_i:

$$K_i = \frac{y_i}{x_i} \qquad (1\text{-}1)$$

The variation of K-values with temperature, pressure and composition has been studied experimentally for many years. Most of the work has been done at fairly low pressures and medium to high temperatures. Many different components have been studied, usually in binary or ternary systems. Likewise, theoretical development and correlation work has been extensive at the same conditions.

Some interesting phenomena, not known or expected until recently, are found at high pressure or low temperatures. Multicomponent systems are very complex and many interesting phenomena can be expected to be discovered through the study of such systems and conditions.

This work involves the study of vapor-liquid equilibrium in the multicomponent system carbon dioxide-normal

paraffins. The data are taken in the medium to high pressure range and at medium temperatures. Carbon dioxide concentrations are fairly high in order to study their effect on the K-values of the normal paraffins.

The experimental conditions chosen are also of practical interest. Hydrocarbon separation processes are sometimes designed to operate at the selected conditions. A more likely application of the K data at these conditions is in the secondary recovery of petroleum utilizing high pressure gas drives.

CHAPTER II

PREVIOUS INVESTIGATIONS

Experimental Technique

The techniques and apparatii used to obtain vapor-liquid equilibrium data were reviewed in some detail by Hipkin[29], Robinson and Gilliland[58] and Hala, et al.[26] The simplest and commonest type of apparatus is the constant volume bomb. The mixture is placed into the bomb and either agitated or allowed to sit for a long time to reach equilibrium. The main failure of this type of apparatus is that the mass of material in the gas phase at low pressure is quite small. Withdrawing a sample can upset the equilibrium appreciably. This failure is reduced if the bomb is used for measurements at high pressure where the gas phase is much denser.

The disturbance due to sampling can be reduced by the use of a variable volume cell which also is fairly commonly used, for instance, Evans and Harris[23] and Sage and Lacey.[61] The pressure disturbance due to sampling is reduced by maintaining the equilibrium pressure as the sample is withdrawn by compressing the mixture with a piston. The piston may be a mechanical device or a slug of mercury. The use of a

mercury piston causes some concern when used at high temperatures due to the toxicity of mercury vapor.

A third method for obtaining vapor liquid equilibrium data is the bubble and dew point method. A mixture of known composition is introduced into a variable volume cell. The temperature is maintained constant and the pressure varied until a bubble in the liquid or a drop in the vapor inside the cell is observed in the windowed cell. Another way to establish the dew and bubble points is to plot the pressure isotherm and obtain the points from the discontinuities in the curve. However, the discontinuities are not always well defined. This method is applicable to binary systems only since the fixing of temperature and pressure is not sufficient to define the multicomponent systems.

In the dynamic flow method gas is bubbled slowly through a series of cells containing the liquid. If the bubbling rate is low enough, phase equilibrium should be established between the phases. However, a pressure gradient is necessary to drive the gas, and hence there is some question about the establishment of equilibrium. This method is much more easily adapted for low pressure usage than for high pressure.

In the liquid recirculation method the vapor rising from the still is condensed and recycled to the still. If the vapor rising from the still is not in equilibrium with the liquid, then the continued recirculation merely maintains a steady state condition, since the condensate is of

the same composition as the vapor. This type of still is widely used for work near and at atmospheric pressure. Hala et al.[26] list fourty-nine references of various modifications of this type of still.

The vapor recirculation method probably reaches equilibrium after some time. The reason for that is that the vapor being recirculated is allowed to bubble through the liquid thus ensuring good contact. However, as in the dynamic flow method the flow is produced by some small pressure gradient. Thus, there is a small concentration gradient in the cell from the top to the bottom. Dodge and Dunbar[17] moved the vapor through a mercury pump outside the temperature bath. That produced pressure variations due to temperature and volume variations. Aroyan and Katz[3] used a magnetic pump to produce a constant enclosed volume. Roberts and McKetta[57] and Stuckey[70] placed the magnetic pump into the constant temperature bath. The current flowing through the coils of the magnetic pump produces heat, thus tending to upset the thermal equilibrium if the current is not held constant. Slight super-heating of the vapor is produced but that is not nearly as bad as subcooling would be since the latter would cause condensation.

The weakest part in obtaining the equilibrium data is the analysis of the samples for composition. A binary system is accurately determined by the procedure described under variable volume cells. However, multicomponent systems have to be sampled and analyzed for each data point.

The withdrawal of samples is difficult. A small sample must be taken in such a manner as to disturb the system as little as possible. The compositions of the phases are normally analyzed by means of a gas chromatograph. That is particularly true if relatively non-volatile components are present. The error introduced due to the chromatograph can be analyzed but the upset of equilibrium due to sampling is an entirely subjective matter.

Experimental Data

The vapor-liquid equilibria of many different hydrocarbon-carbon dioxide systems have been investigated experimentally. Of course, the systems studied the most have been the binary and ternary systems. References 2, 16, 18, 40, 41, 49, 50, 52, 54, 59, 69 and 74 are part of the work on normal paraffin-carbon dioxide systems.

The data from binary systems have been used extensively in K-value correlations to account for the effect of carbon dioxide on hydrocarbon systems. Normally the effect of carbon dioxide is correlated as a correction factor with which to multiply the K-value for hydrocarbon-hydrocarbon systems as Lenoir[34] has done.

The use of only binary hydrocarbon-carbon dioxide data give reliable K predictions for systems with relatively high carbon dioxide concentrations, i.e., binary or ternary systems. However, the application of these correlations to the calculation of K-values in multicomponent systems is

uncertain. Although it is reasonable to expect them to give a satisfactory value, it is desirable to assess the effect on systems of low carbon dioxide concentrations, i.e., multicomponent, experimentally.

The number of published carbon dioxide systems with more than two hydrocarbon components present is rather low. Usually the carbon dioxide is present only because it was in the natural gas used in the equilibrium studies. Standing and Katz[67], Weinaug and Bradley[76] and Davis et al.[15] ran equilibrium studies with both carbon dioxide and nitrogen in their systems. Jacoby and Rzasa,[30] Gore et al.,[24] Smith and Yarborough,[66] and Vagtborg[72] ran their systems with hydrogen sulfide present in addition to the above gases. In all of the above systems not only is the carbon dioxide concentration low, but in addition, non-hydrocarbon gases other than carbon dioxide are present. Because of the latter reason it is virtually impossible to assign a separate effect to carbon dioxide since it could well be masked by the presence of the other gases. The data are nevertheless valuable for qualitative investigations. For instance, they show little effect on the hydrocarbon K-values due to the presence of all three gases as long as they are present in amounts of a few mole per cent or less.

The effect of the presence of carbon dioxide was studied more directly by Poettmann and Katz.[42] They published the first study of a hydrocarbon-carbon dioxide multicomponent system with carbon dioxide being the only inorganic

gas present. The overall concentrations were up to 10 mole per cent carbon dioxide, 65 per cent methane, 20 per cent heptanes plus fraction and very little of the intermediate hydrocarbons. They found no variation in the carbon dioxide K-values with changes in the carbon dioxide composition, but there was a large deviation from the ideal K-value for carbon dioxide. Since the carbon dioxide composition varied but a little, the authors probably could not measure any significant deviations in the K-values. The discovery that the K-values deviate greatly from the ideal K-values is significant and as expected. The authors did not measure the hydrocarbon K values, and hence the effect of carbon dioxide on hydrocarbons cannot be assessed.

The second article was published by Poettman[43] on a natural gas-crude oil-carbon dioxide system. The data reported covered a temperature range of 38 to 202°F and a pressure range of 600 to 8500 psia. The overall carbon dioxide concentration ranged up to 12 mole per cent. Again Poettmann found no effect on either carbon dioxide or hydrocarbon K-values due to variation of carbon dioxide concentration. However, he did notice that the carbon dioxide K-values were lower in the crude oil system than in the distillate.

It is interesting to note that the natural gas-crude oil-CO_2-N_2-H_2S system of Jacoby and Rzasa[30] showed higher K-values for methane, CO_2 and ethane than did Poettmann's crude oil system, but nearly the same as Poettmann's

distillate system. To investigate the reason for this disagreement Jacoby and Rzasa[31] ran systems similar to the former but with different amounts of condensate present. Again the Jacoby and Rzasa values agreed well with Poettmann's distillate system.

This perplexing problem was discussed by Poettman[30] based on the tacit assumption that the presence of N_2 and H_2S in Jacoby and Rzasa's systems had very little effect on the results. His conclusion was that much of this apparent discrepancy can be explained by the presence of intermediate components in one case and very little in the other. It appears, on the basis of the results of the above four publications, that carbon dioxide, when present in low concentrations, has less effect on the K-values of hydrocarbons than the presence or absence of intermediate components.

K-Value Correlations

Much emphasis is being placed on the development of calculation methods that can be used readily on a digital computer. However, a literature survey shows that very few K-value correlations of this type have been published. The first one was the Chao and Seader[10] procedure. It was based on the regular solution theory developed by Scatchard and Hildebrand[27,28] and used the Redlich and Kwong[55] equation to calculate vapor phase imperfections.

No radically different correlation has been presented since then although the Chao-Seader method has received wide

attention. A number of papers[9,20,22] have been presented which apply the Chao-Seader correlation to various practical calculations. Lenoir[35] has recently investigated the accuracy with which the Chao-Seader correlation predicts K-values. He found that the range of conditions for which the K-values are given to within 10 per cent is rather restricted.

Grayson and Streed[25] have extended the range of conditions on the correlation and Erbar[22] has extended it to such permanent gases as carbon dioxide and nitrogen. The wide variety of the use of the Chao-Seader correlation illustrates the versatility and ease of application of this correlation.

Another type of correlation that holds high promise is of the type of Starling[68] and Wilson.[77] Procedures of this kind select a good equation of state and then proceed to either modify the form or the constants of the equation until the K-values are represented as well as possible. More will be said about this in Chapter III.

CHAPTER III

THEORETICAL CONSIDERATIONS

It is well known to students of thermodynamics that the fugacity of a component distributed between two phases in equilibrium with each other has the same value in either phase. Mathematically it is expressed as

$$\hat{f}_i^L = \hat{f}_i^V \qquad (3\text{-}1)$$

where superscript L refers to the liquid phase and V to the vapor phase.

All K-value correlations which are based to some extent on theoretical considerations are developed from Equation (3-1). The fugacities in Equation (3-1) can be evaluated in a variety of ways, hence there are several different K correlations published and many more are likely to be developed.

The most direct procedure is to calculate the equilibrium pressure and composition from an equation of state so that Equation (3-1) is satisfied. This is readily done even with a complicated equation of state such as the Benedict, Webb, and Rubin[6,7,8] equation, provided a digital computer is available. The difficulty with direct calculation from an equation of state is that the constants for equations of state are determined from pressure-volume-temperature

data of limited accuracy. That is, there is an inherent error in all available equations of state. The expression for the fugacity in either a liquid or a vapor mixture is derived from

$$\ln\left(\frac{\hat{f}_{i2}}{\hat{f}_{i1}}\right) = \frac{1}{RT}\int_{P_1}^{P_2} \bar{V}_i \, dP \qquad (3\text{-}2)$$

Obviously a differentiation and then an integration has to be performed on the equation of state to obtain an expression for fugacity. Thus the error inherent in the volume or pressure calculated from the equation of state is increased when it is used to calculate fugacity. The famous Kellogg K charts[32] were developed from the BWR equation as described above.

A slightly more complicated but more accurate way to correlate K values is to select an equation of state and either determine or modify the constants in it so that Equation (3-1) is as nearly satisfied as possible. Experimental K data are needed to develop this type of correlation. This simple approach has been used by Starling[68] for high molecular weight normal paraffins and Klekers[33] for normal paraffins and some aromatics and naphthenes. Barner and Schreiner[5] used the same technique to fit enthalpy data.

The use of an equation of state to develop a calculational scheme for K-values is good if care is utilized. First of all, the best equation available should be selected. For most purposes only two equations and their modifications are worth considering. One is the Redlich and

Kwong[55] equation. The advantages of this equation are that it is generalized and therefore applicable to any component for which the critical temperature and pressure are known. In addition, it can be solved directly for the density roots in the two phase region. However, it is not quite as accurate as the Benedict, et al. equation.

The Benedict, et al. equation has some drawbacks of its own. The constants in this equation are evaluated for each component from experimental PVT data. Thus, unless generalized constants such as those of Edmister, et al.[21] are available, the equation is restricted to use on components for which the constants have been determined. The use of generalized constants reduces the accuracy of the equation, however.

The above drawbacks not withstanding, both the Redlich, et al. and the Benedict, et al. equations can be used to calculate fugacity coefficients for the vapor phase with acceptable accuracy. The Chao and Seader correlation used the Redlich-Kwong equation and this work uses the Benedict, et al. equation with the generalized coefficients[21] to calculate the vapor phase fugacity coefficients, ϕ_i. Thus Equation (3-1) becomes

$$f_i^L = y_i \phi_i P \tag{3-3}$$

With the introduction of the definition of the K-value Equation (3-3) becomes

$$\frac{f_i^L}{x_i} = \frac{y_i}{x_i} \phi_i P = K_i \phi_i P \tag{3-4}$$

The right hand side can be readily evaluated from experimental data and an equation of state. The left hand side applies to the liquid phase and is difficult to evaluate in this form. If it is multiplied and divided by the reference fugacity, f_i^L, then Equation (3-4) becomes

$$\frac{\hat{f}_i^L}{x_i} = \gamma_i f_i^L = K_i \phi_i P \qquad (3\text{-}5)$$

where γ_i is the activity coefficient.

The reference fugacity may be defined as the fugacity of the component in either the pure state or a mixture of a given composition, in liquid or vapor phase or state of aggregation and at any pressure that is desired. The only requirement is that it be at the same temperature as the system under consideration.

From the above definition it is clear that several different reference states are possible. The most commonly used definition is that of pure liquid at system pressure and temperature. Edmister[19] as well as others have applied it to many calculations. Prausnitz[12,39,44,45] has tried to define the reference fugacity as above for heavier components, but the light component reference fugacity is taken to be Henry's law constant for that component. This definition gets away from evaluation of liquid fugacity at conditions under which the pure component is actually gaseous. A disadvantage of this definition is that the evaluation of Henry's law constant requires data at very low concentrations. Such data are hard to obtain.

A third definition that has been suggested by Prausnitz[44] and tested by Weber[75] is to take the reference fugacity at system temperature and pressure but in the state of aggregation that the pure component really exists. Thus, if the temperature is high enough and pressure is low enough for the component to be in the gaseous state, then the reference fugacity for the liquid phase would be that of a gas. Such a definition makes it easy to evaluate the reference fugacity, but the calculation of the activity coefficient becomes difficult. Little is achieved by defining the reference fugacity at one state and then trying to correct it to a different pressure so that the standard equations for activity coefficients can be used.

A fourth definition also suggested and used by Prausnitz[36,46] is to define the reference state as pure liquid at system temperature and zero pressure. Obviously, all fugacities are in the hypothetical state by such a definition. However, one needs only to recall that hypothetical fugacities were also required for the more volatile components under the first definition.

From the above discussion it can be seen that, regardless of which definition of the reference state is selected some difficulties will be encountered. In this work it was decided to select the definition described first, that is, pure liquid at system temperature and pressure. With this definition a number of equations for the calculation of liquid activity coefficients are readily available. The

regular solution theory has been used by Chao and Seader in their correlation with some success. Strictly speaking, the Scatchard and Hildebrand equation is only approximately correct and is supposed to apply to systems containing molecules of approximately equal molecular volumes. Since it performs reasonably well at least at fairly low pressures, it was selected for use in this work. This application will be a test of the ability of the Hildebrand equation to predict the free energy of mixing at high pressures as well as low.

With the selection of the definition of the reference fugacity, Equation (3-5) becomes

$$f_i^L = \frac{K_i \phi_i P}{\gamma_i} \qquad (3\text{-}6)$$

where the right hand side is now known and the left hand side needs to be calculated and correlated.

If the Benedict, et al. equation of state is used to calculate f_i^L, a value different from that given by Equation (3-6) is obtained. In the case of components below their critical temperatures it means that errors in experimental K-values, errors in calculation of liquid activity coefficient and errors caused by the equation of state combine to cause this difference. The same thing can be said about supercritical components. In addition and probably overriding the above errors is the calculation of a liquid activity coefficient at conditions where the pure component is actually a gas. The proper density to use in this

hypothetical calculation could be calculated. Since the Benedict equation is not exactly accurate even for subcritical calculations and they need some correlation, it was decided to correlate the liquid fugacity calculations in the same manner for both subcritical and supercritical calculations.

A correlation constant ϵ_i can be defined as follows

$$\epsilon_i = f_i^L / f_i^{BWR} \tag{3-7}$$

where f_i^{BWR} is the fugacity calculated from the Benedict, et al. equation. For supercritical temperatures it is to be calculated at system temperature and pressure. For subcritical temperatures the Plank[56] equation was used to calculate the vapor pressure. The saturated liquid fugacity f_i^{SL} and saturated vapor fugacity f_i^{SV} were calculated at this vapor pressure. The fugacity at the system temperature and pressure was calculated from

$$f_i^{BWR} = f_i^{SV} f_i^{SP} / f_i^{SL} \tag{3-8}$$

where f_i^{SP} is the fugacity at the system pressure as given by the Benedict, et al. equation. If the equation was accurate enough, Equation (3-8) would not be necessary. Since it is not and since the vapor pressure is calculated by another equation, this procedure should do better than direct calculation of the fugacity from the Benedict, et al. equation. Equation (3-8) may seem to be a complicated way to go about the correlation but in reality it does not

involve any more calculation than the determination of vapor pressures from the Benedict, et al. equation would involve.

Equation (3-8) expresses the liquid reference fugacity as given by the Benedict, et al. equation as follows. The saturated vapor fugacity is deemed to be reasonably accurate. The saturated liquid fugacity and the liquid fugacity at system pressure are not given accurately. However, the difference between the two may be reasonably accurate. Hence, adding the difference to the saturated vapor fugacity would provide a fairly accurate reference fugacity for the subcritical components.

The correlation constants as given by Equation (3-7) were calculated for all components of the published binary data selected for use in developing the correlation. The development of the equation to calculate the correlation constants is described in Chapter VIII. The K-values are then calculated from the following equation

$$K_i = \frac{\epsilon_i f_i^{BWR}}{P} \frac{\gamma_i}{\phi_i} \qquad (3\text{-}9)$$

which is similar to the Chao-Seader equation in form. The ϕ_i and f_i^{BWR} are calculated from the BWR equation with generalized coefficients,[21] the γ_i from the more exact form of the Scatchard-Hildebrand Equation (27) and ϵ_i from the equations presented in Chapter VIII.

CHAPTER IV

LIQUID ACTIVITY COEFFICIENTS

Several equations have been proposed for the calculation of activity coefficients of components of non-ideal liquid nonelectrolyte solutions. Among the better known equations are the Porter, Margules, Van Laar, Black, Scatchard-Hildebrand and Wilson equations. Van Ness[73] has summarized the derivation of the first three equations. To derive these forms the excess free energy of mixing is expressed empirically as a power series in mole fraction. Thus for a binary mixture one can write

$$\frac{\Delta G^E}{x_1 x_2 RT} = B + C\,(2x_1 - 1) + D\,(2x_1 - 1)^2 + \ldots \qquad (4\text{-}1)$$

The activity coefficient is obtained from Equation (4-1) making use of the following relationship for constant temperature and pressure

$$\ln \gamma_1 = \frac{\Delta G^E}{RT} - x_2 \frac{d(\Delta G^E/RT)}{dx_1} \qquad (4\text{-}2)$$

If all constants except B in Equation (4-1) are set equal to zero, the Porter type equation is obtained

$$\ln \gamma_1 = Bx_2^2 \qquad (4\text{-}3)$$

This equation holds well for systems that are not too dissimilar, which have nearly the same molecular volumes.

If all constants except B and C in Equation (4-1) are set equal to zero, the two constant Margules type of equation is obtained

$$\ln \gamma_1 = x_2^2 (\alpha + 2x_1 (\beta - \alpha)) \qquad (4\text{-}4)$$

This equation fits many more complicated systems. The constants α and β have to be determined from experimental data.

The excess free energy of mixing can also be expressed empirically as

$$\frac{x_1 x_2}{\Delta G^E/RT} = B + C (2x_1 - 1) + D (2x_1 - 1)^2 + \ldots \qquad (4\text{-}5)$$

If all the constants except B are zero, the Porter type equation is obtained again. Setting all the constants except B and C equal to zero yields an equation of the Van Laar type

$$\ln \gamma_1 = \frac{\alpha}{(1 + \frac{\alpha}{\beta} (\frac{x_1}{x_2}))^2} \qquad (4\text{-}6)$$

Although these equations are more complicated than the Margules equations, they fit data more closely for complex systems. The constants have to be determined from experimental data.

The above equations were derived for constant temperature data. Similar expressions are obtained for constant pressure data. The main difference in the forms is that the logarithms of activity coefficients are multiplied by the RT product. The above equations are restrained to binary mixtures and their constants have to be evaluated

from experimental data. They are derived from an empirical expression for excess free energy.

Van Laar derived his equation from the van der Waals equation of state as shown by Hildebrand and Scott.[27] The constants in Equation (4-6) are then given by the van der Waals constants a and b as

$$\alpha = b_1\left(\frac{\sqrt{a_1}}{b_1} - \frac{\sqrt{a_2}}{b_2}\right)^2 \qquad (4\text{-}7)$$

and

$$\beta = b_2\left(\frac{\sqrt{a_1}}{b_1} - \frac{\sqrt{a_2}}{b_2}\right)^2 \qquad (4\text{-}8)$$

The reliance on the van der Waals equation was not necessary as was shown by Wohl.[80] The second order Wohl equation (4-9) reduces to Equation (4-6) for a binary mixture if α and β are allowed to assume the appropriate definitions.

$$\frac{\Delta G^E}{2.3\ RT \sum_i q_i x_i} = \sum_{ij} z_i z_j a_{ij} \qquad (4\text{-}9)$$

The Black equation is an empirical modification of the Van Laar equation defined as

$$\frac{\Delta G^E}{RT} = \left(\frac{\Delta G^E}{RT}\right)_{\text{Van Laar}} + \left(\frac{\Delta G^E}{RT}\right)_{\text{Black}} \qquad (4\text{-}10)$$

This equation is very complicated and the constants have to be determined from experimental data. The equation accounts adequately not only for physical interaction and molecular association in pure liquids but also for inter-association between unlike molecules.

Hildebrand and Scott[27] give a detailed derivation of the Scatchard-Hildebrand equation based on the regular solution theory. Four basic assumptions are introduced in the derivation. First, it is assumed that the mutual energy of two molecules depends only upon the distance between them and their relative orientation and not on the molecules surrounding them or the temperature. The second assumption is that the distribution of the molecules in position and orientation is random. The third assumption is that the volume change of mixing at constant pressure is zero.

With these assumptions the "cohesive energy" of a mole of an n component system can be written as

$$- E_m = \left(\sum_{ij} c_{ij} V_i V_j X_i X_j \right) / \left(\sum X_i V_i \right) \qquad (4\text{-}11)$$

or in terms of volume fractions, X

$$- E_m = \left(\sum_i x_i V_i \right) \left(\sum_{ij} c_{ij} X_i X_j \right) \qquad (4\text{-}12)$$

The energy of mixing is then given by

$$\Delta E^M = E_m - \sum_i E_i x_i = \tfrac{1}{2} \left(\sum_i x_i V_i \right) \left(\sum_{ij} A_{ij} X_i X_j \right) \qquad (4\text{-}13)$$

where

$$A_{ij} = (c_{ii} + c_{jj} - 2c_{ij}) \qquad (4\text{-}14)$$

Since the volume change of mixing was assumed to be zero, one can set the enthalpy of mixing equal to the internal energy of mixing. Then from Equation (4-13)

$$\Delta \bar{H}_k = V_k \left[\sum_i A_{ik} X_i - \tfrac{1}{2} \sum_{ij} A_{ij} X_i X_j \right] \qquad (4\text{-}15)$$

The partial free energy and enthalpy are related by

$$\Delta\bar{G}_k = \Delta\bar{E}_k - T\Delta\bar{S}_k \tag{4-16}$$

Because random mixing was assumed the partial molal entropy of mixing is given by

$$\Delta\bar{S}_k = - R \ln x_k \tag{4-17}$$

Combining Equation (4-16) and (4-17) gives

$$\Delta\bar{G}_k = RT \ln a_k = RT \ln x_k + V_k\left[\sum_i A_{ik} X_i - \tfrac{1}{2} \sum_{ij} A_{ij} X_i X_j\right] \tag{4-18}$$

or

$$\ln \gamma_k = \frac{V_k}{RT}\left[\sum_i A_{ik} X_i - \tfrac{1}{2} \sum_{ij} A_{ij} X_i X_j\right] \tag{4-19}$$

At this point the fourth assumption is introduced. That is

$$A_{ij} = (c_{ii} + c_{jj} - 2\sqrt{c_{ii}c_{jj}}) = (\sqrt{c_{ii}} - \sqrt{c_{jj}})^2 \tag{4-20}$$

With this assumption Equation (4-13) becomes

$$H^M = \tfrac{1}{2}\left(\sum_i x_i V_i\right) \sum_{ij}\left[(\delta_i - \delta_j)^2 X_i X_j\right] \tag{4-21}$$

where $\delta_i = c_{ii}^{\frac{1}{2}}$ and is known as the solubility parameter. Then for a binary mixture

$$\Delta\bar{E}_1 = X_2^2 V_1 (\delta_1 - \delta_2)^2 \tag{4-22}$$

or

$$\ln \gamma_1 = \frac{X_2^2 V_1}{RT} (\delta_1 - \delta_2)^2 \tag{4-23}$$

which is the familiar Scatchard-Hildebrand equation. The Scatchard-Hildebrand equation predicts activity coefficients of many hydrocarbon systems well. It has an advantage over other equations in that experimental solubility

data are not needed to evaluate the constants.

If the simplyfying assumption Equation (4-20) is not used, then the interaction parameters in Equation (4-14) have to be evaluated. That has been done by Cheung and Zander[11] and Chueh and Prausnitz.[13] They have been applied in this work as shown in Chapter VIII.

If the molecules in the mixture are of highly different size, then the assumption of random distribution probably does not hold. Wilson[78,79] has tried to remove the effect of this assumption by a semi-empirical derivation for excess free energy. It is an extension of the theory of athermal solutions developed for polymers. Wilson adds the effect of differing intermolecular forces to the effect due to varying size. The excess free energy is written

$$\frac{G^E}{RT} = - \sum_i x_i \ln \left[\sum_j x_j \Lambda_{ij} \right] \qquad (4\text{-}24)$$

where

$$\Lambda_{ij} = \frac{V_j^L}{V_i^L} \exp \left[- (\lambda_{ij} - \lambda_{ii})/RT \right] \qquad (4\text{-}25)$$

and

$$\Lambda_{ij} = \frac{V_i^L}{V_j^L} \exp \left[- (\lambda_{ji} - \lambda_{jj})/RT \right] \qquad (4\text{-}26)$$

and

$$\lambda_{ij} = \lambda_{ji} \quad \text{but} \quad \Lambda_{ij} \neq \Lambda_{ji}$$

Equation (4-24) gives for a binary mixture

$$\ln \gamma_1 = - \ln(x_1 - \Lambda_{12} x_2) + x_2 \left[\frac{\Lambda_{12}}{x_1 + \Lambda_{12} x_2} - \frac{\Lambda_{21}}{\Lambda_{21} x_1 + x_2} \right] \qquad (4\text{-}27)$$

This equation is very appealing in that it has a built-in temperature dependence. Multicomponent mixtures can be calculated with coefficients from binary mixture data. A disadvantage of this equation compared to the Scatchard-Hildebrand equation is that the constants have to be determined from experimental data.

In the foregoing a number of solubility equations were discussed very briefly. It was pointed out that although almost all of the equations have some theoretical significance behind them, they can be derived from strictly empirical expressions for excess free energy. Likewise, some of the equations can be derived from each other with the proper assumption of the relationship between their parameters. All of the equations except the Scatchard-Hildebrand and the Van Laar using van der Waals constants require experimental solubility data to evaluate their constants. Hence they are difficult to apply to multicomponent mixtures. Of these two the Scatchard-Hildebrand equation is the superior one and therefore was selected for use in this work.

CHAPTER V

EXPERIMENTAL APPARATUS

The experimental investigation was conducted using vapor recirculation to attain phase equilibrium. This chapter presents and describes the flow diagram of the apparatus, details of the equilibrium cell and its supporting equipment, the analytical equipment and the substances used in this study.

Apparatus

The description of the equipment is divided into four parts. They are the feed system, pressure regulation and measurement system, equilibration and temperature regulation system and the analytical system. Figure 1 shows a schematic diagram of the whole experimental apparatus. One equilibrium cell and one recirculation pump were part of another experimental system.

Feed System

The gas mixture was fed from a supply cylinder through a pressure regulator and a needle valve to the gas compressor. 316 stainless steel valves, fittings and 1/8 O.D. x 1/16" I.D. tubing were used in this section. The liquid

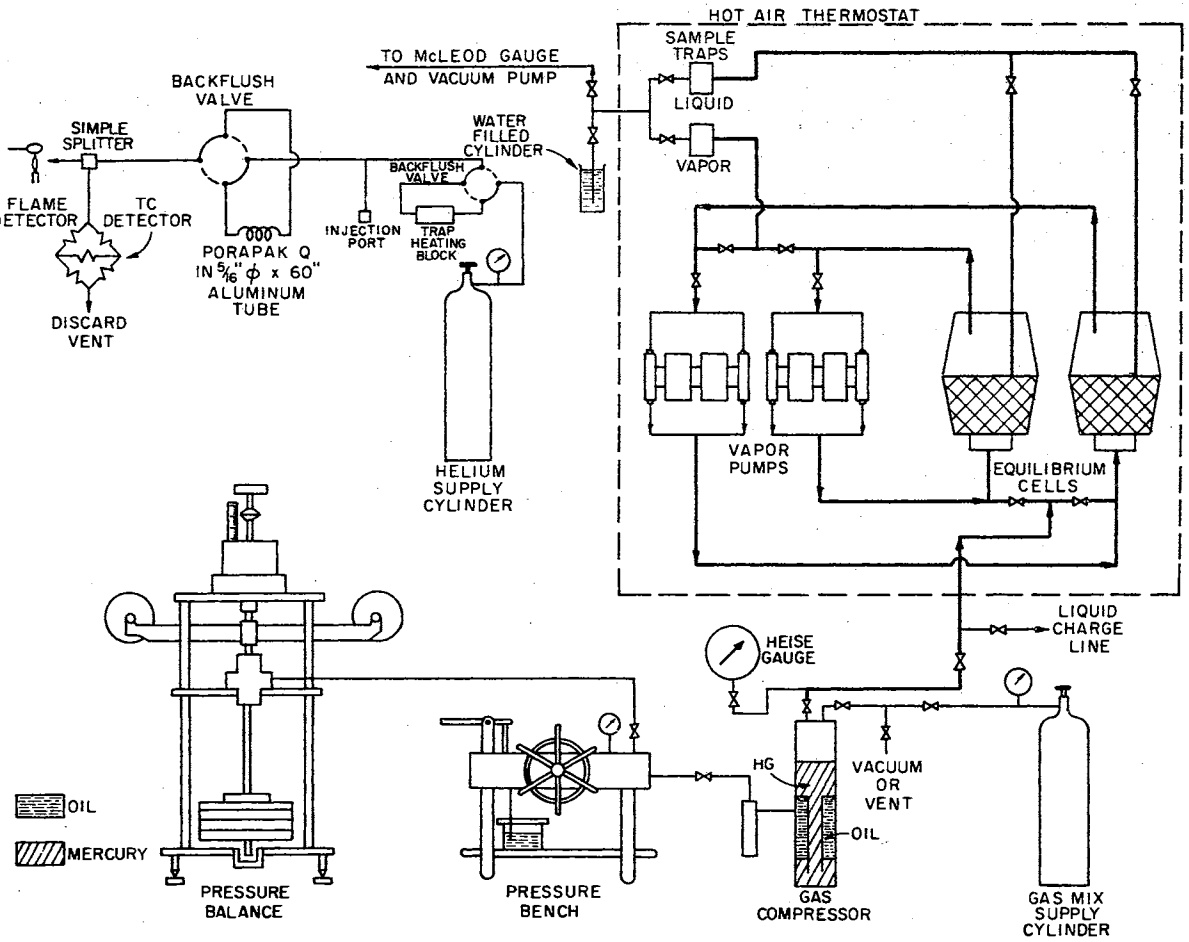

FIGURE 1
SCHEMATIC DIAGRAM OF VAPOR-LIQUID EQUILIBRIUM APPARATUS

hydrocarbon mixture was fed from a 100 cc burette through a section of 1/8" O.D. tubing to a needle valve connected to the line entering the bottom of the equilibrium cell. The connection is labeled "liquid charge line" on Figure 1.

Pressure Regulation and Measuring System

Pressure regulation was accomplished through the use of a pressure gage in conjunction with a gas compressor. A Heise pressure gage was used for pressures below 3000 psia and a Michels pressure balance for pressures above this value. A pressure bench was used to generate and maintain pressure. The pressure bench, pressure balance, and gas compressor were manufactured by W. C. Hart und Zn, Instrumenten-en Apparatenfabriek N. V., Rotterdam, Holland. The Heise pressure gage was manufactured by the Heise Bourdon Tube Co., Inc., Newton, Connecticut.

The Heise gage is a brass Bourdon tube gage with a 0 to 3000 psi range in 2 psi divisions. The gage was read to the nearest 0.5 psi. The Michels pressure balance was checked against the Heise gage and found to give identical results within the accuracy of the Heise gage.

The Michels pressure balance is a dead weight tester using a differential piston. The operation of a dead weight tester is based on the use of a piston in a cylinder of known area and loaded with a known weight. The maximum allowable pressure for the pressure balance is 3000 atm. with a manufacturer's claimed accuracy of about 1 part in

10000. A more detailed description of the Michels pressure balance was given by Stuckey[70] and also Thompson.[71]

The pressure bench contains a hand pump to pump oil from an oil reservoir into the system. A screw press is used to provide a fine control of the system volume. The oil can be pumped to the pressure balance and the gas compressor. A special, filtered petroleum oil having good viscosity-pressure properties was used in this system. The pressure bench is rated for the same maximum operating conditions as the pressure balance.

Figure 2 shows a sectional view of the gas compressor. The upper and lower chambers of the compressor are connected with a short tube. The gas to be compressed is confined in the upper compartment by mercury. Mercury flows from the lower compartment through the connecting center tube into the upper compartment. The mercury is moved by oil flowing from the pressure bench into the upper end of the lower cylinder on top of the mercury.

The position of the mercury in the upper compartment must be known to calculate the system pressure using the Michels pressure balance. The mercury meniscus position is measured by means of a bridge circuit having for one leg a platinum wire which extends the length of the upper compartment. The calibration of the mercury level is a function of the level indicator reading. The calibration is described in Appendix B. The gas compressor has a capacity of 500 cc and a maximum operating pressure of 1500 bars.

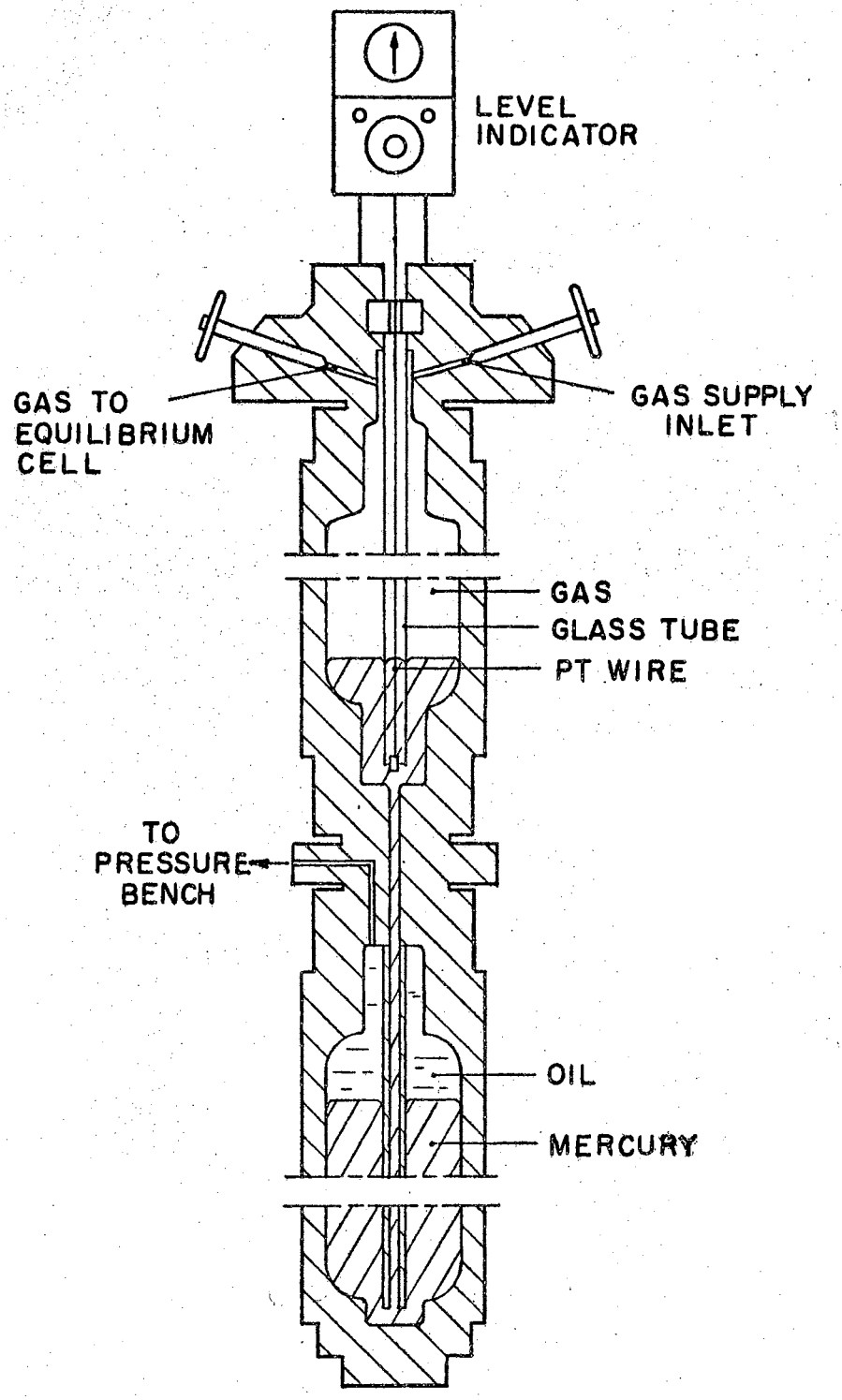

FIGURE 2

SECTIONAL VIEW OF GAS COMPRESSOR

Equilibration and Sampling System

The cell used was designed and manufactured of 316 stainless steel by Autoclave Engineers, Erie, Pennsylvania. The cell was tested to 22,400 psia at 200°F. A cross-sectional view of the cell is presented in Figure 3.

The gas enters at the bottom of the cell through a 1/8" I.D. tube. Next the gas is broken into numerous small streams by the distribution plate holes and the sintered aluminum cone. This arrangement produces less pressure drop across the distribution system than the arrangement described by Stuckey[70] for another equilibrium cell. One line is used to remove vapor phase samples while another line is used to remove the liquid samples. All connecting lines to the cell are 1/8" O.D. tubes. The liquid sampling tube extends to 1/2" above the top of the upper distribution plate. The internal volume of the cell is approximately 150 cc.

In this work a constant volume magnetic pump is used to remove vapor from the top of the cell and to recirculate it through the liquid phase by forcing it into the bottom of the cell. The recirculation rate can be adjusted by varying the speed of the pump. Mechanical details as well as operating information for the pump and its control unit were given by Stuckey.[70] The pumping rate of the pump built for this study was found to be 10% below that reported by Stuckey for his pump.

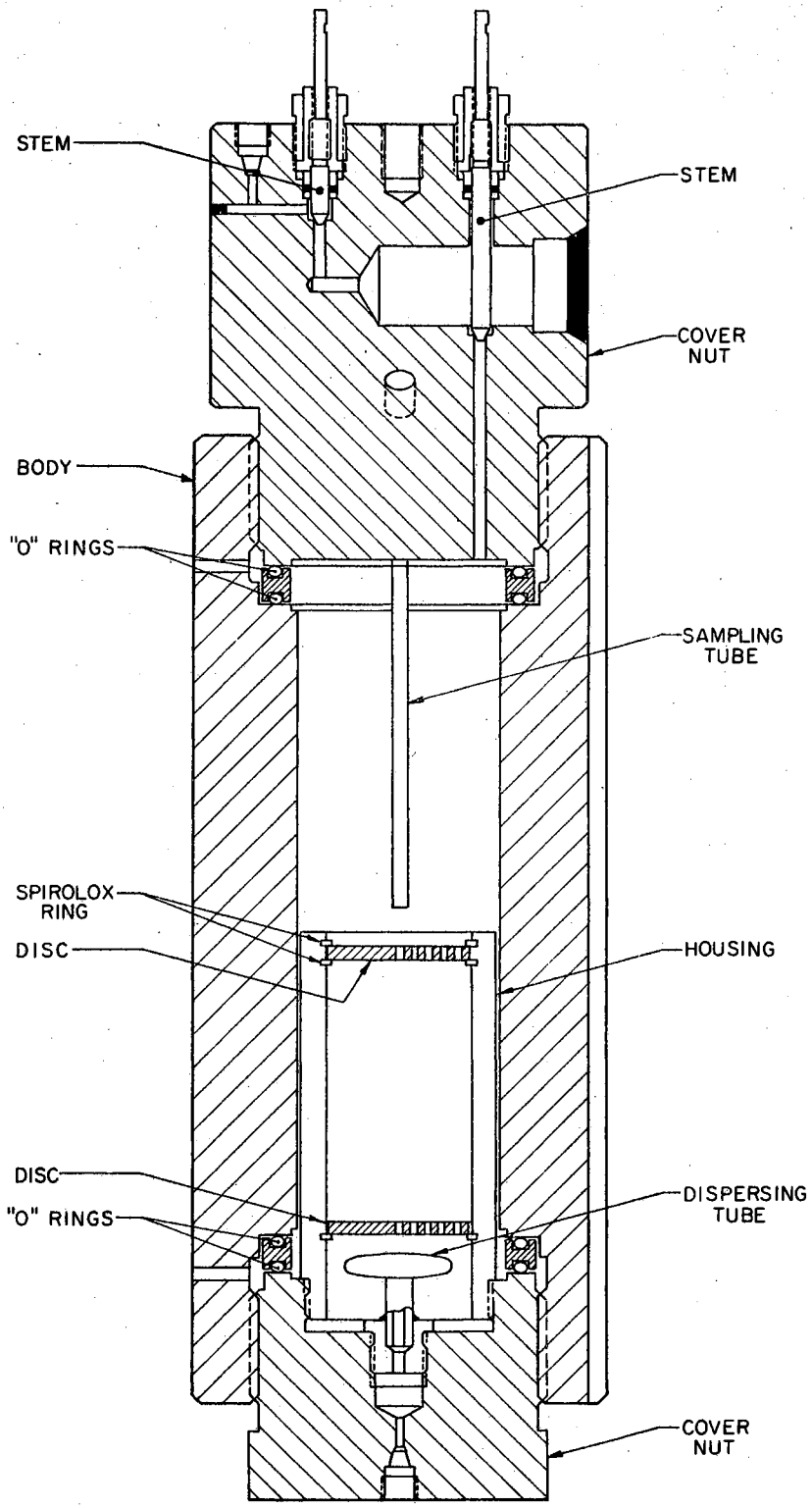

FIGURE 3

EQUILIBRIUM CELL
(AUTOCLAVE)

Samples of both the vapor and the liquid phases were collected in sample traps placed a short distance from the equilibrium cell. The sample traps are illustrated in Figure 4. The sample traps were described by Yarborough and Vogel.[81] The sample trap dimensions are nearly the same as the Autoclave Engineers model 30VM valve. Standard Autoclave valve stems, glands, gland nuts and high temperature glass impregnated Teflon packings were used in their construction. Two piece valve stems were used and the Teflon wafer seals were placed close to the stem tip to give a low dead volume.

The body of the trap was constructed from 416 stainless steel. An insert of 316 stainless steel was used in the area of the sample cavity because 416 steel was too soft to give a good seal for the valve stem. The body was not constructed entirely of 316 stainless steel due to fabrication difficulties. Just above the sample cavity the valve stem has a very loose fit in the valve body allowing fluid to flow around the valve stem and through the valve when the sampling cavity is sealed. The sample cavities were made in two sizes, of about 2 and 40 microliters to give samples of reasonable size for both vapor and liquid phases.

The sample traps were mounted using vise grips and 1/4" Autoclave fittings for easy removal for analysis. The sample traps are connected to the equilibrium cell through 1/8" O.D. stainless steel tubing.

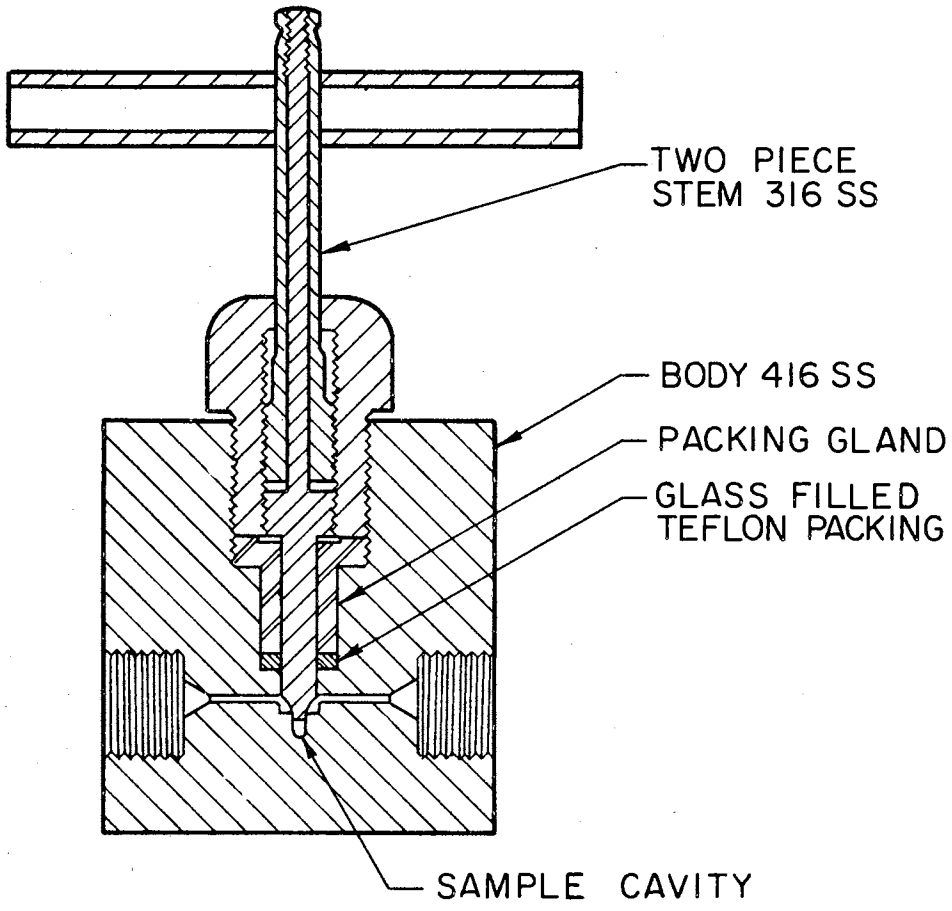

FIGURE 4
SAMPLING VALVE

Temperature Control

A large air thermostat was used as constant temperature bath. The details of the thermostat box construction are given by Stuckey. Air was circulated using a six-inch squirrel cage blower located in a back corner close to the top of the box. The blower was driven by a 1/2 HP electric motor located outside the box. The intake of the blower was located at the bottom of the box and the discharge at the top to provide good air circulation throughout the box. Figure 5 illustrates the blower, heating and cooling coil arrangement.

Eight 250 watt Chromalox PTF-10 finned air heaters supplied the heat input. Four heaters were for constant heat input and controlled by a Superior Type 116 Powerstat. The remaining four heaters were controlled by a Fisher Model 44 temperature controller. Heat was removed from the bath with an 8x8x1$\frac{1}{2}$" finned cooling coil placed before the heaters at the blower intake. Antifreeze was pumped through the coil from a chilling unit at a controlled rate. The temperature sensing element was placed at the outlet end of the blower.

Analytical Section

Analysis of the equilibrium samples was performed using an F&M Model 810 research chromatograph. A diagram of the analytical section can be seen in Figure 1. After removal sample traps were placed in a heated aluminum block and

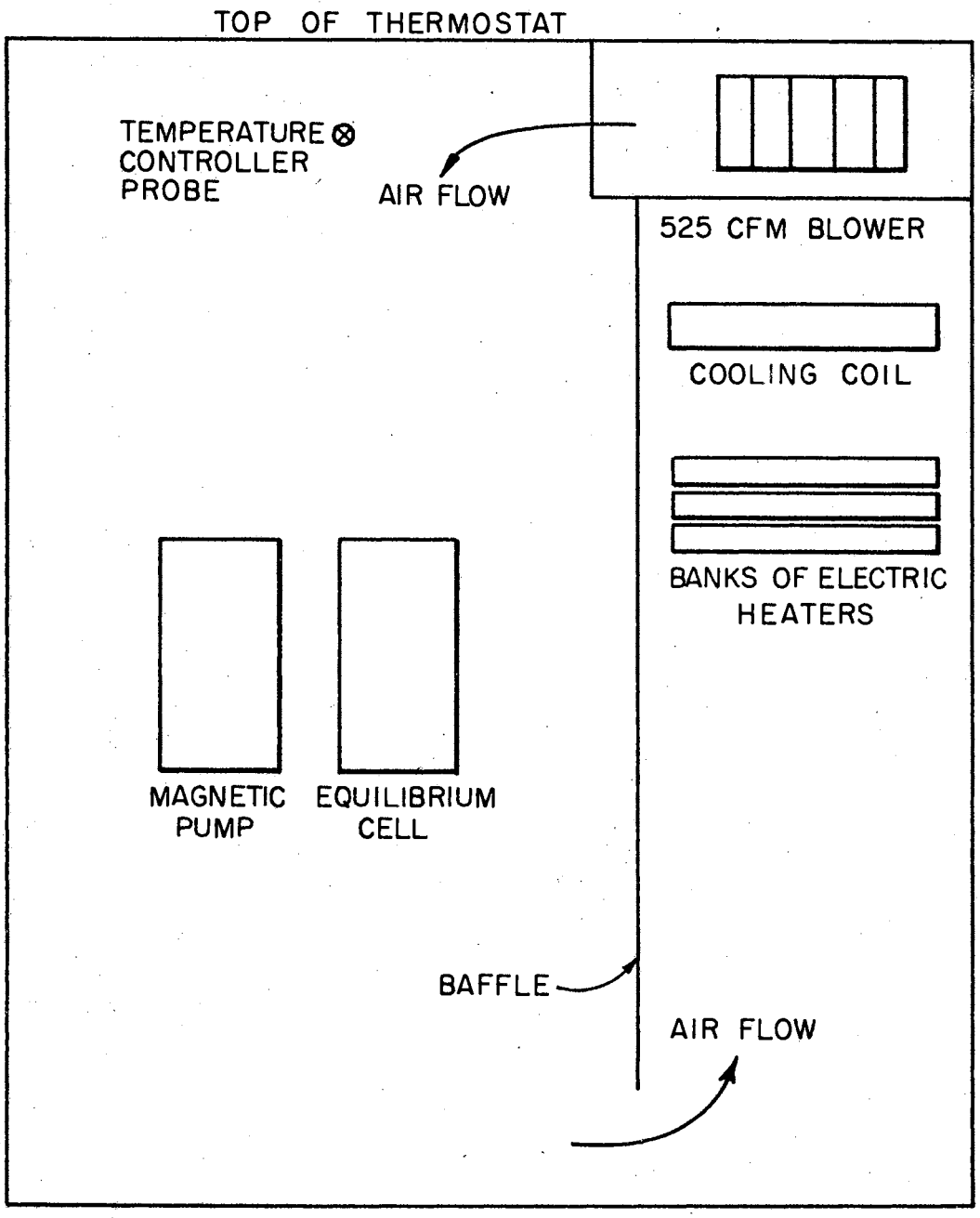

FIGURE 5

BLOWER, COOLER AND HEATER ARRANGEMENT

connected to the chromatograph through heated 1/8" O.D. stainless steel tubing. Separation was performed in 5/16" O.D. aluminum column five feet long and filled with Porapak Q 50-80 mesh base material (Walter Associates Inc.). A standard backflush valve was provided for removing the heaviest component from the column. USP helium was used as the carrier gas. A second backflush valve was placed outside the oven to provide continuous gas flow when no sample trap was connected to the heating block.

The stream leaving the packed column was split in 1:3 ratio. The smaller part was conducted to the flame ionization detector and the larger part to the thermal conductivity detector. The signals from the detectors were recorded on two Honeywell recorders equipped with disc chart integrators. The flame ionization detector response was used for the sample analysis calculations except that CO_2 peaks were taken from the thermal conductivity response. Hydrogen was used as the fuel for the flame with air from a gas cylinder as the oxydizer.

Materials

The gas mixture used in this work was composed of methane, ethane and propane prepared from Phillips Petroleum Company's research grade gases. The gas mixture donated by the company was diluted by the addition of methane. Two additional gas mixtures were prepared with CO_2 as the fourth component. The compositions are given in Table I.

TABLE I

CHARGE GAS COMPOSITIONS

Phillips Petroleum Co. Analyses

	Cylinder 1	Cylinder 2
Methane	0.7572	0.7571
Ethane	0.1512	0.1513
Propane	0.0873	0.0873
Nitrogen	0.0043	0.0043
Oxygen	81 ppm	81 ppm
	1.0000	1.0000

Analyzed at Oklahoma State University

	Base System	Low CO_2 System	High CO_2 System
Methane	0.8869	0.7947	0.6828
Ethane	0.0653	0.0622	0.0459
Propane	0.0478	0.0395	0.0291
CO_2	-	0.1035	0.2421
	1.0000	0.9999	0.9999

NOTE: Compositions given in mole fractions.

The liquid charge mixtures were made using Phillips Petroleum Company's Research grade n-pentane, n-hexane, and n-decane. Technical grade 1-methylnaphthalene was used for the last series of runs.

CHAPTER VI

EXPERIMENTAL PROCEDURE

A four step procedure was followed in the experimental procedure. They were: charging the mixture components, equilibration, sampling and analysis.

Charging of the Cell

Two types of charging procedures were employed. The first procedure was used to charge both liquid and gaseous material to the cell. The second procedure was used to charge only gaseous material to the cell.

The first charging procedure was used at the beginning of a series of runs at a single temperature. At this point the equilibrium cell, gas compressor, sampling lines and sample traps were evacuated to a pressure of 15 to 20 microns by connecting a vacuum pump to the system and leaving it connected for eight hours or longer. The vacuum pump was then shut off and the system pressured up to about 100 psia with the charge gas. After 10 minutes the gas was bled off and the whole system evacuated again. The latter procedure was performed twice.

The equilibrium cell was then isolated from the rest of the system by closing the appropriate valves. A burette

was connected by means of a Tygon line to the cell's drainage line. Approximately 100 cc of deareated liquid charge was then allowed to flow into the evacuated cell. Care was taken to ensure that no air gets into the cell through the burette.

The liquid charge was always a 20-20-60 mole % mixture of n-pentane, n-hexane and n-decane, respectively. This mixture was deareated by slowly bubbling the charge gas through the burette filled with the liquid for five minutes.

After charging the liquid, the equilibrium cell was immediately pressured up to prevent air leakage into the cell. The gas was added to the cell by letting some flow into the mercury piston compressor and then using the compressor to force it into the cell. The gas charge was prepared as described in Chapter IV.

The second charging procedure was used only to increase pressure in the cell. It consisted in letting the charge gas flow into the compressor and then using the compressor to force it into the cell.

Equilibration

After charging the cell initially the thermostat was heated to the desired temperature and allowed to stabilize. The optimum coolant rate setting was found to be 35 and the powerstat setting of 155 watts for operation in the vicinity of 150°F. For operation near 250°F the corresponding settings were 12 and 840 watts.

For runs at pressures less than 3000 psia the pressure was monitored and measured on the Heise gage. At pressures of 3000 psia and higher the Hart pressure balance and bench were utilized. By this type of setup only one pressure cylinder was needed, thus eliminating the need to change them. The weights needed to obtain the operating pressure were placed on the balance. The weights were lightly oiled every time they were handled to prevent corrosion. The valve isolating the pressure balance from the pressure bench was then opened. The hand pump was used to inject oil into the system and lift the piston and the rotating parts to their operating height. The weights were set in rotation. The above procedure was used to check the pressure balance before continuing with the run.

The pressure balance was then isolated from the system. The mercury piston compressor was then filled with the gas. The valve separating the pressure bench and the compressor was opened. Oil was pumped into the compressor until the pressure gage mounted on the pressure bench indicated that the pressure was near the desired operating pressure. At this point the valve separating the gas compressor and the equilibrium cell was slowly opened and the gas allowed to flow into the cell. The pressure on the gage was maintained by the addition of more oil. About this time the magnetic pump control unit was switched on and the vapor circulation line opened. In about 10 minutes most of the liquid had been saturated with gas so that little gas had to be added

afterwards. Then the pressure balance was connected into the system and the pressure brought up to the desired value and maintained there by the addition of oil to the compressor. Meanwhile the temperature was checked frequently by means of a thermocouple inserted into the cell wall. Manual adjustment of the temperature controller set point was necessary to compensate for set point drift over a period of six or more hours.

The vapor was recirculated at the desired operating temperature and pressure for a minimum of two hours. After this period the pump was shut down and isolated from the system. The constant heat input of the powerstat was increased by 100 watts to compensate for the heat given off by the magnet coils. The outlet valves from the equilibrium cell were closed and the contents allowed to settle for 30 minutes.

Sampling

Meanwhile the lines leading to the sampling traps were evacuated. The sample traps were closed and the sample line exhaust shut-off valve was also closed. Then the sampling lines were filled with the fluid from the cell up to the shut-off valves. The vapor line was filled first. The contents were allowed to settle for 15 additional minutes. To compensate for pressure drop in the cell due to filling of the lines additional gas was injected into the cell as the lines were filled. Immediately before filling the lines

enough gas was injected into the cell to raise the pressure by up to 1 per cent of the system pressure.

After the total settling period of 30 minutes, the vapor sample was taken as follows. The tip of the tube on the atmospheric side of the exhaust shut-off valve was dipped into a graduated cylinder filled with water. The valve was very carefully cracked to produce a bubble rate of 1 bubble per second. This was allowed to continue for 15 minutes at which time the valve was closed. The sample trap was opened and then closed thus trapping a vapor sample.

A similar procedure was followed for the liquid sample. However, for low pressure runs decane tended to collect in the cylinder. When 3 ml of decane had collected on the surface of the water, the sampling procedure was terminated. During sampling additional gas was injected to maintain the pressure.

Analysis

After the completion of the sampling process the cell was isolated again and with the sample traps closed the sample lines were emptied. The thermostat door was opened and both sample traps removed from the lines and replaced with fresh traps. The liquid sample trap was left in the thermostat to be maintained at the appropriate temperature. The sample trap removal operation allowed the air temperature to drop about 3 to 5 degrees when executed rapidly.

The vapor trap was purged by blowing air through it to remove most of the fluid left in the crevices and on the surfaces. Then the trap was placed in the heating block, the helium lines connected and helium allowed to flow through it for 6 to 10 minutes. The backflush valve was then turned to the "light end" position and the purging continued for another 10-20 minutes. During this time the amount of material swept into the chromatograph column was monitored on a recorder. When no significant signal was detected anymore, the chromatograph column was cooled down from 200°C during the purge stage to 40°C with the cooling water turned on.

At the start of the analytical run the sample trap in the heating block was opened. At the same time the temperature programmer injection start button was depressed. The temperature programmer was always set on a four-minute delay which was necessary for the complete separation of CO_2 and ethane. Three minutes from the start of the analysis the cooling water was shut off and the line blown out with compressed air for one minute. At the end of four minutes the air was shut off and the temperature programmer started heating the oven at the temperature rate of 10°C/min. Twenty-six minutes after the start of the analysis the backflush valve was turned to the heavy end position. That reversed the flow of helium in the column and eluted the n-decane through the inlet end. The complete analysis of one sample took 45 minutes.

After the vapor sample was analyzed the same procedure was followed with the liquid sample trap. During the purge periods the cell was raised to the next higher pressure and the equilibration started to speed up the overall process. In this manner three runs could be made in a 12-hour day but prevented reruns on the same charge if the sample traps had leaked or the analysis was ruined in some other way.

CHAPTER VII

EXPERIMENTAL RESULTS

Experimental Results

Composition data of the two coexisting phases were taken at a series of pressures at each of two temperatures. One temperature was 150°F and the other was 250°F. For each isotherm equilibrium was established at 8 to 11 different pressures starting with 100 psia and going to the single phase pressure. A sample from each phase was taken and analyzed for composition.

The experimental apparatus was described in Chapter IV and experimental procedure in Chapter VI. The conversion of experimental pressure and temperature measurements is presented in Appendix A and Appendix B, respectively. A sample calculation is given in Appendix E. The chromatograph calibration for conversion of raw data to mole fraction data is presented in Appendix C.

Altogether three systems were run at each of the two temperatures. The first one was the base system composed of the normal paraffins, methane, ethane, propane, pentane, hexane and decane. The vapor and liquid mole fractions and corresponding K-values of each component are presented in

Table D-I for the 150°F isotherm and Table D-II for the 250°F isotherm.

The second set of data was made after preparing a pressuring gas containing carbon dioxide. The feed gas composition is shown in Table I under "low CO_2 system." The phase equilibrium data were obtained at the same conditions as the base system. These data are presented in Table D-III for the 150°F isotherm and Table D-IV for the 250°F isotherm.

After the above runs were completed a new feed gas was made up. The composition of this gas is presented in Table I under "high CO_2 gas." The results of the runs with this feed gas are presented in Table D-V for the 150°F and Table D-VI for the 250°F isotherm.

A seventh isotherm was run at 250°F. This isotherm was run together with Klekers.[33] It differs from the runs in Table D-VI by 1-methylnaphthalene being substituted for normal decane. The results of this run are presented in Table D-VII.

The K data of Tables D-I, D-II, D-III, D-IV, D-V, D-VI and D-VII are presented in graphical form as Figures 6, 7, 8, 9, 10, 11 and 12, respectively.

Experimental Errors

As will be seen presently the measurement of the phase compositions contributes much more to the error in K-values than either temperature or pressure measurements. As discussed in Appendix A the thermocouples in the constant

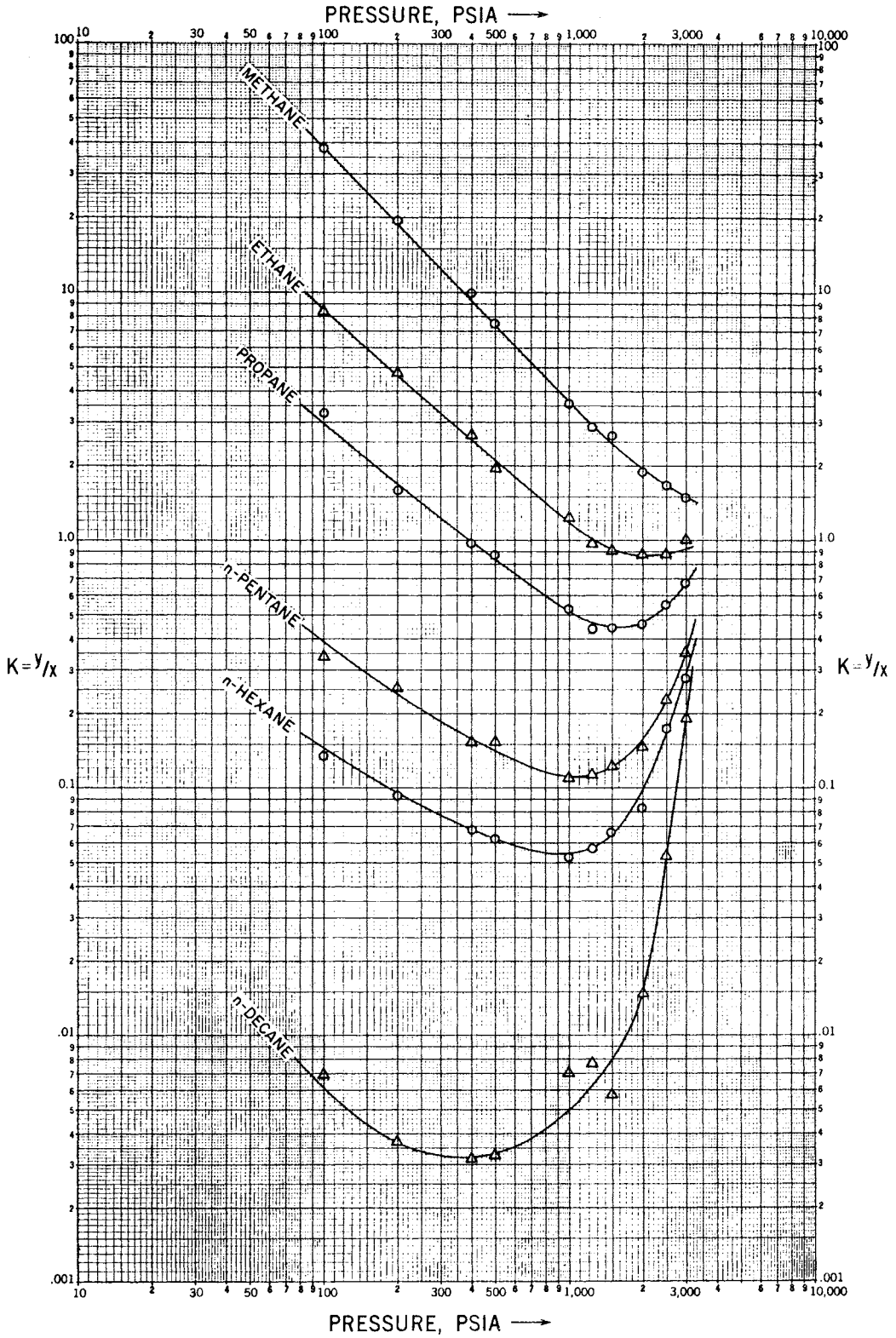

FIGURE 6

EXPERIMENTAL K-VALUES AT 150°F
BASE SYSTEM

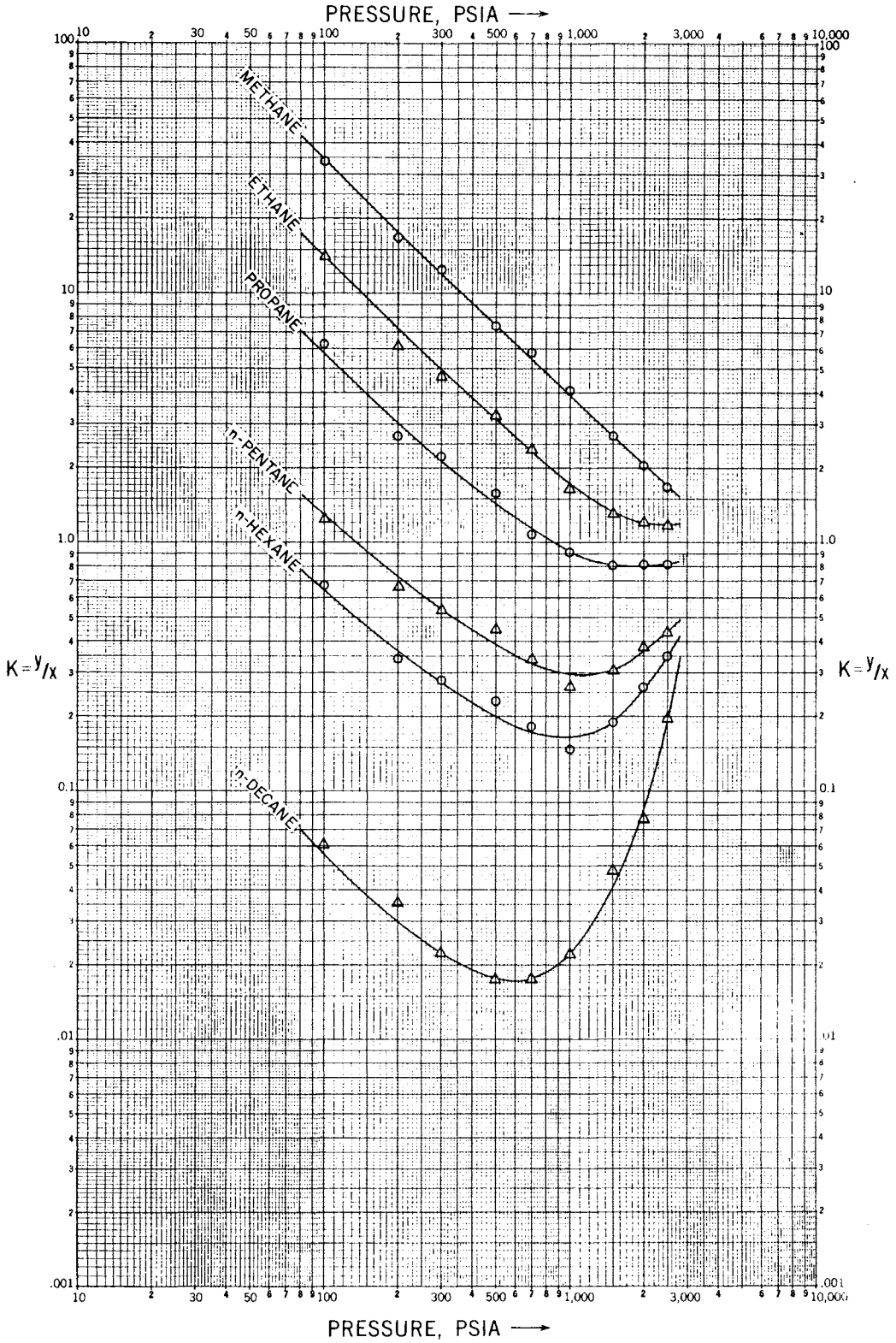

FIGURE 7

EXPERIMENTAL K-VALUES AT 250°F
BASE SYSTEM

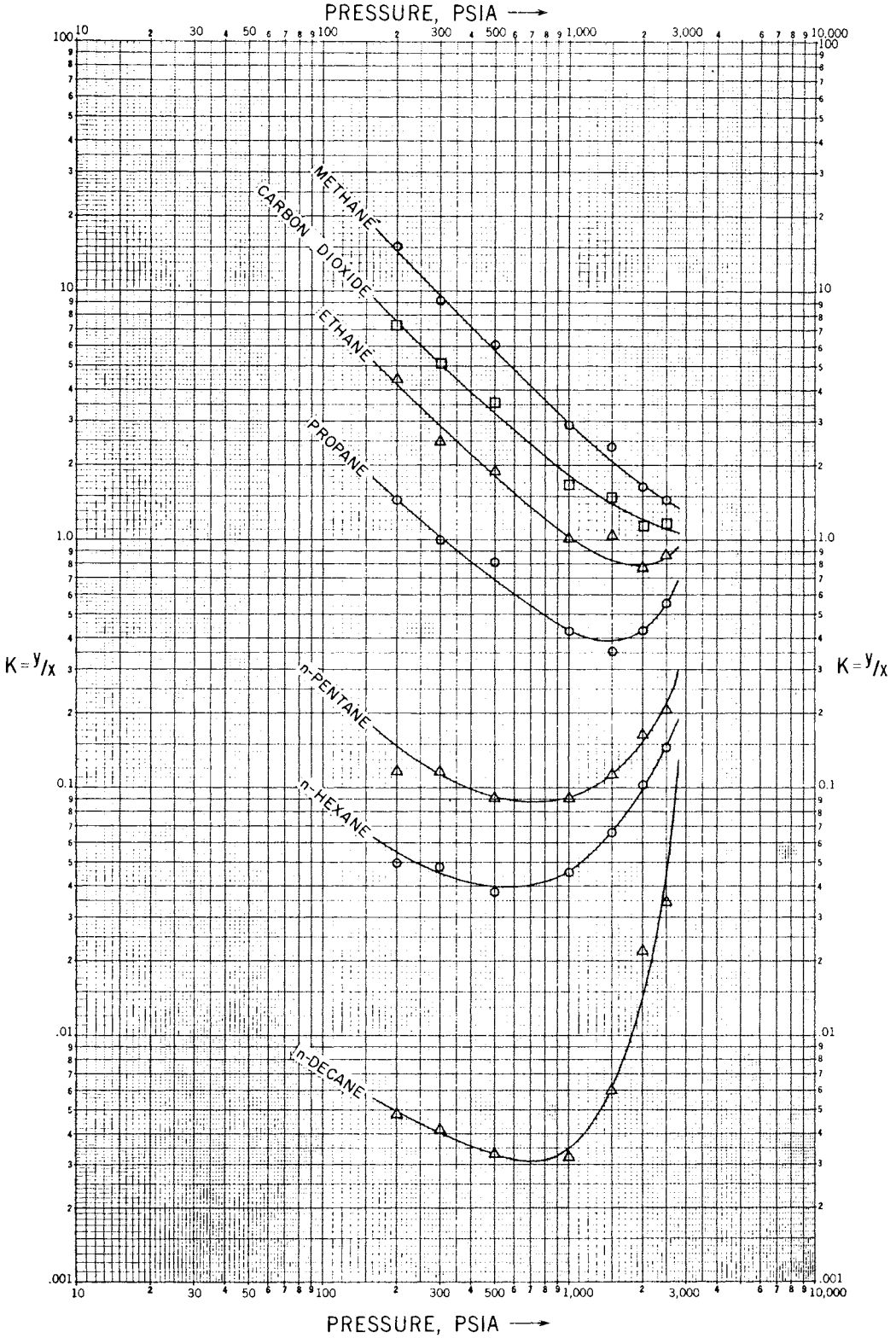

FIGURE 8

EXPERIMENTAL K-VALUES AT 150°F
BASE SYSTEM WITH LOW CO_2 ADDITION

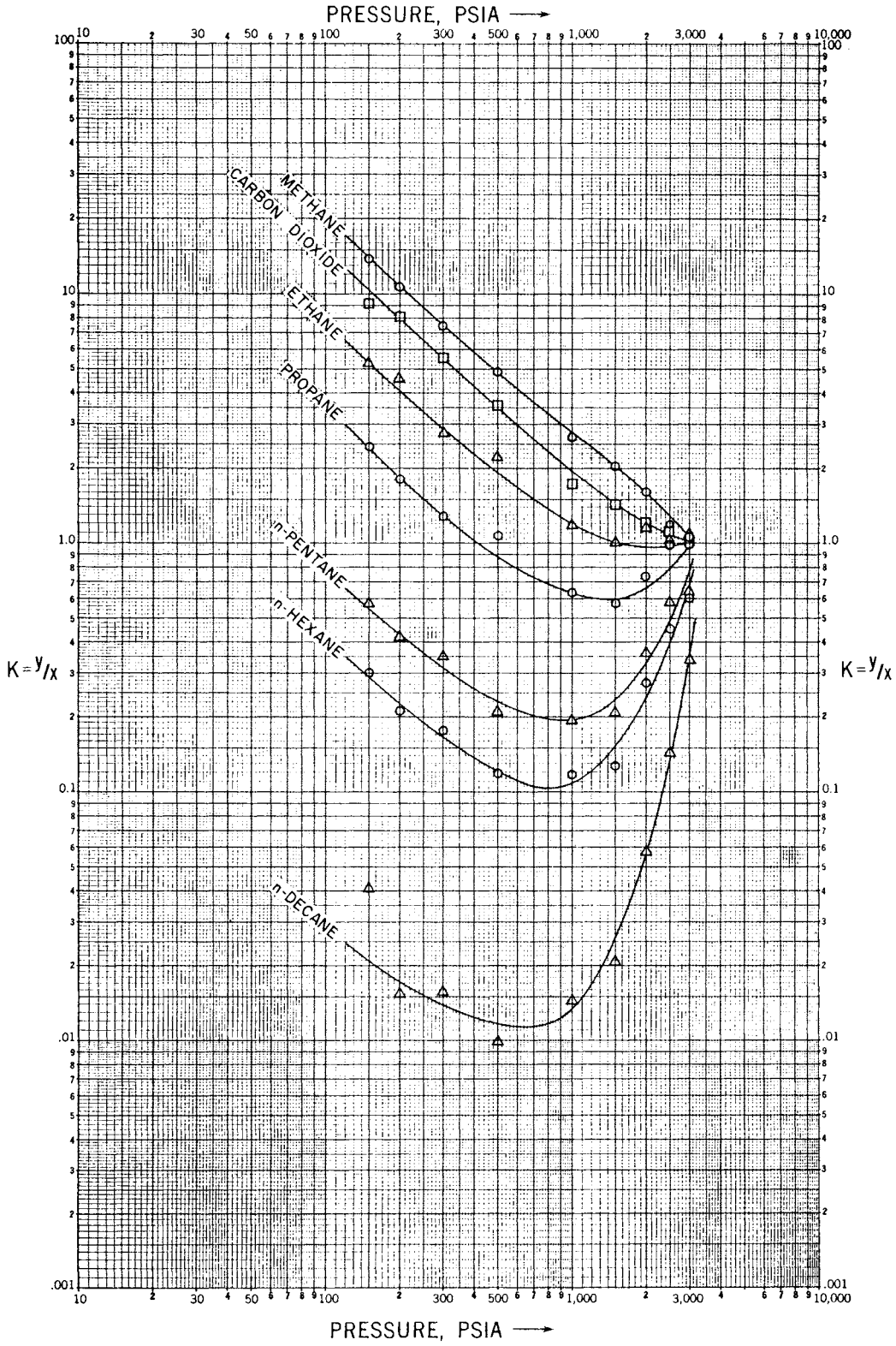

FIGURE 9

EXPERIMENTAL K-VALUES AT 250°F
BASE SYSTEM WITH LOW CO_2 ADDITION

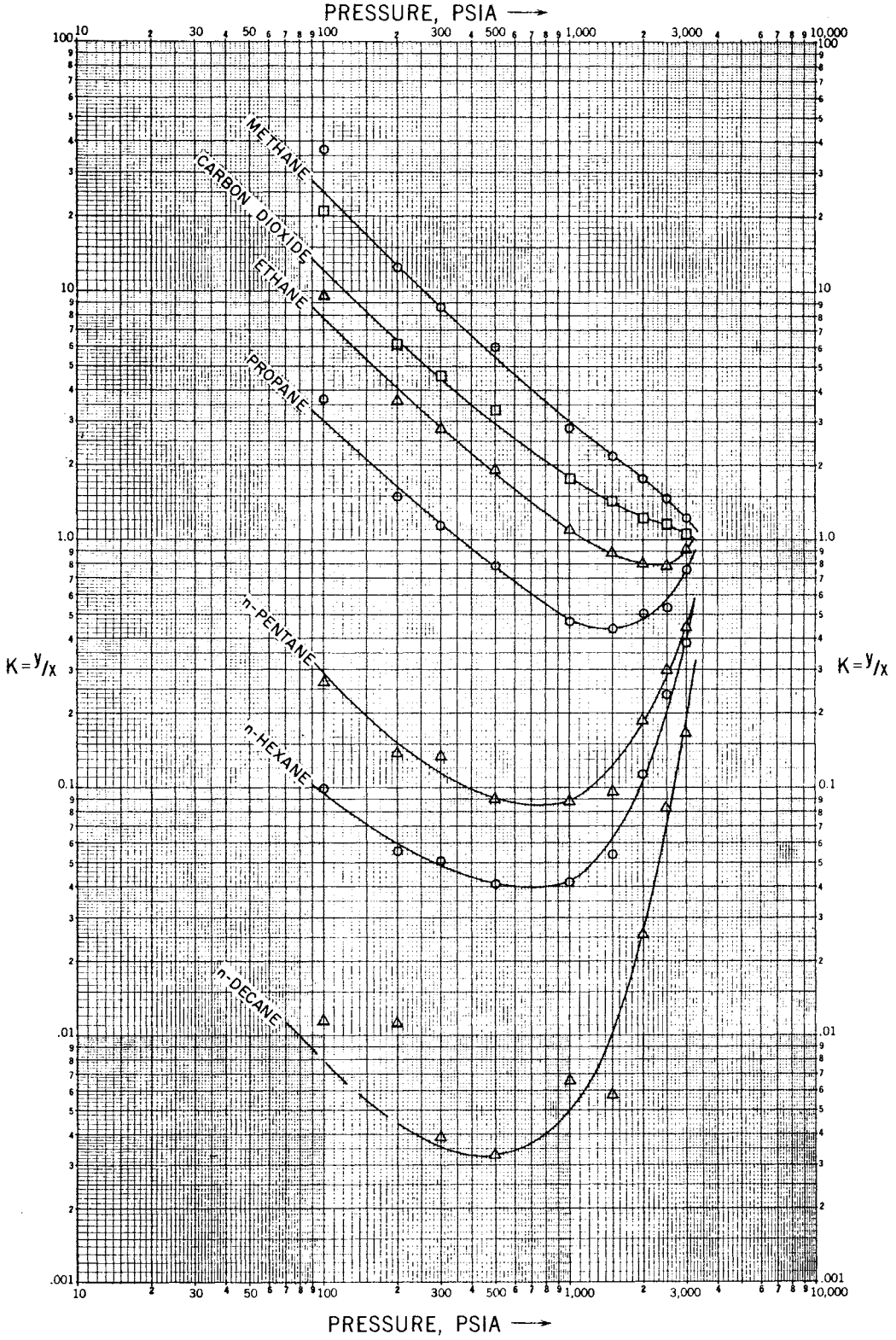

FIGURE 10

EXPERIMENTAL K-VALUES AT 150°F
BASE SYSTEM WITH HIGH CO_2 ADDITION

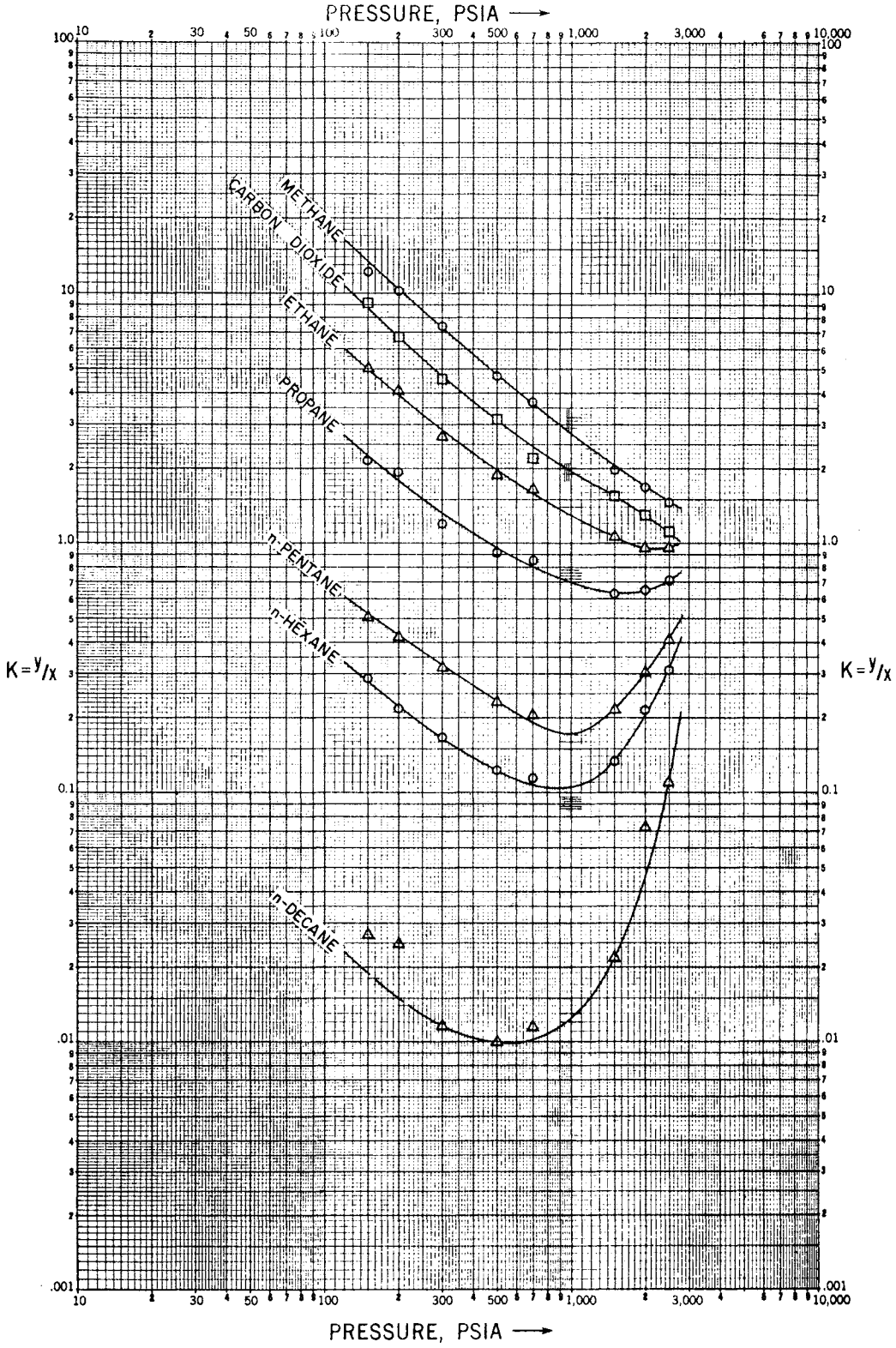

FIGURE 11

EXPERIMENTAL K-VALUES AT 250°F
BASE SYSTEM WITH HIGH CO_2 ADDITION

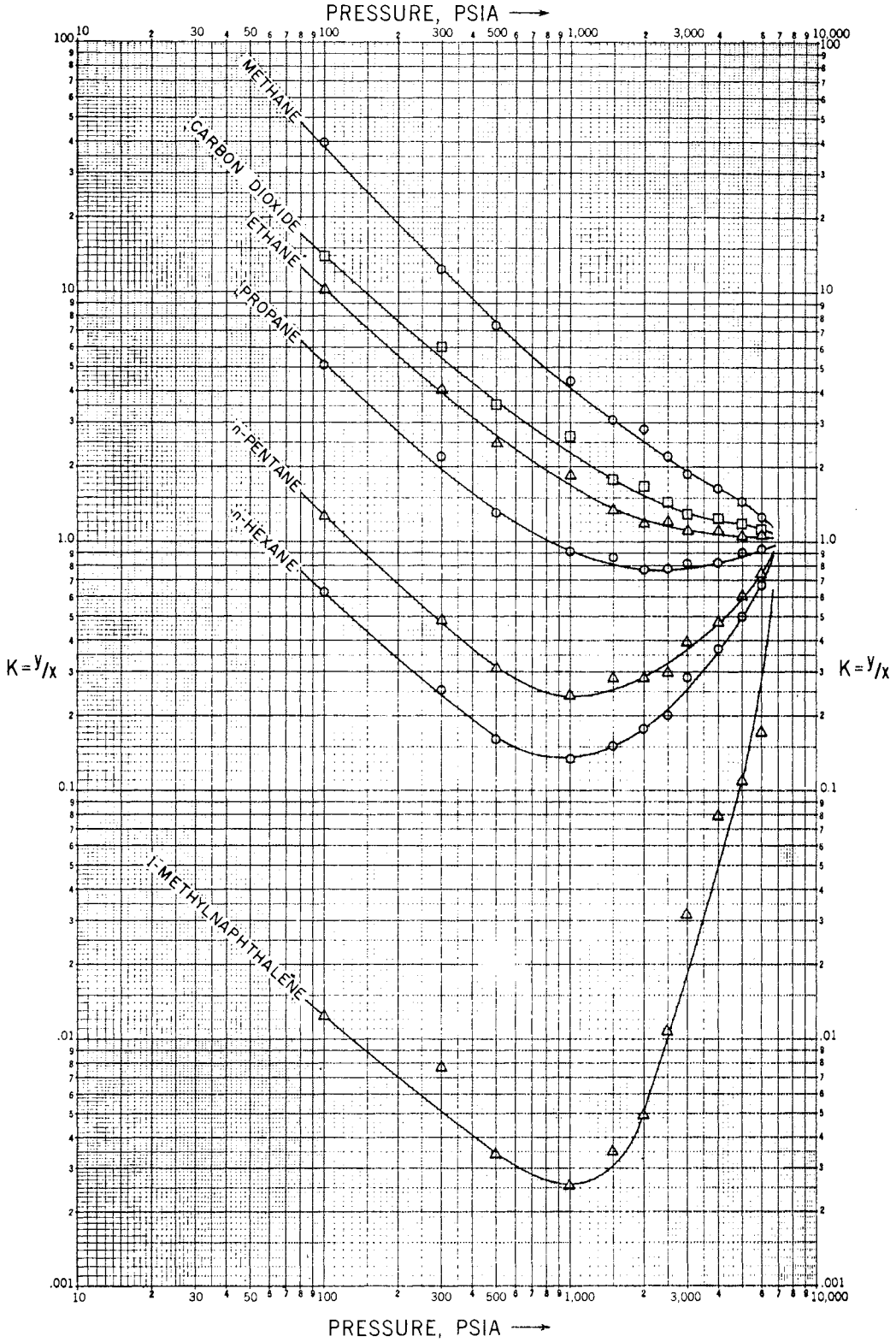

FIGURE 12

EXPERIMENTAL K-VALUES AT 250°F - BASE SYSTEM WITH CO_2 AND 1-METHYLNAPHTHALENE SUBSTITUTED FOR N-DECANE

temperature air bath were calibrated to read to ± 0.02°F. The temperatures for the experimental data are reported as being ± 0.5°F of the reported value. Actually in all but a few cases the temperature deviation was only about half of this value during a given run. This deviation represents on a percentage basis a deviation of less than 0.1 of a per cent. Since the K-value response to changes in temperature as given by Jacoby and Rzasa[30] is reasonably flat, the error in the experimental K-values due to errors in temperature measurements may be assumed to be negligible. If the pressure is very close to the apparent convergence pressure, then this deviation is accentuated but is probably negligible anyway.

Pressure measurements below 3000 psia were made on the Heise pressure gage which could be read to ± 0.5 psia. That represents an error of 0.5 to 0.01 per cent, depending on the absolute pressure. For pressures above 3000 psia the Hart pressure balance was used. These pressures were read to ± 0.1 psia and hence represent an error of 0.003% or less. Therefore the contribution due to pressure inaccuracies can also be neglected.

The precision with which area ratios could be measured was determined by the chromatographic analysis of several injection samples taken from the same sample bottle. It was found that the areas could be determined within approximately three per cent of the mean value. Thus the expected error in the K-values is about six per cent. Obviously, the

errors due to composition analysis far exceed those due to temperature and pressure measurements.

A six per cent deviation in K-values is not enough to explain the deviations in the experimental data. Consequently, an analysis was made as described in Appendix F to determine the maximum possible error in the K-value of each component of each experimental data point. The values of area and slope deviations given in Table F-1 were used in the calculations. The area deviations are due to inaccurate recorder operation and the slope deviations are possible errors introduced due to scatter of calibration data.

The range of maximum expected deviation in K-values is indicated for most data points on Figures 13, 14, 15, 16, 17, 18 and 19 along with the experimental data points. In areas where the hash marks would have been too confusing some of the marks were omitted. Since the smooth line drawn through the data points usually falls within the range of deviation of the K-values, it is concluded that in these cases any scatter in the data points is due mostly to chromatographic analysis. In those cases where the deviation range does not bracket the line, it must be concluded that some other factors influenced the experimental results. The most likely cause is the sampling technique. It is quite possible that a truly representative sample was not obtained in some cases.

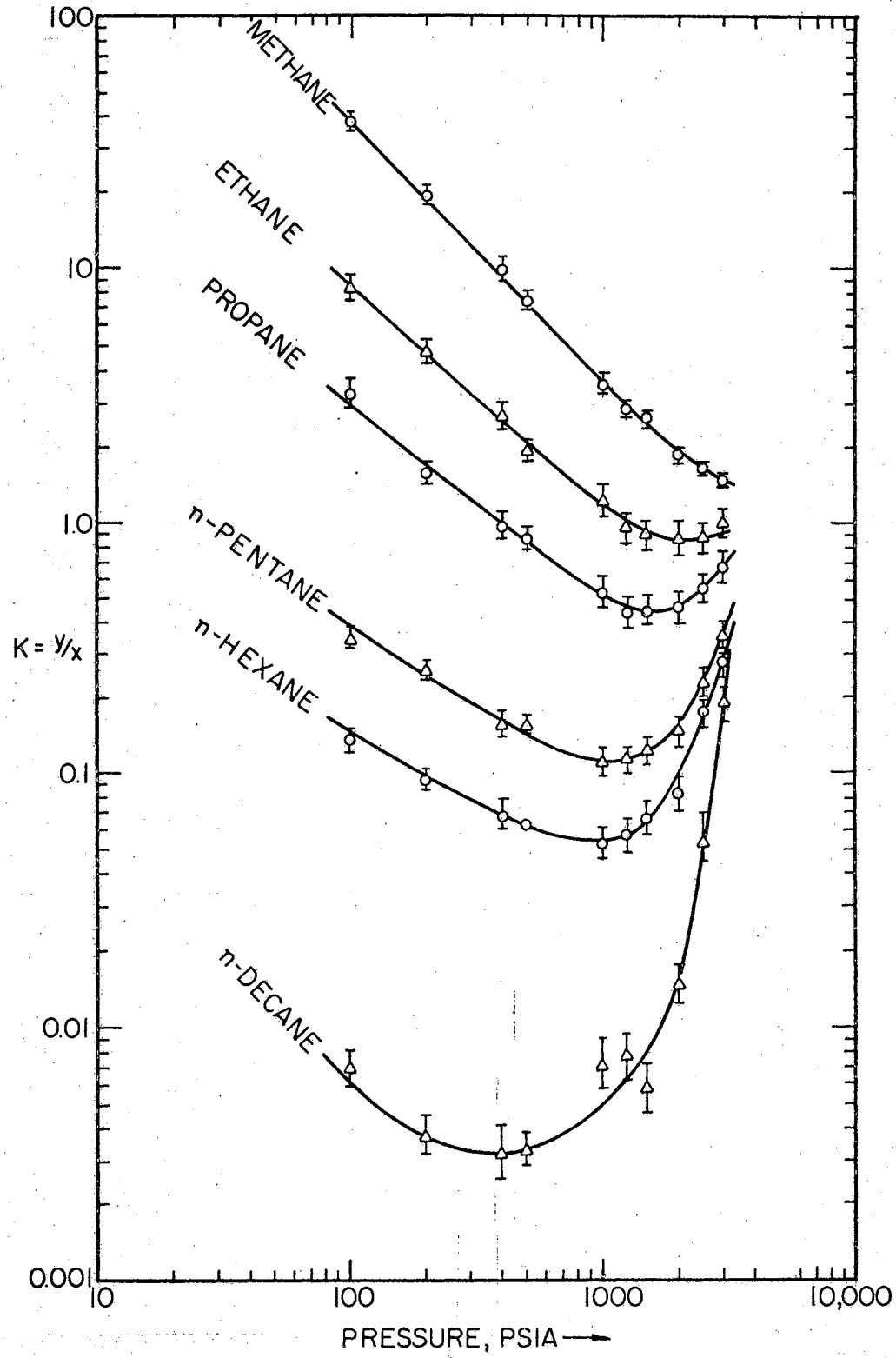

FIGURE 13

MAXIMUM EXPECTED ERROR AT 150°F
BASE SYSTEM

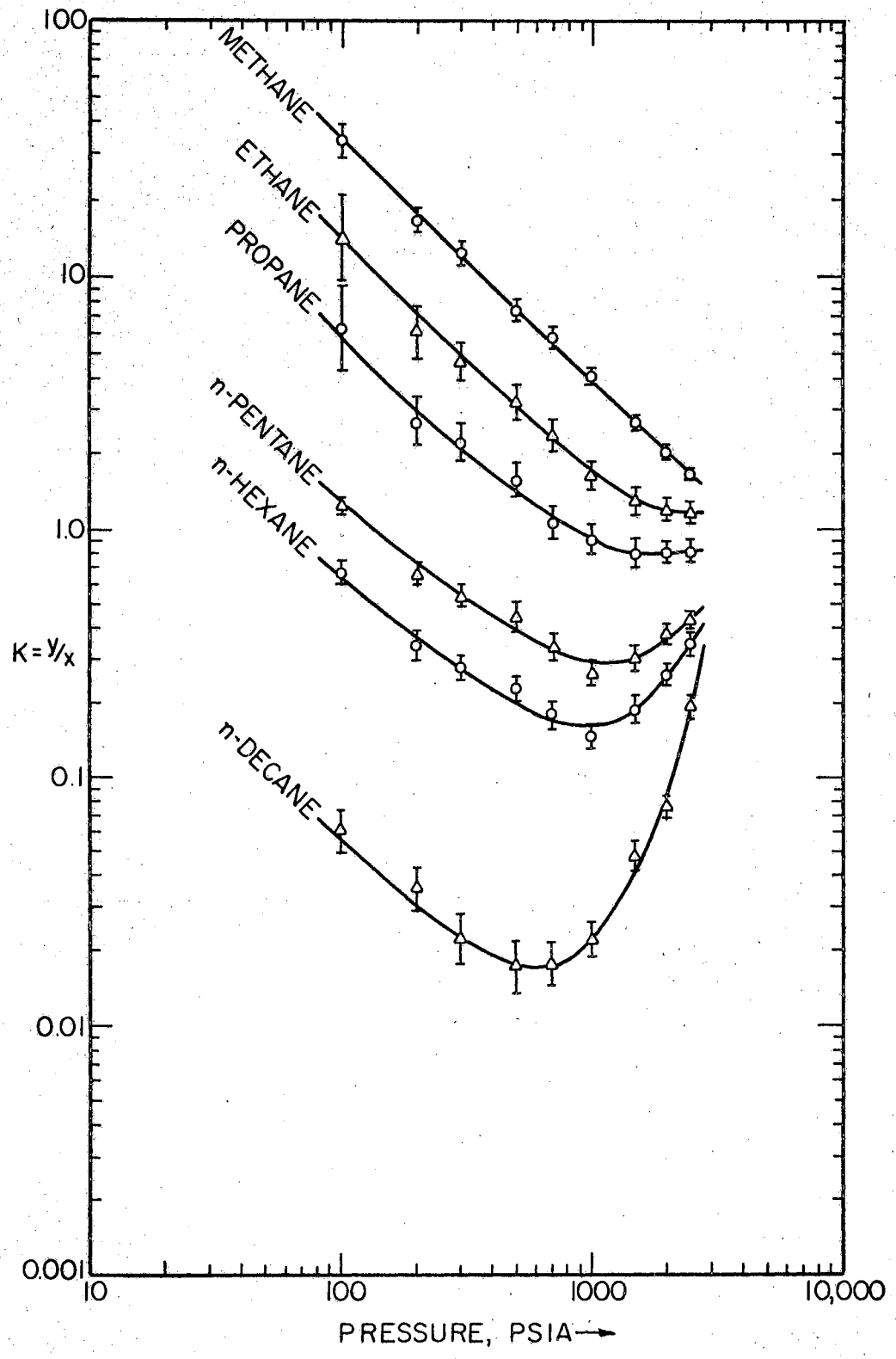

FIGURE 14

MAXIMUM EXPECTED ERROR AT 250°F
BASE SYSTEM

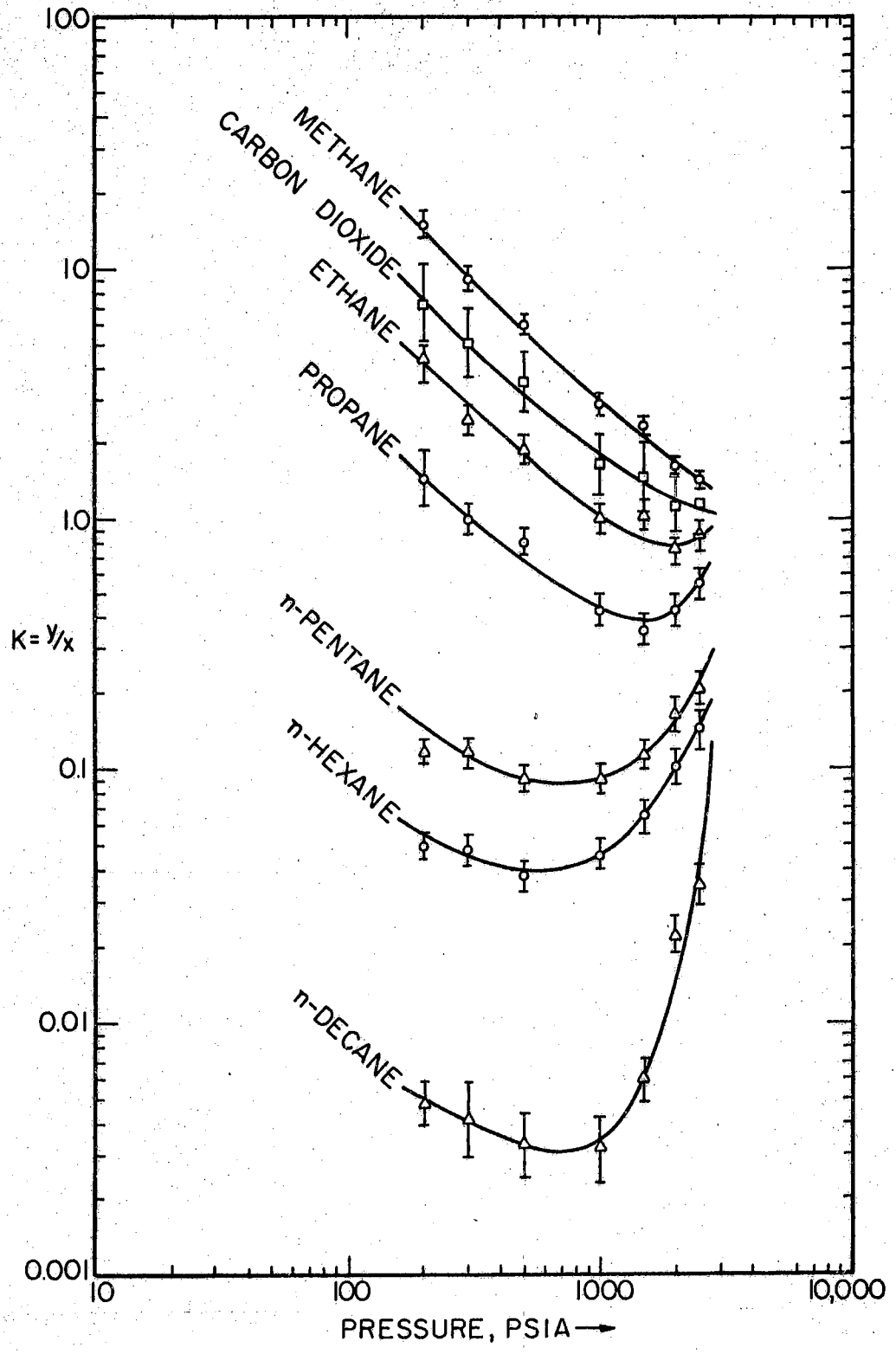

FIGURE 15

MAXIMUM EXPECTED ERROR AT 150°F
BASE SYSTEM WITH LOW CO_2 ADDITION

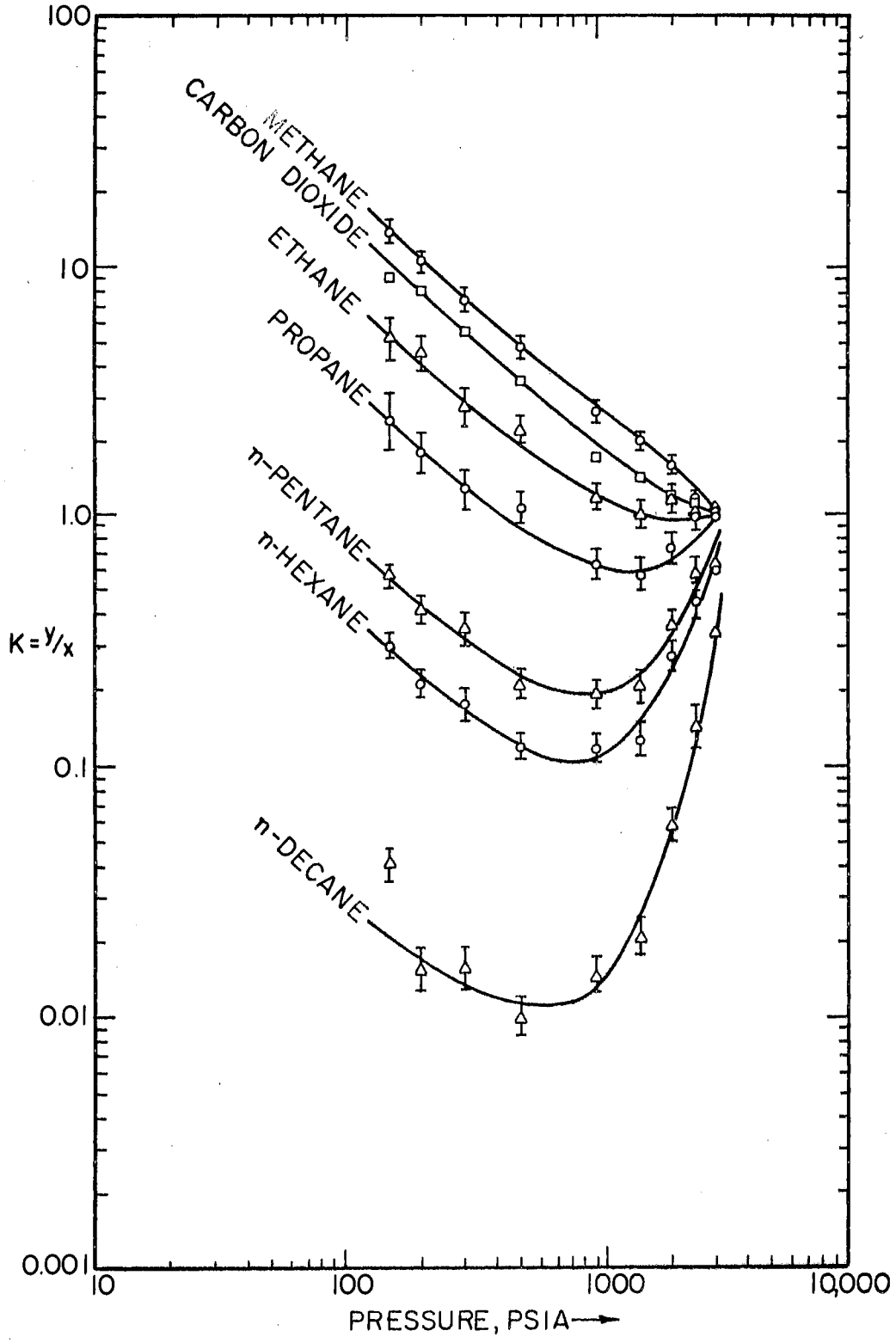

FIGURE 16

MAXIMUM EXPECTED ERROR AT 250°F
BASE SYSTEM WITH LOW CO_2 ADDITION

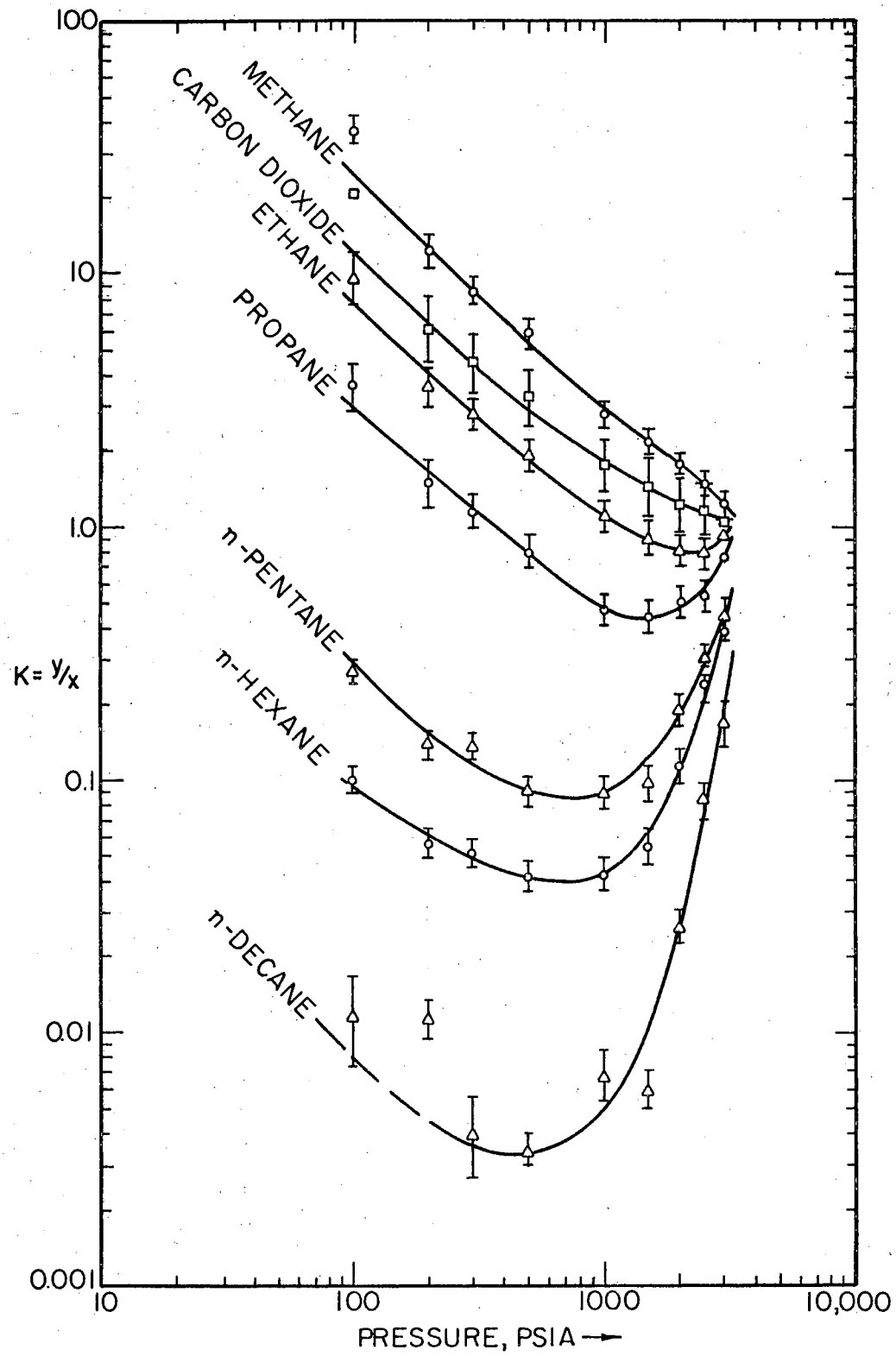

FIGURE 17

MAXIMUM EXPECTED ERROR AT 150°F
BASE SYSTEM WITH HIGH CO_2 ADDITION

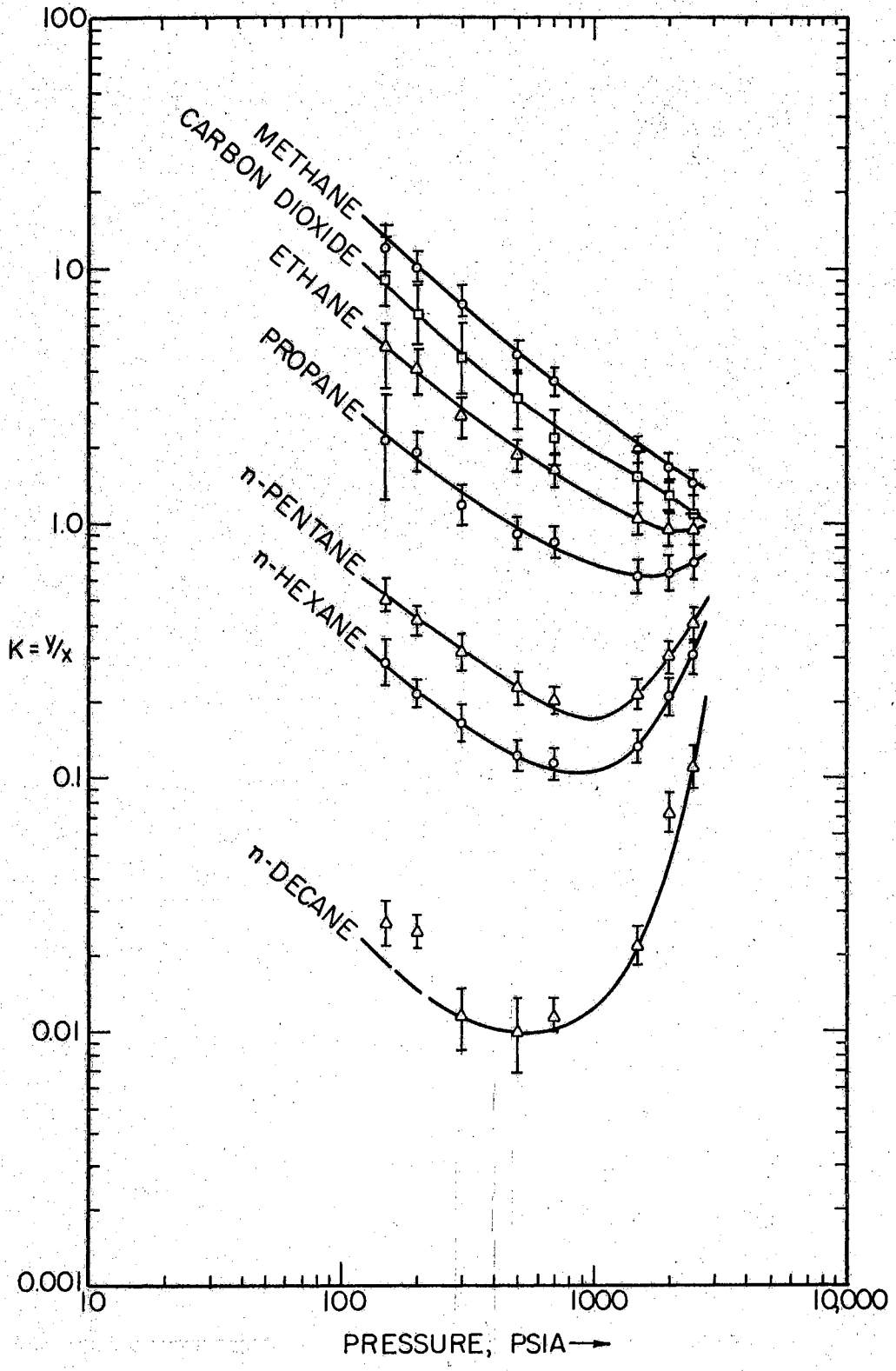

FIGURE 18

MAXIMUM EXPECTED ERROR AT 250°F
BASE SYSTEM WITH HIGH CO_2 ADDITION

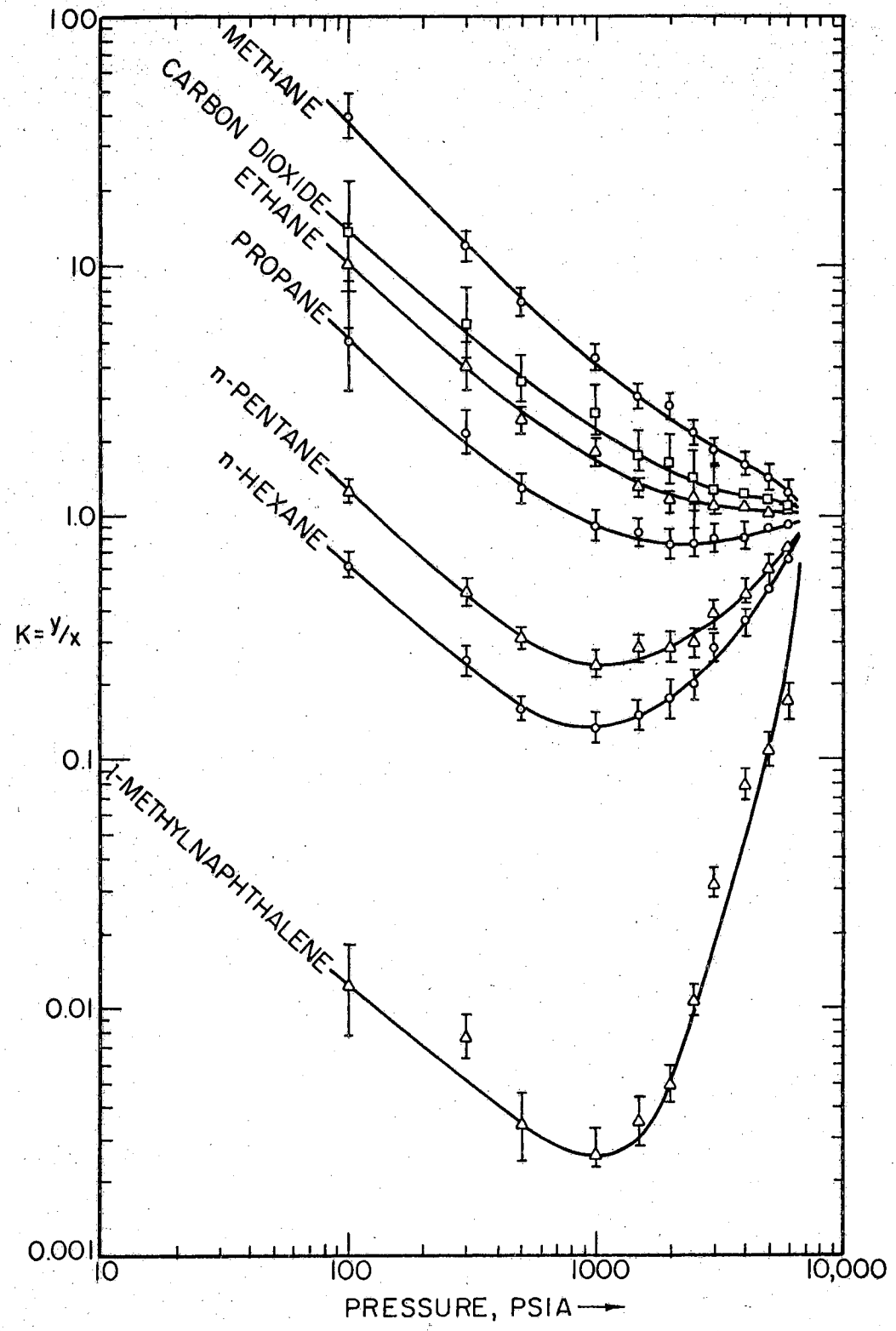

FIGURE 19

MAXIMUM EXPECTED ERROR AT 250°F - BASE SYSTEM WITH CO_2 AND 1-METHYLNAPHTHALENE SUBSTITUTED FOR N-DECANE

Comparison of Results

A comparison of the experimental data for the base system at 150°F and the NGPA K-values from (38) interpolated for a convergence pressure of 4000 psia is presented in Figure 20. As can be seen the agreement is good except for decane. Figure 21 shows a similar comparison between the base system at 250°F and the NGPA K-values at 3000 psia convergence pressure. Again the agreement is good except for decane. The n-decane K-values are more dependent on the convergence pressure than those of the other five components. Since the system composition was changing from run to run, the actual convergence pressure is not known. Selection of somewhat different convergence pressure for comparison purposes could give as good an agreement for decane as for other values.

The K-values for all components at pressures near the convergence pressure should depend greatly on the convergence pressure. Examination of Figures 20 and 21 shows that indeed the K-values deviate more from the NGPA K-values at pressures above 1000 psia than below. This indicates that the values selected for the convergence pressure were somewhat in error as was surmised before.

No comparison was made with the data containing CO_2 since the NGPA K-values obviously would not agree well with them. The reason is that the NGPA values do not account for the difference due to the presence of CO_2. Hence the lack of agreement is to be expected.

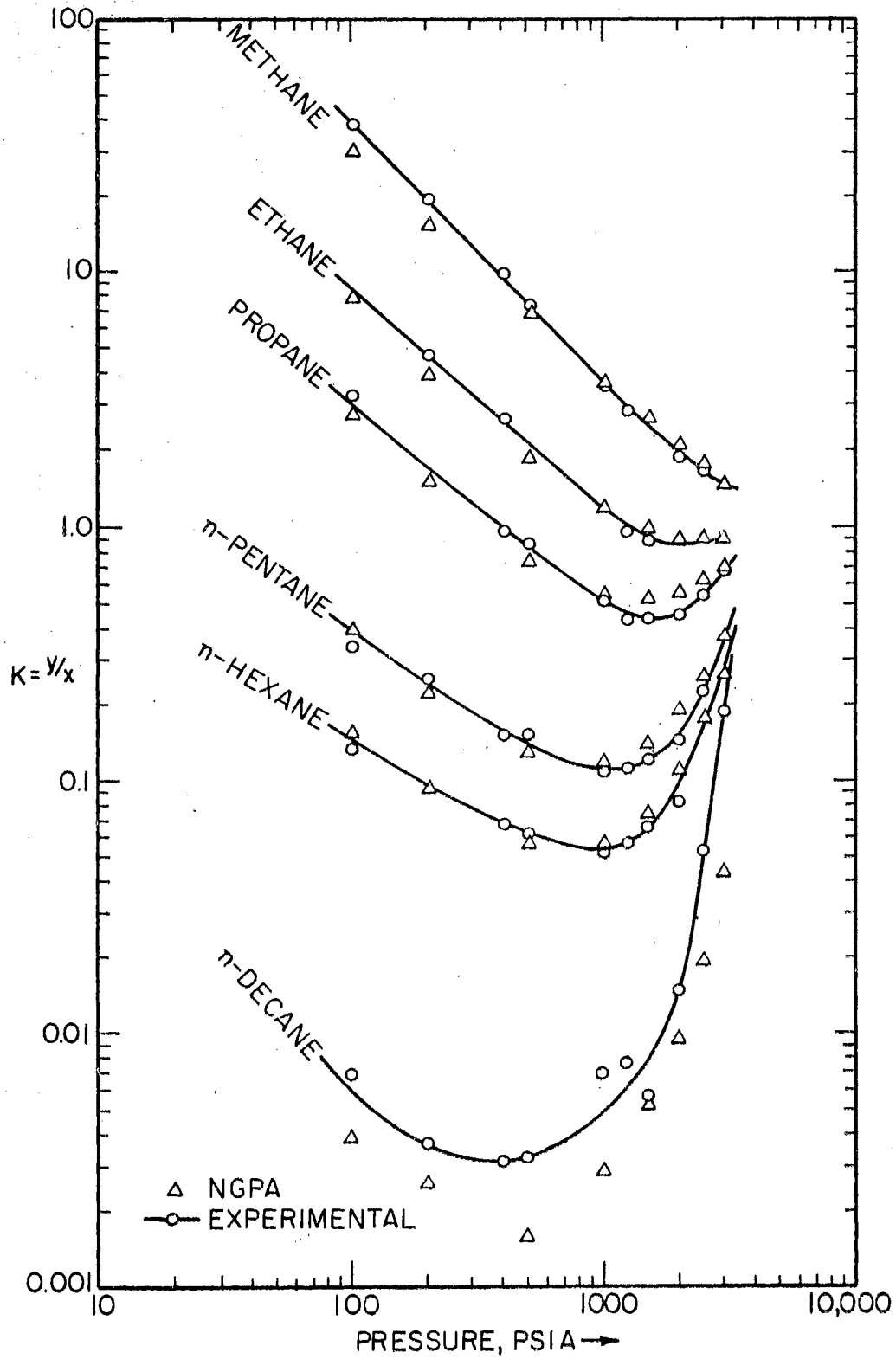

FIGURE 20

COMPARISON OF EXPERIMENTAL K-VALUES WITH NGPA AT 150°F - BASE SYSTEM

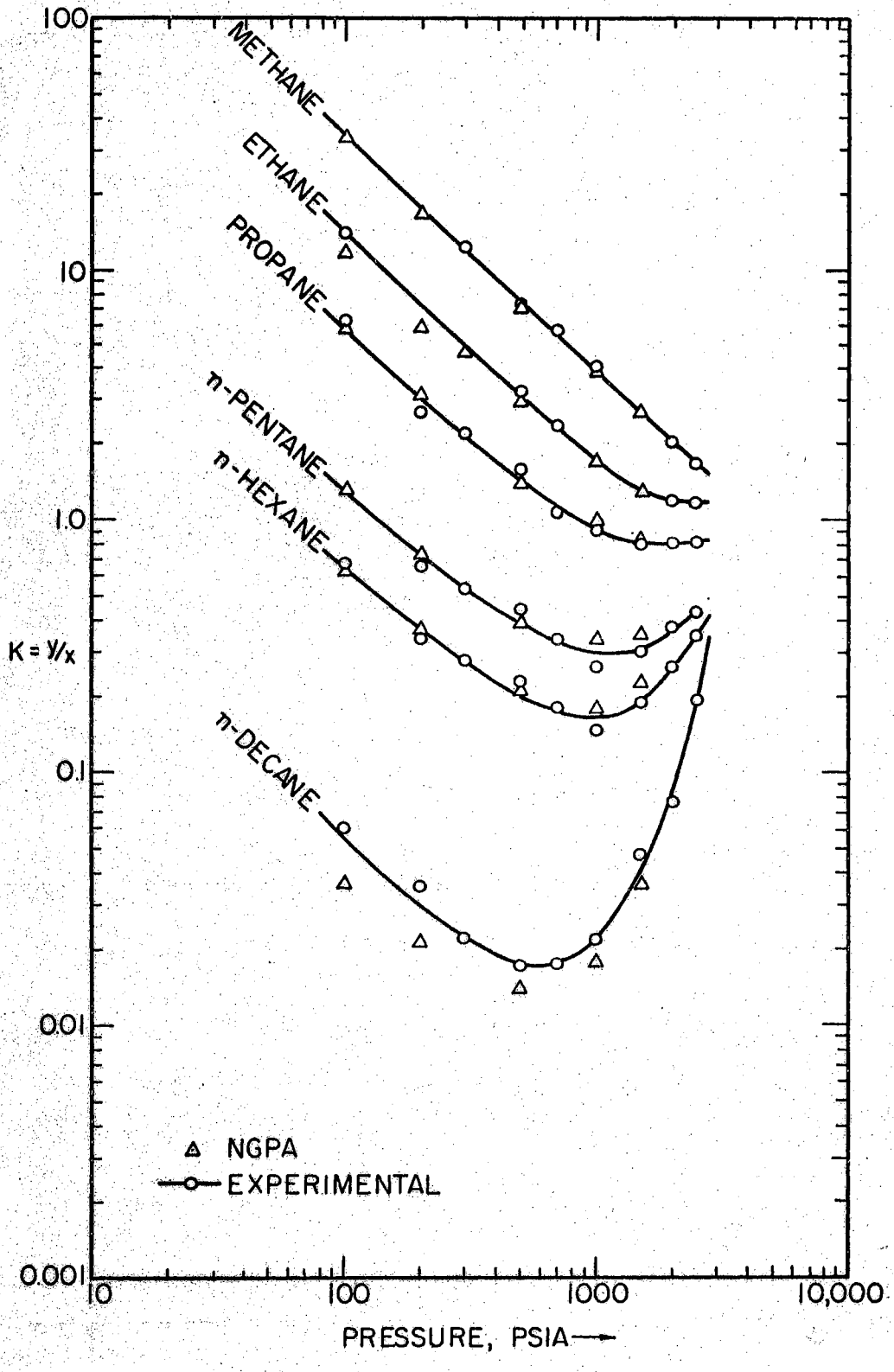

FIGURE 21

COMPARISON OF EXPERIMENTAL K-VALUES WITH NGPA AT 250°F - BASE SYSTEM

A comparison was run between the experimental data and the Chao-Seader correlation.[10] The average absolute per cent deviations of the Chao-Seader values from the experimental values are given in Table II for each component. The number of data points in each of eight per cent deviation groups are shown. The deviations were calculated according to % deviation = $100(\frac{K_{cs} - K_{exp}}{K_{exp}})$. The K-values calculated from the Chao-Seader correlation were obtained in an overconstrained manner. That is, the experimental temperature, pressure and both phase compositions were substituted into the correlation to give a K-value directly. Actually one of the variables like the vapor composition should have been determined from the trial and error flash calculation with the correlation. Not knowing the overall composition of the mixture it was necessary to use the direct substitution. This may account for some of the rather large deviations from the experimental data. In addition the correlation was developed for pressures less than 2000 psia. In the comparison with the experimental data the pressures ran considerably above this value. Hence, it is not surprising that some very large per cent deviations were obtained. The agreement between the correlation and the experimental data is much better for the base systems than those with carbon dioxide. The reason for this is that the Chao-Seader correlation was not developed from data on systems containing carbon dioxide. As can be seen from the experimental data the presence of carbon dioxide alters the

TABLE II

COMPARISON OF CHAO-SEADER PREDICTIONS AND UNSMOOTHED EXPERIMENTAL K-VALUES

Component	Average Absolute % Dev.	Number of Points in the % Deviation Range of: Less Than -20	-20 to -10	-10 to -5	-5 to 0	0 to 5	5 to 10	10 to 20	More Than 20
Base System at 150°F (11 points)									
Methane	30.8		3		1			1	6
Ethane	12.9	3	2	2	2	2			
Propane	6.6		2	2	2	3	1	1	
n-Pentane	13.1	1	2	2	1	1	3	1	
n-Hexane	16.9	3	2	1	1	3		1	
n-Decane	54.0	11							
Base System at 250°F (10 points)									
Methane	24.4					2	2	2	4
Ethane	25.3	4	1	1	1			2	1
Propane	15.2	3	2	1	2	1		1	
n-Pentane	12.4	1	4	2		3			
n-Hexane	16.0	1	4	3	1	1			
n-Decane	42.6	7	3						
System with Low CO_2 Addition at 150°F (8 points)									
Methane	45.7							1	7
Ethane	15.3	2	1	1		1	1	1	1
Propane	19.6	1			2			3	2
n-Pentane	39.1	1					2		5
n-Hexane	35.6	1	1		1		1		4
n-Decane	49.9	8							
Carbon Dioxide	15.8		2	1	1	1	1	1	1
System with Low CO_2 Addition at 250°F (10 points)									
Methane	76.6								10
Ethane	53.4	4		1					5
Propane	44.2	4					1		5
n-Pentane	43.2	3	1						6
n-Hexane	42.6	4							6
n-Decane	45.5	5		1			1	1	2
Carbon Dioxide	23.2	1	3		2	1			3

TABLE II (Continued)

System with High CO_2 Addition at 150°F (10 points)									
Methane	46.6			1					9
Ethane	11.6		2		3	1	2	1	1
Propane	12.3		1	2		2		2	3
n-Pentane	37.2		2			1		1	6
n-Hexane	41.0		3				1		6
n-Decane	55.3		8			2			
Carbon Dioxide	34.1		1	2	1	1		2	3
System with High CO_2 Addition at 250°F (9 points)									
Methane	72.8								9
Ethane	56.9		3	1					5
Propane	40.9		1	1	1		1		5
n-Pentane	39.9		1		1			1	6
n-Hexane	36.0		1	1			1		6
n-Decane	39.5		3		1		2		3
Carbon Dioxide	17.7		2		3			1	3

hydrocarbon K-values somewhat. Hence the Chao-Seader correlation cannot be expected to agree as well with these systems as with the base systems. The variation of hydrocarbon K-values in carbon dioxide systems was treated by Lenoir[34] but for binary systems only.

In the above comparison the correlation constants of Erbar, et al.[22] were used for carbon dioxide. Since that represents a direct correlation of the data, it should be expected that in these systems the carbon dioxide K-values are represented fairly closely. The agreement for carbon dioxide is significantly better.

In Table III are shown the results of bubble point calculations on mixtures using the experimental equilibrium liquid compositions. The Chao-Seader correlation was used to arrive at the results. For each of the seven experimental isotherms the average absolute per cent deviation in bubble point, the average per cent deviations, the total number of data points and the number of data points used in the bubble point calculations are shown. All of the data points could not be utilized in the bubble point calculations since the Chao-Seader method would not give convergence beyond certain pressures. This can be attributed to the range of the applicability of the correlation being narrower than the range of the experimental data.

Examination of Table III shows that the Chao-Seader method gives bubble points that are too high on the average. The more CO_2 is present the less accurate is the calculation.

TABLE III

RESULTS OF BUBBLE POINT CALCULATION WITH THE CHAO-SEADER EQUATION

System	Total Number of Points	Number of Points Converged	Average Absolute % Deviation	Average % Deviation
Base at 150°F	11	7	26.6	14.6
Base at 250°F	10	8	20.5	20.5
Low CO_2 at 150°F	8	4	33.6	33.6
Low CO_2 at 250°F	10	5	81.2	81.2
High CO_2 at 150°F	10	5	31.4	27.2
High CO_2 at 250°F	9	5	72.4	72.4
1-Methylnaphthalene at 250°F	11	4	66.4	66.4

A dew point calculation was not performed because it is very sensitive to the concentration of heavy components in the vapor phase. This is particularly true in condensate systems to which the systems of this study are very similar. The concentrations of n-decane in the vapor phase are much more uncertain than the liquid phase concentrations and hence the dew point calculation was felt to be an unfair test of the Chao-Seader correlation in this case.

Effect of Carbon Dioxide

Examination of Figures 6 through 11 and Tables D-I through D-VI shows that the mixtures with carbon dioxide present have a markedly lower single phase pressure. That of course was to be expected from the knowledge of the behavior of binary carbon dioxide-hydrocarbon systems. This was accompanied generally by a decrease in the K-values of the hydrocarbon components. The exception to that generalization is decane at 150°F in the more highly concentrated carbon dioxide system. Here the opposite trend was observed. These trends can be observed in Table IV where the ratios of the K-value in the system with carbon dioxide present to the K-value in the base system for each component at five selected pressures are presented. Smoothed K-values were used in calculating the ratios. Pressures below 1000 psia were selected to stay well below the convergence pressure areas.

TABLE IV

RATIOS OF K-VALUES IN SYSTEMS WITH CO_2 TO THE K-VALUES OF BASE SYSTEMS

Pressure	200	300	400	700	1000	Average Ratio
			Low CO_2 Concentration at 150°F			
Methane	.770	.781	.783	.791	.797	.784
Ethane	.913	.877	.863	.844	.874	.874
Propane	.858	.836	.818	.818	.827	.836
n-Pentane	.612	.611	.627	.727	.829	.681
n-Hexane	.579	.584	.603	.723	.818	.662
n-Decane	1.324	1.231	1.109	.805	.700	1.034
Average	.843	.820	.800	.785	.808	.811
			High CO_2 Concentration at 150°F			
Methane	.668	.707	.728	.771	.811	.737
Ethane	.891	.877	.874	.888	.933	.893
Propane	.964	.959	.929	.924	.923	.940
n-Pentane	.629	.622	.620	.702	.793	.673
n-Hexane	.632	.636	.647	.705	.764	.677
n-Decane	1.189	1.092	1.016	.948	1.000	1.049
Average	.829	.816	.802	.823	.871	.828
			Low CO_2 Concentration at 250°F			
Methane	.611	.630	.648	.664	.727	.656
Ethane	.555	.592	.584	.652	.694	.615
Propane	.617	.613	.600	.640	.685	.631
n-Pentane	.589	.583	.578	.571	.661	.597
n-Hexane	.616	.600	.609	.610	.654	.618
n-Decane	.577	.622	.647	.646	.604	.619
Average	.594	.607	.611	.631	.671	.623
			High CO_2 Concentration at 250°F			
Methane	.589	.605	.626	.654	.714	.638
Ethane	.534	.582	.597	.696	.751	.632
Propane	.593	.623	.647	.702	.761	.665
n-Pentane	.589	.602	.600	.543	.583	.583
n-Hexane	.611	.600	.613	.622	.636	.617
n-Decane	.500	.511	.542	.577	.568	.540
Average	.569	.587	.604	.632	.669	.612

Although the ratios presented in Table IV vary with pressure, the average value for each component is also shown. Examination of the average values for both temperatures shows that the presence of carbon dioxide in the two amounts studied affects the K-values of the hydrocarbons methane, ethane and propane independently of the amount of carbon dioxide present. For n-pentane, n-hexane and n-decane the effects were different for the two isotherms. At 150°F the K-values of these three hydrocarbons were lowered by the presence of carbon dioxide but less markedly at the high carbon dioxide concentration than at the lower one. At 250°F additional carbon dioxide continued to decrease the K-values of these three hydrocarbons.

The average ratios for all hydrocarbons in each of the four systems presented in Table IV allow one to draw a very approximate conclusion as to the effect of carbon dioxide on normal paraffin K-values. That is, at 150°F the hydrocarbon K-values are 80% and at 250°F, 60% of the values at the corresponding temperatures when no carbon dioxide is present. This rough conclusion implies that the amount of carbon dioxide has no large effect on the K-values of normal paraffins whereas temperature has a marked effect.

At this point it is interesting to note the differences in the conclusions about the effect of CO_2 on n-paraffin K-values drawn above and those of Lenoir.[34] Lenoir studied binary hydrocarbon systems in the temperature range -60°F to 120°F. He concluded that the ratios discussed above

became "1 at temperatures above 120°F, and shows that at higher temperature levels CO_2 does not produce a significant effect upon the volatility of light paraffin or olefin hydrocarbons." The data of this study show that his conclusion may not be correct. The curves in his Figure 3 should extend below unity for higher temperatures. The comparison of Lenoir's curves and averages from Table IV is shown in Figure 22. There are no theoretical reasons for the ratios being unity or less than unity at higher temperatures. In fact at temperatures much above 90°F one might expect strange behavior since at these temperatures CO_2 is a supercritical gas. Its solubility characteristics cannot be expected to be like those at lower temperatures. Therefore, its effect on the hydrocarbon activity in the liquid phase might also be different.

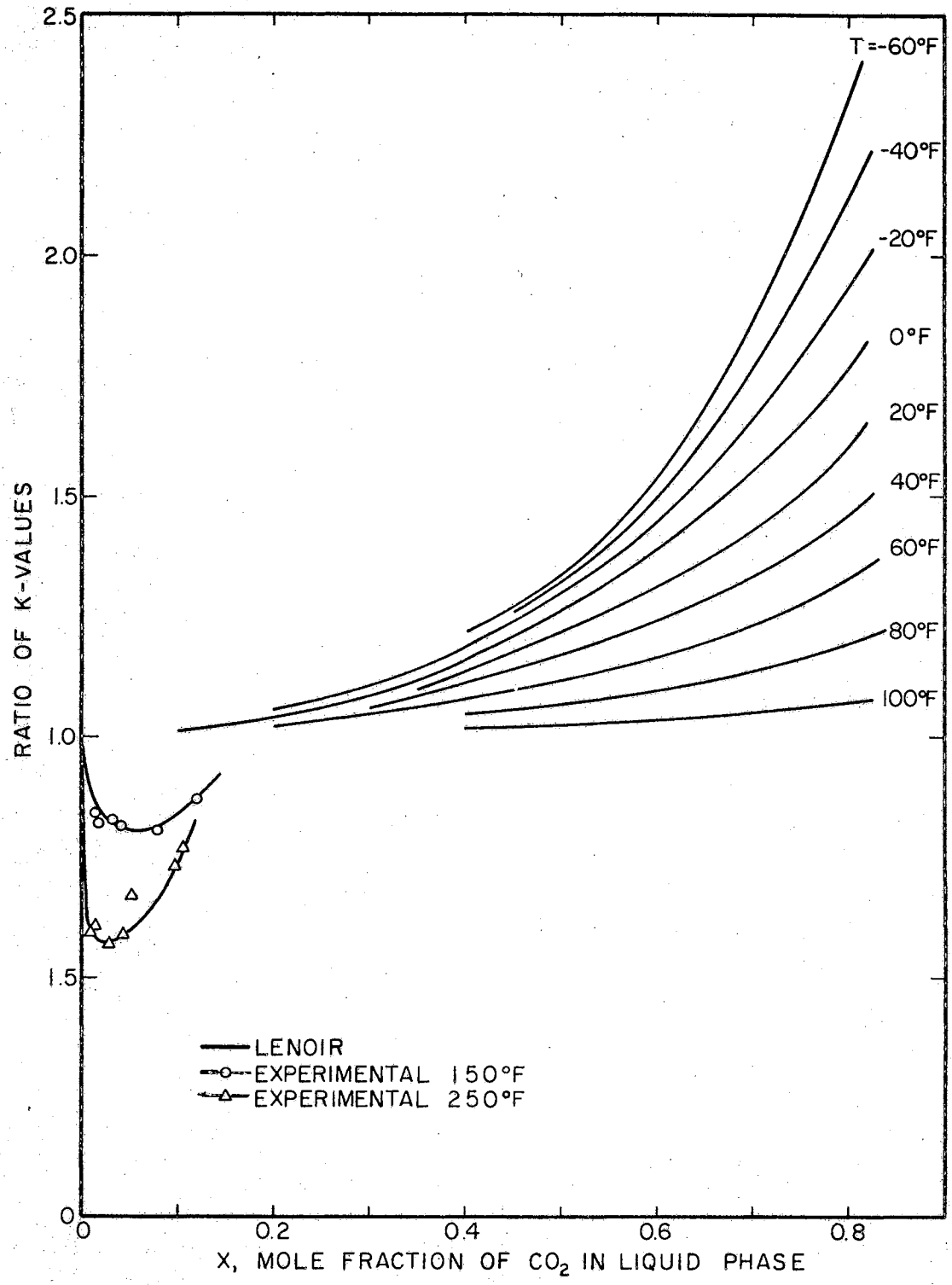

FIGURE 22

RATIOS OF K-VALUES

CHAPTER VIII

CORRELATION RESULTS

Development of Correlation

Binary K-value data[1,2,4,18,37,47,48,51,52,53,54,62,63,65] on paraffin and paraffin-CO_2 systems were used to develop a semi-empirical K-value correlation for computer applications. The experimental data in this work were then used to check the correlation and compare the differences against those obtained from the Chao-Seader correlation.

Calculation of Reference Fugacity

The first step in the correlation work was to calculate f_i^L values using Equation (3-6). The right hand side contains values of pressure and K-values both of which were obtained from the published binary experimental data. The values of the fugacity coefficients in the vapor mixture were calculated using the Benedict, et al. equation with the generalized coefficients of Edmister, et al.[21] The activity coefficients were evaluated by the Scatchard-Hildebrand equation.[27] However, in place of the usual representation of the interaction contribution to the solubility parameter, a more accurate representation of the binary interaction coefficients for the solubility parameters was used.

Expanding Equation (4-19) for component 1 in a binary mixture and simplifying yields

$$\ln \gamma_i = \frac{V_1}{RT} A_{21} X_2^2 \qquad (8\text{-}1)$$

where A_{21} is given by Equation (4-14) instead of Equation (4-20). Letting $C_{11} = \delta_1^2$, $C_{22} = \delta_2^2$ and representing the interaction coefficient C_{12} by

$$C_{12} = (1 - k_{12})\delta_1\delta_2 \qquad (8\text{-}2)$$

one obtains the more rigorous form of the Scatchard-Hildebrand equation

$$\ln \gamma_1 = \frac{V_1}{RT} X_2^2 (\delta_1^2 + \delta_2^2 - 2 (1 - k_{12})\delta_1\delta_2) \qquad (8\text{-}3)$$

In this equation k_{12} represents the interaction coefficient and the δ's are the solubility parameters of the components in question.

Cheung and Zander[11] determined the interaction coefficients, k_{12}, for carbon dioxide dissolved in light liquid hydrocarbons. It is interesting to note that Cheung and Zander found that their values of k_{ij} agreed well with those of Chueh and Prausnitz[13] which were determined from saturated vapor phase PVT data. In addition the interaction coefficients were found to be almost independent of temperature. For these reasons it was decided to use the interaction parameters of Chueh and Prausnitz in Equation (8-3). Since the two groups of authors had not determined all of the interaction parameters needed in this work, some of them had to be determined by extrapolation of the available values.

The extrapolation was performed in the following manner. The k_{ij} values were plotted versus the carbon number of the other molecule, for all methane binaries, ethane binaries and propane binaries. The subscript r refers to the reference substance, that is, methane, ethane or propane. The subscript i refers to the component interacting with the component r. The plots can be seen on Figure 23. The best line was drawn through the points and extrapolated to n-decane. To get pentane and hexane interaction with decane a curve was plotted with n-decane as the reference substance. This curve is also shown on Figure 23. The literature and extrapolated or interpolated values are shown in Table V.

For carbon dioxide binaries the interaction parameters were plotted against the carbon atoms in the hydrocarbon molecule on log-log scale and extrapolated to decane. The curve is shown in Figure 24 and the values tabulated in Table V.

Calculation of Correlation Factor

With the experimental K-values and pressure known, the ϕ_i for the vapor phase calculated by the Benedict, et al. equation and γ_i for the liquid phase given by Equation (8-3), the pure liquid fugacities were determined from Equation (8-6). These values represented the fugacities one should be able to calculate in order to get an accurate representation of the K-values.

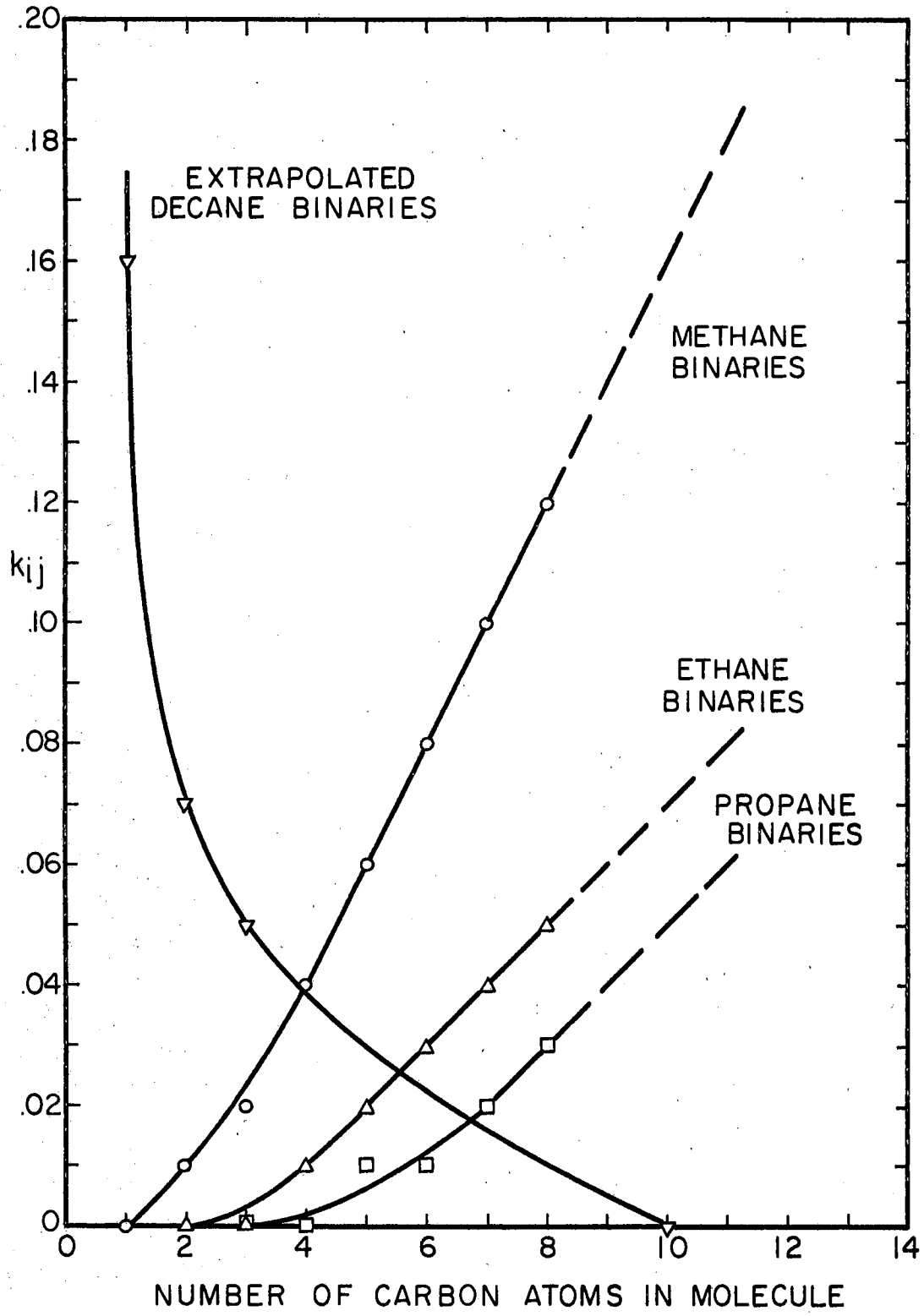

FIGURE 23

EXTRAPOLATION OF INTERACTION PARAMETERS
FOR HYDROCARBONS

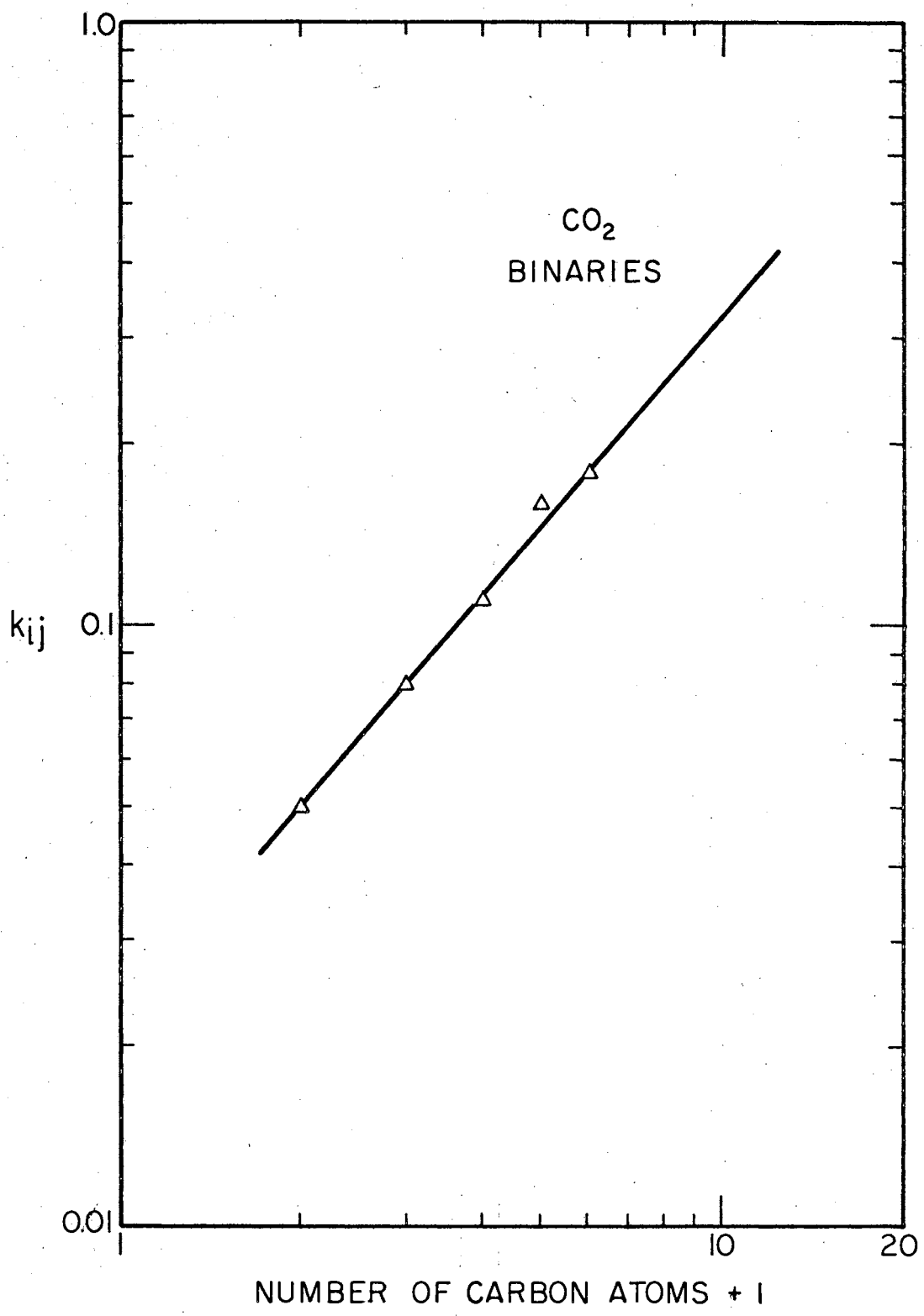

FIGURE 24

EXTRAPOLATION OF INTERACTION PARAMETERS
FOR CO_2 BINARIES

TABLE V

LITERATURE AND EXTRAPOLATED
INTERACTION COEFFICIENTS

	Chueh and Prauznitz[13] k_{ij}	Extrapolated k_{ij}
Methane-		
Ethane	.01	
Propane	.02	
Butane	.04	
Pentane	.06	
Hexane	.08	
Heptane	.10	
Octane	.12	
Decane		.16
Ethane-		
Propane	.00	
Butane	.01	
Pentane	.02	
Hexane	.03	
Heptane	.04	
Octane	.05	
Decane		.07
Propane-		
Butane	.00	
Pentane	.01	
Hexane	.01	
Heptane	.02	
Octane	.03	
Decane		.05
Pentane-		
Hexane	.00	
Heptane	.00	
Octane	.00	
Decane		.03
Hexane-		
Heptane	.00	
Octane	.00	
Decane		.02
Carbon Dioxide-	Cheung and Zander[11]	
Methane	.05	
Ethane	.08	
Propane	.11	
Butane	.16	
Pentane	.18	
Hexane		.22
Decane		.36

Next the BWR equation was used to calculate f_i^{BWR} values from Equation (3-8). Since the fugacities of the pure liquid as given by Equation (3-8) did not equal the required fugacities as given by Equation (3-6), a correlation factor had to be introduced. The correlation factor was calculated by Equation (3-7).

The correlation of the correlation factor ϵ_i was performed empirically by curve fitting. It was decided that different equations would be needed to represent the ϵ_i for super and subcritical components. The supercritical hydrocarbon components were fitted with

$$\epsilon_i = a_1 + a_2 T_R + (a_3 + a_4 T_R)/d + a_5/d^2 + \omega\left[a_6 + a_7 T_R + (a_8 + a_9 T_R)/d + a_{10}/d^2\right] \qquad (8\text{-}4)$$

It was found that a separate correlation equation was necessary for methane and carbon dioxide. Carbon dioxide was fitted with the following equation:

$$\epsilon_{CO_2} = a_1 + a_2 T_R + (a_3 + a_4 T_R)/d + a_5/d^2 \qquad (8\text{-}5)$$

and methane with

$$\epsilon_{C_1} = (a_1 + a_2 T_R + a_3 T_R^2)/d \qquad (8\text{-}6)$$

The constants for Equations (8-4), (8-5) and (8-6) determined by curve fitting are shown in Table VI.

An attempt was made to fit the ϵ_i values for the subcritical components, but it met with total failure. A review of the values showed that in most cases they were near unity. At first it was decided to let the ϵ_i equal unity for the subcritical components. However, on testing

TABLE VI

CORRELATION COEFFICIENTS FOR
SUPERCRITICAL COMPONENTS

Constants	ϵ for Supercritical Hydrocarbons Equation 8-4	ϵ for CO_2 Equation 8-5	ϵ for Methane Equation 8-6
a_1	3.9840	.06030	.3301
a_2	-2.5062	.1674	.0186
a_3	- .1302	-.06036	-.0283
a_4	.1332	.05865	
a_5	.0005660	.0001352	
a_6	-25.4132		
a_7	19.3556		
a_8	.3760		
a_9	-.03101		
a_{10}	-.004062		

this correlation against the experimental data of this work it was found that somewhat better results were obtained by letting

$$\omega_i = 0.6 + \omega \qquad (8\text{-}7)$$

Consequently, it was decided to use this relationship for the subcritical components of this correlation. The critical constants used in the correlation are tabulated in Table VII.

The standard deviations of the curve fit for methane, carbon dioxide and the generalized equation were 24.9, 18.5 and 5.2 per cent, respectively. The corresponding number of points in each of the fits was 241, 33 and 82 (70 ethane and 12 propane). The average absolute per cent deviations between ϵ_i from Equation (8-7) and the binary data were 33.4, 18.8, 23.0 and 24.1 per cent for propane, pentane, hexane and decane, respectively. The corresponding number of points were 126, 88, 51 and 121.

Testing of Correlation

The resulting correlation for ϵ_i was used in Equation (3-9) to compare the calculated K-values against the experimental multicomponent K-value data taken in this work. The γ_i values in the multicomponent systems were calculated from Equation (4-19) instead of Equation (8-3) which is the expanded binary form of the former. The average absolute per cent deviations were calculated as 100 (calc-exp)/exp.

TABLE VII

CONSTANTS USED IN CORRELATION

Component	T_c °R	P_c psia	ω	δ $(cal/cc)^{\frac{1}{2}}$	V cc
Methane	343.13	669.7	0.013	6.80	38
Ethane	549.77	708.3	0.105	7.60	55
Propane	665.68	616.3	0.152	7.40	76
n-Pentane	845.08	487.3	0.252	7.05	116
n-Hexane	913.14	436.6	0.290	7.30	132
n-Decane	1111.7	304.0	0.4869	7.75	197
Carbon Dioxide	547.43	1071.0	0.225	8.90	38

Note: T_c, P_c and ω from reference (38)

δ and V from reference (27)

They are shown in Table VIII. This table is similar to Table II for the comparison of the Chao-Seader correlation.

The standard and average deviations for the fit of ϵ values can be compared to the average deviations in Table VIII since the per cent deviations between calculated and experimental or desired K-values and ϵ's are equal. It soon becomes apparent that for the base systems the average deviations are about the same as the standard deviations. That is not true for the systems of CO_2. That is probably because most of the binary data were from all hydrocarbon systems.

A similar comparison was made with the data presented in Table D-VII as well as the data taken by Klekers.[33] It should be noted that there was no realistic basis for the selection of an interaction coefficient between the aromatic and naphthenic compounds and the normal paraffins in Klekers' systems. Hence, the same values were used as for the other systems. The average absolute per cent deviations of the calculated values for these systems are tabulated in Table IX. Since the correlation was not developed for aromatics and naphthenes the results are poorer.

A bubble point calculation was performed on the experimental liquid phase using this correlation. The results are tabulated in Table X in the same way as for the Chao-Seader correlation.

It is interesting to note the results from the comparison of the Chao-Seader correlation and the correlation of

TABLE VIII

COMPARISON OF CORRELATION PREDICTIONS AND UNSMOOTHED EXPERIMENTAL K-VALUES

Component	Average Absolute % Dev.	Number of Points in the % Deviation Range of: Less Than -20	-20 to -10	-10 to -5	-5 to 0	0 to 5	5 to 10	10 to 20	More Than 20
Base System at 150°F (11 points)									
Methane	22.9	5	1	2	3				
Ethane	10.6	1	4		2	1	1	2	
Propane	14.8	3	4	2	1	1			
n-Pentane	15.4	3	4	1	2				1
n-Hexane	19.8	4	5		1			1	
n-Decane	97.8	10							1
Base System at 250°F (10 points)									
Methane	19.8	4	2		2		2		
Ethane	13.8	2	5	1	2				
Propane	24.3	4	1				2	1	2
n-Pentane	18.4	2	4		1	1		2	
n-Hexane	19.9	4	2	2	1	1			
n-Decane	29.7	7	3						
Base System with Low CO_2 Addition at 150°F (7 points)									
Methane	25.2	3				1		1	2
Ethane	10.8		2	1		1	1	2	
Propane	13.1	1	2			1			
n-Pentane	40.4	2		1			1		3
n-Hexane	35.1	3		1					3
n-Decane	35.7	6		1					
Carbon Dioxide	13.4		3		1	1			2
Base System with Low CO_2 Addition at 250°F (10 points)									
Methane	40.9	3	1	1				1	4
Ethane	24.9	3	1				1	1	4
Propane	59.1	4		1			1		4
n-Pentane	47.6	4			1			1	4
n-Hexane	40.9		1		1				4
n-Decane	27.1	2	1	1	1			1	4
Carbon Dioxide	26.5	2	1				1	2	4
Base System with High CO_2 Addition at 150°F (8 points)									
Methane	26.3	3			1	1		1	2
Ethane	4.7	1			3	3	1		
Propane	14.3	3	3	1		1			
n-Pentane	35.8	2						2	4
n-Hexane	29.9	1	1				1	1	4

TABLE VIII (Continued)

Base System with High CO_2 Addition at 250°F (9 points)							
Methane	47.3	3	1				5
Ethane	23.0	1	1	1	1	1	4
Propane	60.6	3	1				5
n-Pentane	42.2	3		1			5
n-Hexane	33.3	3		1			5
n-Decane	45.4		1		1	3	4
Carbon Dioxide	17.2		1	1	2		5

TABLE IX

COMPARISON OF CORRELATION PREDICTIONS AND UNSMOOTHED EXPERIMENTAL K-VALUES FOR SYSTEMS CONTAINING NAPHTHENES AND AROMATICS

Component	Average Absolute % Dev.	Number of Points in the % Deviation Range of: Less Than -20	-20 to -10	-10 to -5	-5 to 0	0 to 5	5 to 10	10 to 20	More Than 20
Base System with High CO_2 Addition and 1-methylnaphthalene Substituted for n-Decane at 250°F (11 points)									
Methane	37.5	8			1	2			
Ethane	16.5	5	3		1	1	1		
Propane	34.4	7	1						3
n-Pentane	18.8	3	3	1				1	3
n-Hexane	14.6	2	4	1			1	3	
1-Methyln.	202.7								11
Carbon Dioxide	14.9	1	1		1	1	3	3	1
Base System with 1-methylnaphthalene Substituted for n-Decane at 150°F (13 points)									
Methane	41.4	8	1						
Ethane	13.0	3	3	3	1	1	2		
Propane	22.7	7	3		1	2			
n-Pentane	24.8	4	3			1		1	4
n-Hexane	22.7	8	1		1	1	2		
1-Methyln.	132.3	3					1	1	8
Base System with 1-methylnaphthalene Substituted for n-Decane at 250°F (15 points)									
Methane	35.3	10	1	1	1	1	1		
Ethane	16.8	5	9		1				
Propane	30.1	9	1				1		4
n-Pentane	22.1	6	1	1	1			2	4
n-Hexane	23.7	6	2	1		1	2	2	1
n-Methyln.	114.8								15
Base Systems with Decahydronaphthalene Substituted for n-Decane at 150°F (16 points)									
Methane	69.7	6			1				9
Ethane	45.4	1	1			1	3		10
Propane	46.7	2	2	2		1	1		8
n-Pentane	75.9	1			1		1	2	11
n-Hexane	54.2	2	1	1			1	3	8
Decahydon.	753.9	11	1						4

TABLE IX (Continued)

	Base System with Decahydronaphthalene Substituted for n-Decane at 250°F (12 points)							
Methane	47.8	5			1			6
Ethane	22.3	1		1	2	1	2	5
Propane	54.8	2			2	1	1	5
n-Pentane	64.4		2	1				9
n-Hexane	52.0	2	1				1	8
Decahydron.	122.1	7	3				1	1

TABLE X

RESULTS OF BUBBLE POINT CALCULATION
WITH THE CORRELATION

System	Total Number of Points	Number of Points Converged	Average Absolute % Deviation	Average % Deviation
Base at 150°F	11	10	18.3	-18.0
Base at 250°F	10	10	20.9	-17.6
Low CO_2 at 150°F	8	7	28.1	- 5.6
Low CO_2 at 250°F	10	10	41.0	+ 9.8
High CO_2 at 150°F	10	8	23.3	- 3.5
High CO_2 at 250°F	9	8	44.3	21.6
CO_2 + 1-methylnaphthalene at 250°F	13	9	30.6	24.0

this work. In the case of direct substitution the average absolute per cent deviations are comparable for the two correlations, sometimes one being better, sometimes the other for the base system. For the systems with CO_2 present the per cent deviations are more nearly like those for the base systems when this correlation is used than when the Chao-Seader correlation is used. This can be attributed to the use of the interaction parameters k_{ij} in the Scatchard-Hildebrand equation. From this comparison the present correlation does not seem to be much better or worse than the Chao-Seader equation.

A comparison of the tables showing results of the bubble point calculations shows the present correlation to be better than the Chao-Seader correlation. That can be attributed to the superiority of the BWR equation over the RK equation. It should be noted that the present correlation was developed for the same range of conditions as the Chao-Seader, and hence both correlations are being used equally beyond their intended range. In addition, the BWR equation does not predict two phases at 150°F for pressures of 3000 psia and above, whereas the RK does.

It can be concluded that the equations used in this work are more likely to yield good results than those used in the Chao-Seader correlation. The failure to obtain a markedly better correlation can be blamed on erratic prediction of vapor phase non-idealities by the BWR equation. Recommendations for improvement are presented in Chapter IX.

CHAPTER IX

CONCLUSIONS AND RECOMMENDATIONS

The sample traps used in the experimental work seem to work well. Considerable care had to exercised to obtain representative samples. It is believed that the lighter the system the better will the sample traps and the sampling system used in this work perform. The presence of decane caused considerable difficulties due to condensation.

The Porapak Q chromatographic analysis columns also seemed to perform well once the temperature programming schedule could be maintained constant. In this case the presence of decane necessitated backflushing which was generally undesirable due to peak spreading. The small sample size reduced the system disturbance but made the sample analysis less reliable, the reason being that the stream had to be split so CO_2 could be analyzed on the thermal conductivity detector.

The experimental data indicate that the presence of CO_2 in multicomponent systems in significant quantities affects the K-values of the hydrocarbons slightly, especially at high pressures because CO_2 lowers the apparent convergence pressure. At low and intermediate pressures the difference in the K-values is not as great, especially for the lighter hydrocarbons.

The K-value correlation obtained in this work is as good as or better than the Chao-Seader correlation. This is also true for the subcritical components for which no correlation other than the inclusion of the solubility parameter interaction parameters and Equation (8-5) were made. The only exception is propane above its critical temperature. Apparently the data used in the propane correlation did not agree well with the present data.

For future work it is recommended that the equipment be modified to a windowed cell with a movable piston. That would be particularly desirable, if components heavier than decane are used since then it is possible to obtain multiple phases. Metering pumps for accurate measurement of charge gas volumes would also be desirable.

For general K-value correlation work along the lines of this investigation, it is suggested that the following procedure be followed.

The BWR equation with generalized coefficients does not seem to predict vapor phase non-idealities with consistent accuracy. It has also been shown that[64] the mixing rules predict PVT behavior much more poorly for CO_2-hydrocarbon binaries than for all hydrocarbon binaries. Hence, the following work should be done on the BWR equation. New mixing rules should be developed for CO_2-hydrocarbon mixtures and the generalized coefficients should be adjusted to give vapor phase mixture densities of uniform even if not high, accuracy. Then the modified BWR equation should be used to

calculate phase equilibria in order to check the uniformity of prediction of vapor phase fugacity coefficients in mixtures.

The next step would be to select reliable experimental two and three component phase equilibrium data. For this purpose the modified BWR equation would be used in an appropriate thermodynamic consistency test. It is imperative that only good data be used.

The third and final step would be to follow the procedure used in this correlation.

The correlation recommendations outlined above represent an enormous amount of detailed work. It is necessary if a correlation significantly better than the Chao-Seader is desired. It is the belief of this author that there is enough material for at least two master's theses and one PhD thesis.

BIBLIOGRAPHY

1. Akers, W. W., J. F. Burns, and W. R. Fairchild, I&EC 46, 2531 (1954).

2. Akers, W. W., R. E. Kelley and T. G. Lipscomb, I&EC 46, 2535 (1954).

3. Aroyan, H. J. and D. L. Katz, I&EC 43, 185 (1931).

4. ASME Symposium, Inst. of Gas Tech. (Febr. 23-26, 1959).

5. Barner, H. E. and W. C. Schreiner, Hydrocarbon Processing 45, 161 (1966).

6. Benedict, M., G. B. Webb and L. C. Rubin, J. Chem. Phys. 8, 334 (1940).

7. _____, J. Chem. Phys. 10, 747 (1942).

8. _____, CEP 47, 419 (1951).

9. Cavett, R. H., presented at 27th Midyear Meeting of the API Division of Refining, San Francisco, Calif. (May, 1962).

10. Chao, K. C. and J. D. Seader, AIChEJ 7, 598 (1961).

11. Cheung, H. and E. H. Zander, CEP Symposium Series, 64, No. 88, (1968).

12. Chueh, P. L., N. K. Muirbrook and J. M. Prausnitz, AIChEJ 11, 1097 (1965).

13. Chueh, P. L. and J. M. Prausnitz, I&EC Fund 6, 492 (1967).

14. Condon, E. U. and H. Odishaw, Handbook of Physics, McGraw-Hill Book Co., New York (1958).

15. Davis, P. C., A. F. Bertuzzi, T. L. Gore and F. Kurata, AIME Trans. 201, 245 (1954).

16. Davis, P. C., N. Rodewald and F. Kurata, AIChEJ 8, 537 (1962).

17. Dodge, B. F. and A. K. Dunbar, JACS 49, 591 (1927).

18. Donelly, H. G. and D. L. Katz, I&EC 46, 511 (1954).

19. Edmister, W. C., Applied Hydrocarbon Thermodynamics, Gulf Publishing Co., Houston, (1961).

20. Edmister, W. C., C. L. Persyn and J. H. Erbar, Proceedings of 42nd NGPA Annual Convention, Houston (March, 1963).

21. Edmister, W. C., J. Vairogs and A. J. Klekers, AIChEJ 14, 479 (1968).

22. Erbar, J. H., C. L. Persyn and W. C. Edmister, Proceedings of 43rd NGPA Annual Convention, New Orleans (1964).

23. Evans, R. B. and D. Harris, JC&ED 1, 45 (1956).

24. Gore, T. L., P. C. Davis, and F. Kurata, AIME Trans. 195, 279 (1953).

25. Grayson, H. G. and C. W. Streed, Sixth World Petroleum Congress, Frankfort, Maine (June, 1963).

26. Hala, E., J. Pick, V. Fried and O. Vilim, Vapor-Liquid Equilibrium, Pergamon Press, New York (1958).

27. Hildebrand, J. H. and R. L. Scott, The Solubility of Non-Electrolytes, 3rd edition, Reinhold Publishing Co., New York (1960).

28. _____, Regular Solutions, Prentice-Hall, Englewood Cliffs, New Jersey (1962).

29. Hipkin, H., presented at Thermodynamics Conference, Oklahoma State University, Stillwater (1959).

30. Jacoby, R. H. and M. J. Rzasa, AIME Trans. 195, TP 3312 (1952).

31. _____, AIME Trans. 198, TP 3652 (1953).

32. Kellogg Company, "Liquid-Vapor Equilibria in Mixtures of Light Hydrocarbons," MWK Co., New York (1950).

33. Klekers, A. J., PhD Thesis, School of Chemical Engineering, Oklahoma State University, Stillwater (1969).

34. Lenoir, J. M., Hydrocarbon Processing 46, 191 (1967).

35. Lenoir, J. M. and C. R. Koppany, Hydrocarbon Processing 46, 249 (1967).

36. Lyckman, E. W., C. A. Eckert and J. M. Prausnitz, ChSci 20, 685 (1965).

37. Matschke, D. E. and G. Thodos, I&EC 7, 232 (1962).

38. NGSMA, Engineering Data Book, Tulsa, Okla. (1967).

39. O'Connell, J. P. and J. M. Prausnitz, I&EC Fund 3, 347 (1964).

40. Olds, R. H., H. H. Reamer, B. H. Sage, and W. N. Lacey, I&EC 41, 475 (1949).

41. Poettmann, F. H. and D. L. Katz, I&EC 37, 847 (1945).

42. _____, I&EC 38, 53 (1946).

43. Poettmann, F. H., AIME Trans. 192, 141 (1951).

44. Prausnitz, J. M., AIChEJ 6, 78 (1960).

45. _____, ChESci 18, 613 (1963).

46. Prausnitz, J. M., C. A. Eckert, R. V. Orye and J. P. O'Connell, Computer Calculations for Multicomponent Vapor-Liquid Equilibria, Prentice-Hall, Englewood Cliffs, N. J. (1967).

47. Price, A. R. and R. Kobayashi, JC&ED 5, 40 (1959).

48. Reamer, H. H., R. H. Olds, B. H. Sage and W. N. Lacey, I&EC 34, 1526 (1942).

49. _____, I&EC 36, 88 (1944).

50. _____, I&EC 37, 688 (1945).

51. Reamer, H. H., B. H. Sage and W. N. Lacey, I&EC 46, 534 (1950).

52. _____, I&EC 43, 2515 (1951).

53. Reamer, H. H. and B. H. Sage, I&EC 7, 161 (1962).

54. _____, JC&ED 8, 508 (1963).

55. Redlich, O. and J. N. S. Kwong, Chem. Revs. 44, 233 (1949).

56. Reid, R. C. and T. K. Sherwood, The Properties of Gases and Liquid, McGraw-Hill Co., New York (1967).

57. Roberts, L. R. and J. J. McKetta, AIChEJ 7, 173, (1961).

58. Robinson, C. S. and E. R. Gilliland, Elements of Fractional Distillation, 4th ed. McGraw-Hill Co., New York (1950).

59. Robinson, D. B. and A. C. Saxena, NGPA Proc., 58 (1966).

60. Rossini, F. D. et al., "Selected Values of Physical and Thermodynamic Properties of Hydrocarbons and Related Compounds," Carnegie Institute of Technology, Pittsburgh (1953).

61. Sage, B. H. and W. N. Lacey, AIME Trans. 136, 136 (1940).

62. _____, I&EC 32, 992 (1940).

63. Sage, B. H., H. H. Reamer, R. H. Olds and W. N. Lacey, I&EC 34, 1108 (1942).

64. Sass, A., B. F. Dodge and R. H. Bretton, JCED 12, 168 (1967).

65. Shim, J. and J. P. Kohn, JC&ED 7, 3 (1962).

66. Smith, L. R. and L. Yarborough, SPED 8, 87 (1968).

67. Standing, M. B. and D. L. Katz, AIME Trans. 155, 232 (1944).

68. Starling, K. E., SPEJ 6, 363 (1966).

69. Sterner, C. J., Adv. Cryo. Engr. 7, 106 (1961).

70. Stuckey, A. N., Jr., PhD Thesis, Oklahoma State University, Stillwater (1966).

71. Thompson, R. E., PhD Thesis, Oklahoma State University, Stillwater (1963).

72. Vagtborg, H. J., AIME Trans. 201, 31 (1954).

73. Van Ness, H. C., "Classical Thermodynamics of Non-Electrolyte Solutions," MacMillan Co., N.Y. (1964).

74. Wang, R. H., and J. J. McKetta, JC&ED 9, 30 (1964).

75. Weber, J. H., presented at Houston AIChE Meeting (1967).

76. Weinaug, C. F. and H. B. Bradley, AIME Trans. 192, 233 (1951).

77. Wilson, G. M., Adv. Cryo. Engr. 9, 168 (1964).

78. _____, J. Am. Chem. Soc. 86, 127 (1964).

79. _____, J. Am. Chem. Soc. 86, 133 (1964).

80. Wohl, K., Trans. Am. Inst. Chem. Engrs. 42, 215 (1946).

81. Yarborough, L. and J. L. Vogel, CEPSS 63, No. 81, 1 (1967).

APPENDIX A

CALIBRATION OF GAS COMPRESSOR

APPENDIX A

CALIBRATION OF GAS COMPRESSOR

The calibration of the pressure balance was described by Stuckey.[70] No additional calibration work on the pressure balance and measuring cylinders was deemed necessary, and hence the procedure will not be described here. The Heise pressure gage was calibrated by the manufacturer. The readings taken on the gage agreed well with those taken from the pressure balance.

The mercury piston gas compressor had to be recalibrated, however, for during long usage small mercury droplets might be lost in the oil stream, thus making the previous calibration erroneous. The calibration consists of getting the relationship between the mercury level indicator reading and the height of mercury in the gas compressor.

The procedure was the same as that used by Thompson[71] and therefore the details will not be repeated here. Briefly, pressure indicator readings and manometer readings were taken for a series of mercury heights in the compressor. From the manometer readings the height of mercury above the oil inlet to the measuring cylinder was determined. The data were used to obtain the following expression:

$$\Delta P = 1.47255 + 0.1141903\ h - 0.0002795422\ h^2 + 0.000001902440\ h^3$$

where h is the mercury level indicator reading and ΔP is the pressure correction in psia to be added to the pressure balance reading to account for the measuring cylinder outlet not being level with the equilibrium cell and gas compressor. This type of correction was not necessary for the Heise gage readings because it was connected on the cell side of the gas compressor.

APPENDIX B

CALIBRATION OF THERMOCOUPLES

APPENDIX B

CALIBRATION OF THERMOCOUPLES

Six iron-constantan thermocouples were calibrated against a Leeds and Northrup Model 8163 platinum resistance thermometer. The thermometer had been calibrated by the Bureau of Standards. The thermometer resistance was determined on a Leeds and Northrup Model 8069-B Mueller bridge. A Leeds and Northrup Model 2430 galvanometer was used with the Mueller bridge.

The thermocouple emf was measured with a Leeds and Northrup Model 8686 potentiometer. The reference junctions were inserted in an ice bath of distilled water. The emf of the thermocouples could be measured to $\pm$ 0.001 mv. Readings were taken at three temperatures in the vicinity of 150°F and three temperatures in the vicinity of 250°F. Four readings on each thermocouple at each temperature were taken and averaged.

It was found that thermocouples Nos. 1-5 responded in nearly the same manner, but thercouple No. 6 showed a consistently higher reading. Straight lines were fitted to the average mv readings. For thermocouples 1-5 near 150°F the equation is

$$T = 149.0 + 27.0\ (E - 3.390)$$

and near 250°F

$$T = 248.0 + 31.3\ (E - 6.388)$$

where T is temperature in °F and E is the potentiometer reading in millivolts. Thermocouple No. 6 was not used to measure temperature.

APPENDIX C

CALIBRATION OF CHROMATOGRAPH COLUMNS

APPENDIX C

CALIBRATION OF CHROMATOGRAPH COLUMNS

The phase compositions were analyzed on an F&M Model 810 chromatograph equipped with thermal conductivity and flame ionization detectors. The signal from the flame ionization detector was recorded on a Honeywell Model 16 recorder and from the thermal conductivity detector on a Honeywell Model 15 recorder. The reference and analytical columns were Porapak Q in 5/8" aluminum tubes. Eleven grams of the packing were put in each column. The columns were five feet long.

The calibration was performed as follows. Liquid mixtures of n-pentane, n-hexane and n-decane were prepared in four different composition ratios. These four mixtures were prepared by weighing each of the three components in a small bottle with a narrow neck. The components were introduced with a syringe in the order decane, hexane, and pentane to reduce vaporization losses of the lighter components. Then the vial was frozen into a block of ice and removed from the refrigerator only during sample withdrawal. An 0.8 μl sample was injected into the chromatograph for each run. The weight per cent and area per cent of each component are listed in Table C-I.

TABLE C-I

CHROMATOGRAPH CALIBRATION DATA

Compound	Reference Compound	Flame Ionization Weight Ratio	Flame Ionization Area Ratio	Thermal Conductivity Weight Ratio	Thermal Conductivity Area Ratio
C_2	C_1	7.4207	8.3244	7.4207	6.5321
		1.9016	2.2094	1.9016	1.6619
		1.2180	1.4734	1.2180	1.0893
		0.4816	0.5322	0.4816	0.3936
		0.3746	0.4293	0.3746	0.3069
CO_2	C_1			10.6948	5.8411
				4.1695	2.2724
				1.7594	0.9675
				0.6806	0.3776
C_3	C_1	4.1932	4.1040	4.1932	2.7472
		2.7628	2.8041	2.7628	1.8472
		1.8710	1.9549	1.8710	1.2875
		0.3170	0.3636	0.3170	0.2323
C_5	C_1	3.3234	5.4684		
		1.7429	3.0356		
		0.8413	1.5015		
		0.5032	0.9987		
C_6	C_5	1.5529	1.5721		
		2.2658	2.2426		
		1.1384	1.1437		
		0.5296	0.5374		
C_{10}	C_5	16.5517	19.1376		
		25.6004	26.6757		
		12.0697	12.6856		
		5.7338	6.3065		
C_{11}	C_5	4.9333	5.9936		
		15.1648	17.7055		
		18.3294	20.9428		
		15.3825	17.3325		
		10.0827	11.5531		

Binary mixtures of the other components with methane were prepared volumetrically. A schematic of the apparatus is shown in Figure 25. The apparatus was made of glass with spring loaded Teflon stopcocks. The glass tubing was connected with as short as possible pieces of polyethylene tubing. The measuring bomb was approximately 200 cc in volume. The procedure used was to evacuate the whole system, close off the vacuum pump and sample bomb. Then the whole system was filled with a gas, say propane, and allowed to come to thermal equilibrium. The mercury level in the measuring bomb was then raised to its mark, the pressure of the system read on the TI quartz Bourdon tube pressure gage and the measuring bomb isolated from the rest of the system. The stopcock connecting the sample and measuring bombs was opened and the gas forced into the sample bomb by raising the mercury level. The sample bomb was then sealed off and the mercury drained into its reservoir. Then the whole system was evacuated and the same process repeated with methane.

To ensure complete mixing of the gases the gas mixture was moved back and forth between the sample and measuring bombs by means of the mercury piston. This procedure was repeated three times in quick succession.

Since the constant temperature air bath was maintained at 100°F, extra care was used in preparing the methane-n-pentane mixtures. The vapor pressure of pentane is low at this temperature, and it was necessary to ensure that the

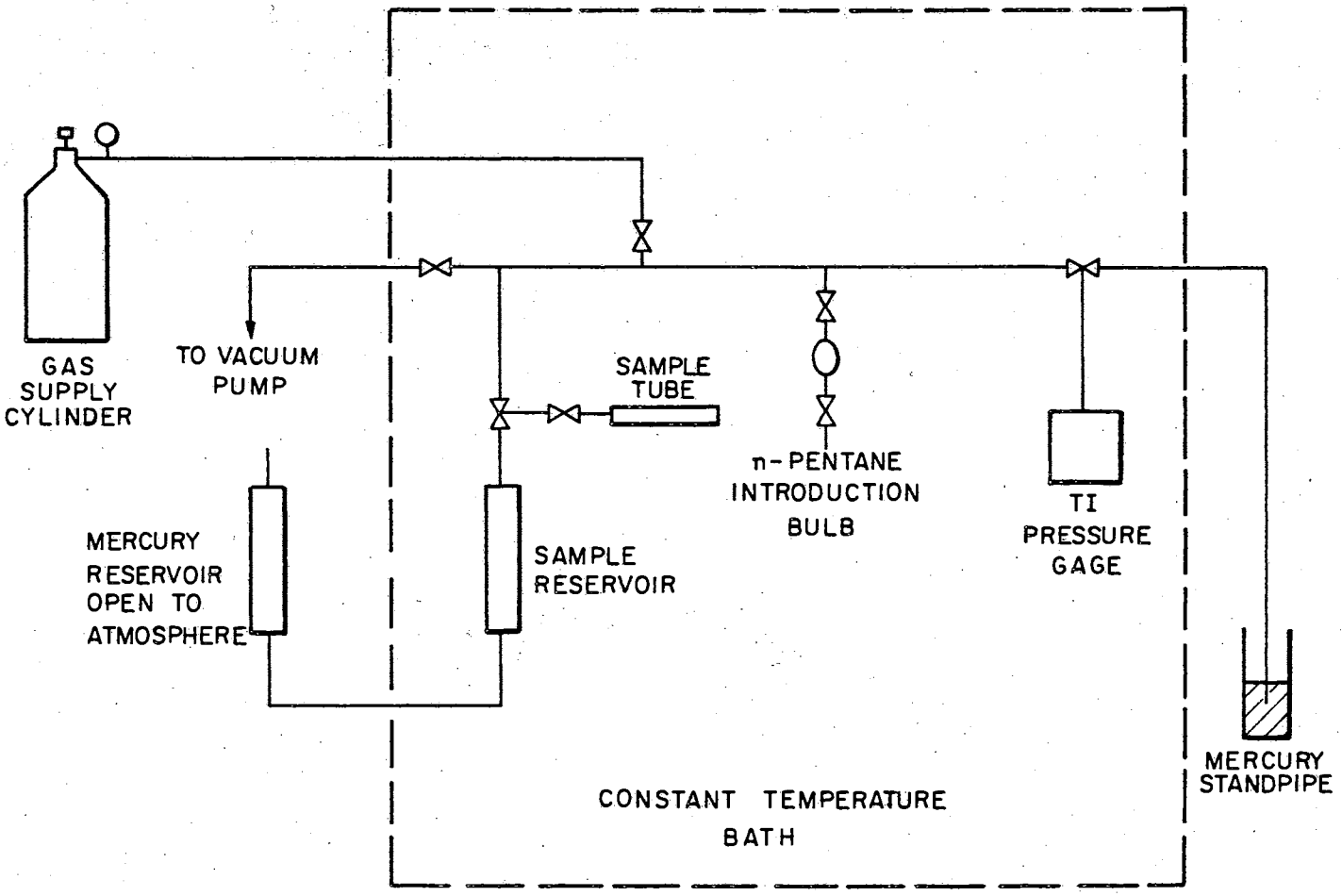

FIGURE 25

APPARATUS FOR PREPARATION OF
GASEOUS CALIBRATION SAMPLES

vapor pressure is never exceeded or condensation would occur.

Three to five mixtures of each binary were prepared and analyzed within eight hours. Before withdrawing a sample, the bomb and syringe were heated well above 100°F to vaporize any component that might have condensed. In the case of the methane-n-pentane mixture some air was always left in the syringe to provide a dilution volume and thus an additional safeguard against condensation. The weight and area percentages are reported in Table C-I.

The calibration results were fitted with the equation

$$R_{ij} = S_{ij}A_{ij}$$

where R is the weight ratio and A is the area ratio for a component. The reference substance was methane for all gaseous samples and n-pentane for all liquid samples. The values of the coefficients are presented in Table C-II.

TABLE C-11

CHROMATOGRAPH CALIBRATION CONSTANTS

Compound	Reference Compound	Slopes (S_{ij} in equation on p. 113) Flame Ionization	Slopes Thermal Conductivity
C_2	C_1	0.8877	1.1365
C_3	C_1	1.0024	1.5716
C_5	C_1	0.5942	
C_6	C_5	1.0013	
C_{10}	C_5	0.9299	
CO_2	C_1		1.8310
C_{11}	C_5	0.8716	

APPENDIX D

EXPERIMENTAL DATA

TABLE D-I

EXPERIMENTAL xy DATA FOR BASE SYSTEM AT 150°F

P, psia		C_1	C_2	C_3	C_5	C_6	C_{10}
100	y	.8712	.0216	.0062	.0701	.0269	.0040
	x	.0226	.0025	.0019	.2023	.2004	.5703
	K	38.6	8.54	3.32	.347	.134	.0069
200	y	.9099	.0263	.0073	.0379	.0162	.0024
	x	.0460	.0054	.0046	.1466	.1713	.6261
	K	19.8	4.86	1.61	.258	.0944	.0037
400	y	.8602	.0617	.0449	.0211	.0103	.0018
	x	.0852	.0228	.0453	.1344	.1486	.5636
	K	10.1	2.70	.991	.157	.0691	.0032
500	y	.9203	.0340	.0115	.0222	.0103	.0018
	x	.1202	.0172	.0130	.1410	.1629	.5457
	K	7.65	1.98	.885	.157	.0630	.0033
1000	y	.9370	.0330	.0081	.0120	.0066	.0033
	x	.2612	.0266	.0152	.1089	.1253	.4628
	K	3.59	1.24	.532	.110	.0528	.0071
1250	y	.9374	.0300	.0099	.0130	.0068	.0029
	x	.3260	.0313	.0226	.1156	.1194	.3851
	K	2.88	.960	.440	.112	.0568	.0076
1500	y	.9275	.0370	.0145	.0119	.0069	.0022
	x	.3513	.0409	.0324	.0979	.1049	.3725
	K	2.64	.904	.447	.122	.0660	.0057
2000	y	.9202	.0413	.0156	.0120	.0071	.0038
	x	.4903	.0474	.0340	.0824	.0859	.2599
	K	1.88	.871	.459	.145	.0829	.0146
2500	y	.8954	.0447	.0201	.0149	.0124	.0124
	x	.5365	.0513	.0366	.0659	.0713	.2384
	K	1.67	.873	.550	.226	.174	.0520
3000	y	.8585	.0414	.0183	.0179	.0172	.0466
	x	.5753	.0409	.0272	.0509	.0616	.2441
	K	1.49	1.01	.672	.352	.279	.191
3999		One Phase					

TABLE D-II

EXPERIMENTAL xy DATA FOR BASE SYSTEM AT 250°F

P, psia		C_1	C_2	C_3	C_5	C_8	C_{10}
100	y	.5986	.0231	.0090	.2103	.1207	.0382
	x	.0177	.0016	.0014	.1694	.1785	.6314
	K	33.9	14.1	6.31	1.24	.676	.0605
200	y	.7736	.0268	.0106	.1092	.0579	.0219
	x	.0461	.0044	.0039	.1643	.1682	.6130
	K	16.8	6.08	2.70	.665	.344	.0357
300	y	.8019	.0360	.0140	.0861	.0487	.0133
	x	.0644	.0077	.0063	.1574	.1745	.5897
	K	12.4	4.67	2.23	.547	.279	.0224
500	y	.8416	.0345	.0142	.0640	.0356	.0100
	x	.1130	.0107	.0089	.1415	.1536	.5722
	K	7.45	3.24	1.59	.452	.232	.0175
702	y	.8612	.0383	.0139	.0486	.0288	.0092
	x	.1476	.0161	.0129	.1425	.1583	.5226
	K	5.84	2.38	1.08	.341	.182	.0176
1000	y	.8797	.0383	.0165	.0337	.0211	.0105
	x	.2157	.0232	.0180	.1265	.1428	.4737
	K	4.08	1.65	.919	.266	.148	.0222
1500	y	.8691	.0386	.0166	.0337	.0229	.0192
	x	.3212	.0294	.0205	.1109	.1207	.3975
	K	2.71	1.31	.809	.304	.190	.0482
2000	y	.8510	.0415	.0192	.0363	.0261	.0259
	x	.4122	.0342	.0235	.0947	.0993	.3362
	K	2.06	1.21	.818	.383	.263	.0769
2500	y	.8195	.0409	.0195	.0339	.0288	.0575
	x	.4879	.0349	.0236	.0780	.0818	.2938
	K	1.68	1.17	.825	.435	.352	.196
3001		One Phase					

TABLE D-III

EXPERIMENTAL xy DATA FOR BASE SYSTEM
WITH LOW CO_2 ADDITION AT 150°F

P, psia		C_1	CO_2	C_2	C_3	C_5	C_6	C_{10}
200	y	.8253	.1170	.0243	.0053	.0175	.0076	.0030
	x	.0542	.0162	.0055	.0037	.1513	.1530	.6161
	K	15.2	7.21	4.43	1.44	.116	.0496	.0048
300	y	.8307	.0905	.0399	.0127	.0168	.0070	.0024
	x	.0901	.0178	.0160	.0126	.1449	.1461	.5726
	K	9.22	5.09	2.49	1.00	.116	.0478	.0042
500	y	.8370	.0911	.0397	.0132	.0122	.0051	.0018
	x	.1370	.0257	.0209	.0161	.1340	.1352	.5311
	K	6.11	3.54	1.89	.817	.0913	.0379	.0033
1000	y	.8046	.1318	.0367	.0101	.0100	.0053	.0015
	x	.2784	.0793	.0365	.0235	.1092	.1149	.3583
	K	2.89	1.66	1.01	.431	.0912	.0462	.0042
1500	y	.8402	.0848	.0469	.0110	.0094	.0057	.0021
	x	.3535	.0570	.0448	.0308	.0836	.0862	.3441
	K	2.38	1.49	1.05	.355	.113	.0658	.0060
2000	y	.8201	.0921	.0504	.0197	.0079	.0052	.0046
	x	.4996	.0808	.0654	.0457	.0485	.0513	.2088
	K	1.64	1.14	.770	.431	.163	.102	.0220
2500	y	.8113	.0948	.0513	.0219	.0083	.0063	.0061
	x	.5609	.0808	.0591	.0395	.0404	.0430	.1763
	K	1.45	1.17	.868	.554	.206	.146	.0346
3001		One Phase						

TABLE D-IV

EXPERIMENTAL xy DATA FOR BASE SYSTEM
WITH LOW CO_2 ADDITION AT 250°F

P, psia		C_1	CO_2	C_2	C_3	C_5	C_6	C_{10}
150	y	.7255	.0764	.0300	.0077	.0876	.0475	.0253
	x	.0521	.0083	.0057	.0032	.1527	.1577	.6203
	K	13.9	9.18	5.27	2.44	.573	.301	.0407
200	y	.7705	.0838	.0335	.0098	.0607	.0323	.0095
	x	.0722	.0104	.0073	.0054	.1442	.1522	.6082
	K	10.7	8.06	4.58	1.82	.421	.212	.0155
300	y	.7937	.0777	.0347	.0106	.0484	.0257	.0091
	x	.1053	.0142	.0126	.0083	.1385	.1456	.5756
	K	7.54	5.49	2.76	1.29	.349	.177	.0158
500	y	.8129	.0923	.0365	.0104	.0265	.0162	.0053
	x	.1667	.0260	.0162	.0097	.1256	.1360	.5198
	K	4.87	3.55	2.25	1.07	.211	.119	.0101
1000	y	.8228	.0870	.0413	.0137	.0178	.0116	.0058
	x	.3059	.0504	.0350	.0215	.0918	.0983	.3972
	K	2.69	1.73	1.18	.640	.194	.118	.0146
1500	y	.8186	.0887	.0449	.0162	.0152	.0098	.0066
	x	.4016	.0625	.0443	.0276	.0726	.0765	.3150
	K	2.04	1.42	1.01	.587	.209	.128	.0210
2000	y	.8182	.0758	.0427	.0185	.0160	.0123	.0165
	x	.5048	.0625	.0362	.0249	.0441	.0446	.2828
	K	1.62	1.21	1.18	.744	.362	.275	.0584
2500	y	.8031	.0863	.0441	.0201	.0156	.0123	.0185
	x	.6769	.0772	.0434	.0202	.0266	.0270	.1287
	K	1.19	1.12	1.02	.992	.586	.455	.144
2990	y	.7885	.0934	.0489	.0213	.0142	.0118	.0219
	x	.7443	.0828	.0451	.0212	.0222	.0196	.0648
	K	1.06	1.13	1.08	1.00	.640	.605	.338
3500		One Phase						

TABLE D-V

EXPERIMENTAL xy DATA FOR BASE SYSTEM
WITH HIGH CO_2 ADDITION AT 150°F

P, psia		C_1	CO_2	C_2	C_3	C_5	C_6	C_{10}
100	y	.6931	.1917	.0208	.0105	.0573	.0202	.0063
	x	.0186	.0092	.0022	.0029	.2137	.2027	.5507
	K	37.3	20.8	9.64	3.59	.268	.0994	.0114
200	y	.7315	.1979	.0236	.0089	.0219	.0100	.0062
	x	.0589	.0325	.0064	.0060	.1595	.1786	.5582
	K	12.4	6.08	3.69	1.49	.137	.0561	.0111
300	y	.7354	.1911	.0263	.0120	.0241	.0092	.0019
	x	.0844	.0422	.0094	.0104	.1792	.1797	.4946
	K	8.71	4.53	2.80	1.15	.135	.0512	.0039
500	y	.7203	.2153	.0298	.0129	.0140	.0066	.0011
	x	.1199	.0650	.0155	.0163	.1561	.1615	.4657
	K	6.01	3.31	1.91	.790	.0896	.0410	.0023
1000	y	.7213	.2145	.0321	.0151	.0098	.0049	.0022
	x	.2537	.1215	.0293	.0322	.1114	.1181	.3340
	K	2.84	1.77	1.10	.470	.0883	.0418	.0066
1500	y	.7126	.2227	.0328	.0172	.0083	.0049	.0016
	x	.3268	.1556	.0371	.0390	.0864	.0899	.2652
	K	2.18	1.43	.885	.442	.0961	.0542	.0058
2000	y	.7189	.2041	.0339	.0201	.0106	.0064	.0060
	x	.4045	.1674	.0423	.0398	.0565	.0574	.2321
	K	1.78	1.22	.801	.505	.188	.112	.0258
2500	y	.6797	.2175	.0388	.0255	.0136	.0118	.0132
	x	.4600	.1880	.0500	.0478	.0458	.0495	.1589
	K	1.48	1.16	.776	.533	.298	.239	.0827
2999	y	.6690	.2165	.0414	.0295	.0144	.0128	.0163
	x	.5466	.2054	.0449	.0389	.0328	.0332	.0982
	K	1.22	1.05	.922	.760	.439	.386	.166
3499		One Phase						

TABLE D-VI

EXPERIMENTAL xy DATA FOR BASE SYSTEM
WITH HIGH CO_2 ADDITION AT 250°F

P, psia		C_1	CO_2	C_2	C_3	C_5	C_6	C_{10}
150	y	.5874	.2163	.0299	.0154	.0873	.0479	.0158
	x	.0479	.0237	.0060	.0071	.1702	.1665	.5787
	K	12.3	9.13	5.02	2.16	.513	.288	.0272
200	y	.6344	.2025	.0295	.0160	.0672	.0362	.0141
	x	.0615	.0304	.0072	.0083	.1591	.1657	.5678
	K	10.3	6.67	4.09	1.92	.423	.219	.0248
300	y	.6791	.1967	.0288	.0157	.0478	.0257	.0062
	x	.0916	.0431	.0107	.0131	.1504	.1535	.5376
	K	7.41	4.56	2.68	1.20	.318	.168	.0115
500	y	.6882	.2142	.0304	.0154	.0302	.0168	.0048
	x	.1471	.0683	.0161	.0167	.1305	.1367	.4846
	K	4.68	3.13	1.89	.922	.232	.123	.0099
700	y	.6939	.2138	.0326	.0163	.0243	.0141	.0051
	x	.1869	.0974	.0198	.0190	.1187	.1239	.4344
	K	3.71	2.20	1.64	.857	.204	.114	.0116
1500	y	.6862	.2237	.0332	.0202	.0190	.0118	.0059
	x	.3444	.1445	.0314	.0321	.0884	.0883	.2710
	K	1.99	1.55	1.06	.628	.215	.134	.0219
2000	y	.6781	.2130	.0337	.0218	.0218	.0154	.0161
	x	.4018	.1644	.0353	.0335	.0721	.0715	.2214
	K	1.69	1.30	.955	.651	.303	.215	.0729
2500	y	.6802	.2008	.0358	.0238	.0228	.0173	.0193
	x	.4623	.1807	.0373	.0333	.0559	.0555	.1749
	K	1.47	1.11	.958	.713	.408	.312	.110
3000		One Phase						

TABLE D-VII

EXPERIMENTAL xy DATA FOR BASE SYSTEM WITH CO_2 ADDITION AND 1-METHYLNAPHTHALENE SUBSTITUTED FOR N-DECANE AT 250°F

P, psia		C_1	CO_2	C_2	C_3	C_5	C_6	C_{11}
100	y	.5052	.1365	.0157	.0070	.2193	.1084	.0079
	x	.0129	.0099	.0015	.0014	.1731	.1720	.6293
	K	39.2	13.8	10.3	5.06	1.27	.630	.0125
300	y	.6714	.1709	.0232	.0131	.0763	.0405	.0046
	x	.0546	.0285	.0057	.0060	.1571	.1602	.5879
	K	12.3	6.00	4.09	2.20	.485	.253	.00774
500	y	.7026	.1873	.0242	.0133	.0461	.0246	.0018
	x	.0957	.0530	.0097	.0102	.1481	.1527	.5306
	K	7.34	3.53	2.49	1.31	.311	.161	.00344
1000	y	.6897	.2141	.0327	.0165	.0292	.0166	.0013
	x	.1566	.0816	.0178	.0179	.1199	.1234	.4828
	K	4.40	2.62	1.84	.922	.243	.134	.00276
1500	y	.7050	.1972	.0322	.0203	.0279	.0158	.0014
	x	.2287	.1101	.0237	.0236	.0992	.1048	.4098
	K	3.08	1.79	1.35	.863	.282	.151	.00352
2000	y	.7127	.1953	.0312	.0199	.0233	.0155	.0020
	x	.2521	.1184	.0262	.0258	.0828	.0863	.4083
	K	2.83	1.65	1.19	.772	.283	.179	.00496
2500	y	.6828	.2142	.0364	.0231	.0234	.0167	.0035
	x	.3103	.1482	.0300	.0296	.0780	.0828	.3211
	K	2.20	1.45	1.21	.780	.300	.201	.0108
2999.3	y	.6746	.2084	.0366	.0257	.0258	.0199	.0090
	x	.3573	.1617	.0330	.0316	.0653	.0694	.2818
	K	1.89	1.29	1.11	.815	.395	.286	.0320
3999.5	y	.6533	.2165	.0385	.0273	.0239	.0200	.0204
	x	.3959	.1755	.0347	.0333	.0505	.0537	.2565
	K	1.65	1.23	1.11	.820	.475	.373	.0795
4998.8	y	.6330	.2262	.0390	.0305	.0248	.0223	.0241
	x	.4351	.1909	.0368	.0336	.0411	.0440	.2184
	K	1.46	1.18	1.06	.909	.604	.507	.110
5998.6	y	.6254	.2220	.0418	.0326	.0256	.0240	.0286
	x	.4920	.1971	.0389	.0349	.0347	.0354	.1671
	K	1.27	1.13	1.07	.936	.740	.676	.171
6996.6		One Phase						

APPENDIX E

SAMPLE CALCULATION OF EXPERIMENTAL DATA

APPENDIX E

SAMPLE CALCULATION OF EXPERIMENTAL DATA

A sample calculation of P-T-x-y data from the experimental measurements is presented in this appendix. The actual calculations were made with a digital computer. The data used in the sample calculations below are those from the base system at 250°F and 2990 psia. All constants and conversion factors were taken from the API Project 44 compilations.[60]

Temperature

The temperature in the equilibrium cell was determined from the potentiometer reading for the iron-constantan thermocouple located in the wall of the equilibrium cell. The calibration for the thermocouples appears in Appendix B. In the 250°F range the calibration equation for this thermocouple is as follows:

$$T = 248.0 + 31.3\ (E - 6.388)$$

where E is the potentiometer reading in millivolts. The emf reading at the start of sampling was 6.454 mv and at the end of sampling 6.465 mv. Hence the average reading was 6.459 mv which corresponds to a temperature of 250.2°F.

Pressure

The pressure in the equilibrium cell was determined from the pressure balance pressure corrected for the hydrostatic head of oil and mercury. The pressure at the balance was corrected for the buoyancy of air, thermal expansion of the measuring cylinder and the hydrostatic head of oil acting against the pressure balance guide pin. The barometric pressure was added to this pressure to obtain the absolute pressure.

The pressure at the pressure balance outlet is represented by the following equation:

$$P_{bal} = \frac{Mg}{Ag_c} + P_{bar} - P_{oil}$$

where P_{bal} is pressure at the pressure balance outlet, g is local acceleration of gravity, g_c is the conversion factor 980.665, M is mass of all rotating parts corrected for buoyancy, A is effective area of piston corrected for thermal expansion, P_{bar} is barometric pressure and P_{oil} is pressure correction due to head of oil on guide pin.

The local acceleration due to gravity was calculated from the following equation:[14]

$$g = 978.0524\left[1 + 0.005297 \sin^2 x - 0.0000059 \sin^2 2x + 0.0000276 \cos^2 + \cos 2(\lambda + 25^\circ)\right] - 0.000060\ h$$

where x is latitude, λ is longitude (positive east of Greenwich) and h is feet above sea level. At Stillwater $x = 36^\circ$ 7' N, $\lambda = 97^\circ$ 4' W and h = 930 ft. Substituting these data

in the above equation gives $g = 979.777$ cm/sec^2 from which $g/g_c = 0.999094\ Kg_f/Kg_m$.

A Texas Instruments Model 141A servo-nulling precision pressure gage was used for determining barometric pressure. Two readings were necessary: the counter reading and the temperature of the instrument. The instrument has been calibrated over the entire range by Texas Instruments. The calibration data were fitted to the equation

$$P = 0.019336842 \left[1 + 1.3\ 10^{-4} \left(\frac{T - 32.0}{1.8} - 24.0\right)\right] \left[0.03167 + 9.9358826\ R - 0.8743147\ 10^{-3} R^2 - 0.16175319\ 10^{-5}\ R^3\right]$$

where P is pressure in psia, R is scale reading and T is temperature at gage in $^{\circ}F$. Substitution of the data yielded a barometric pressure of 741.0 mm Hg or 0.9750 atm.

The 300-600 Kg/cm^2 piston with weights No. 1, 2, 12, 13, 14 and 15 plus 235 grams in the weight pan were used to determine the pressure. The total weight uncorrected for buoyancy is summed below.

Base weight		33.2816 Kg_m
Piston, etc.		0.5598
Weight No.	1	25.0131
	2	25.0120
	12	0.9974
	13	1.0036
	14	1.0042
	15	1.0046
Extra weights		0.235
Total weight		88.1113 Kg_m

Let V = the volume of a steel weight of in vacuo mass M_o

d = density of steel = 7.8 gm/cm^2

ρ_1 = density of air at temperature T_1 and pressure P_1

ρ_2 = density of air at 20°C and 1 atmosphere

M = effective mass of M_o in air at T_1 and P_1

M' = effective mass of M_o in air at 20°C and 1 atm.

$$M = V(d - \rho_1) = M_o \left[1 - (\rho_1/d)\right]$$

$$M = v(d - \rho_2) = M_o \left[1 - (\rho_2/d)\right]$$

Combining M and M' gives

$$M \cong M' \left(1 + \frac{\rho_2 - \rho_1}{d}\right)$$

If the ideal gas law is used to evaluate the air density then

$$M \cong M' \left[1 + 0.000155 \left(1 - (293\ P_1/T_1)\right)\right]$$

With T = 297.2°K and P_1 = 0.9750 atm the corrected mass becomes M = 88.1113 (1.0000059) = 88.1118 Kg.

The linear expansion coefficient of the steel in the measuring cylinder is 11 x 10^{-6} $^oC^{-1}$. The area expansion coefficient is twice the linear coefficient.

$$A = A' \left[1 + 0.000022 \ (T_1 - 293)\right]$$

where A' is the effective piston area at 20°C and A is the effective piston area at T_1. The area of the piston is 0.41938 cm^2. Then

$$A = 0.41938 \ (1 + 0.000088) = 0.41942 \ cm^2$$

The height of the oil above the bottom of the guide pin on the pressure balance is equal to the height of the oil in the guide pin reservoir plus 1.6 cm. The force transmitted to the rotating shaft is

$$F_{oil} = h\ \rho_o A_{gp} (g/g_c)$$

where h_o is reservoir oil reading + 1.6 cm, ρ_o is density

of balance oil, i.e., 0.876 gm/cm^3, A_{gp} is cross-sectional area of the guide pin, i.e., 1.76 cm^2. The pressure correction due to the oil level is, then,

$$P_{oil} = F_{oil}/A = h_o \rho_o \frac{A_{gp}}{A} \frac{g}{g_c}$$

where A is the corrected piston area. Since the oil level reading was 24.3, then h_o = 25.9 and

$$P_{oil} = 25.9 \times 0.876 \times \frac{1.76}{1000. \times 0.41942} \times 0.99909$$

$$= 0.09512 \text{ Kg/cm}^2$$

Combining the above corrections the balance pressure is

$$P_{bal} = \frac{Mg}{Ag_c} - P_{bar} - P_{oil} = \frac{88.1118}{0.41942} \times 0.99909$$

$$+ \frac{74.1 \times 13.5237 \times 0.99909}{1000.} - 0.09512 = 209.8889$$

$$+ 1.0012 - 0.09512 = 210.7950 \text{ Kgf/cm}^2$$

$$= 2998.2215 \text{ psia}$$

The correction for oil and mercury heads in the gas compressor was presented in Appendix A. The equation for this correction is

$$P_{gc} = 1.472555 + 0.1141903\ h - 0.0002795422\ h^2 + 0.00000190244\ h^3$$

where h is the gas compressor level indicator reading. With h = 70.3, P_{gc} = 8.1 psia and P = 2990.1 psia.

Composition

The composition analyses were obtained in the following manner. The peak area was multiplied by the corresponding

attenuation for each component. Then the area ratios were obtained from the products. This was done for both the flame ionization and the early part of the thermal conductivity results. The results below are for the vapor phase:

Flame Ionization

	Peak Area		Attenuation		Area	Area Ratio
C_1	963	x	256	=	246272	7.315
C_2	2016	x	16	=	32256	0.958
C_3	1140	x	16	=	18240	0.542
C_5	1052	x	32	=	33664	1.000
C_6	2089	x	16	=	33424	0.993
C_{10}	6863	x	16	=	109808	3.262

Thermal Conductivity

C_1	1137	x	256	=	291072	1.000
CO_2	1615	x	32	=	51680	0.177

The weight ratio of each component is obtained as follows. Letting W represent weight ratio, A area ratio and S the slopes from Appendix C with the subscripts referring to the components, one gets

$$W_{15} = A_{15}/S_{51}$$

$$W_{25} = A_{25}S_{21}/S_{51}$$

$$W_{35} = A_{35}S_{31}/S_{51}$$

$$W_{55} = 1$$

$$W_{65} = A_{65}S_{65}$$

$$W_{105} = A_{105}S_{105}$$

$$W_{C025} = A_{C021}S_{C021}W_{15}$$

Division of the weight ratio for each component by the corresponding molecular weight gives the number of moles of each component. Normalization yields mole fractions. The calculations are summarized below:

	Weight Ratio	Moles	Mole Fraction
C_1	12.3107	0.7675	0.792
C_2	1.4312	0.0475	0.049
C_3	0.9143	0.0207	0.021
C_5	1.0000	0.0139	0.014
C_6	0.9943	0.0115	0.012
C_{10}	3.0333	0.2130	0.022
CO_2	3.9899	0.0906	0.093

APPENDIX F

MAXIMUM COMPOSITION ERRORS

APPENDIX F

MAXIMUM COMPOSITION ERRORS

The maximum expected errors in K-values due to chromatographic composition analysis were computed in similar manner to the computation of the K-values described in Appendix E. The only difference was that for each area of each component in each phase a maximum error in the area was added to it and also subtracted. Similarly a maximum error in the calibration slope was added and subtracted from the slopes. Then using the minimum expected areas and slopes for the vapor sample a minimum vapor composition was computed. Using the maximum corresponding values a maximum liquid composition was computed to give a minimum K-value. The opposite procedure was followed to obtain a maximum K-value. The area and slope changes are summarized in Table F-I.

TABLE F-I

AREA AND SLOPE DEVIATIONS

Component	Area Dev.	Slope Dev.	
C_1	5	.10	Flame Ionization
C_2	10	.01	Flame Ionization
C_3	10	.01	Flame Ionization
C_5	15	.00	Flame Ionization
C_6	15	.01	Flame Ionization
C_{10}	150	.01	Flame Ionization
C_1	10	.01	Thermal Cond.
CO_2	15	.01	Thermal Cond.

APPENDIX G

NOMENCLATURE

APPENDIX G

NOMENCLATURE

A - area in Appendix E

  - constant in Benedict, et al. equation/BWR/

a - constant in the BWR

B - constant in the BWR

b - constant in the BWR

C - constant in the BWR

c - constant in the BWR

d - density

E - potentiometer reading

F - force

f - fugacity

g - acceleration due to gravity

h - gas compressor level reading

  - oil reservoir level reading in Appendix E

  - elevation above sea level in Appendix E

K - vapor-liquid equilibrium phase distribution ratio

M - mass

P - pressure

R - gas constant

R - pressure gage reading in Appendix E

S - slope in chromatograph calibration

T - temperature

V - volume

W - weight ratio

x - liquid mole fraction

- latitude in Appendix E

y - vapor mole fraction

Greek Symbols

α - constant in the BWR

γ - constant in the BWR

- liquid activity coefficient

ϕ - vapor fugacity coefficient

λ - longitude in Appendix E

ω - acentric factor

Subscripts

c - critical property

i - component i

j - component j

r - reduced property

1 - methane

2 - ethane

3 - propane

5 - n-pentane

6 - n-hexane

10 - n-decane

11 - decahydronaphthalene

Superscripts

L - liquid phase

V - vapor phase

o - simple fluid property

1 - correction to simple fluid property

- - superbar, partial molar quantity

Abbreviations

exp - exponential

ln - logarithm to the base e

BWR - Benedict-Webb-Rubin equation

APPENDIX H

APPENDIX H

EXPERIMENTAL DATA COMPARISONS

In the body of the thesis the expected experimental error was discussed. The data were also compared against results from established K-value correlations. In this appendix the data are compared against previously published data.

At first data were taken on the methane-n-pentane binary system. The purpose for this was to get a check on the accuracy and reproducibility of the results. Many such runs were required before the equipment was developed to the point where acceptable data were obtained. The results of the last six runs made on the binary system are shown in Table H-I. They are not good at the low pressure but at 1350 psia the deviation from the mean is less than the expected $\pm$ 6% and the mean values are within 4% of the Sage and Lacey[63] values.

Yarborough and Vogel[81] published results on a system very similar to the base system. Their data were taken at 200°F. The results from the base system can be compared against their results on a ln K versus T plot. Such plots at three different pressures are shown as Figures 26, 27 and 28. The data lie very nearly on straight lines or have

TABLE H-I

BINARY DATA

Run No.	T °F	P psia	y C_1	y C_5	x C_1	x C_5	K C_1	K C_5
BR42	160	605	.893	.107	.200	.800	4.47	.134
BR43	160	605	.873	.127	.187	.813	4.66	.156
						Average	4.57	.145
						From Reference 63	5.25	.1454
BR44	160	1350	.886	.114	.355	.645	2.50	.177
BR45	160	1350	.888	.112	.379	.621	2.34	.180
BR46	160	1350	.894	.106	.393	.607	2.28	.175
BR47	160	1350	.888	.112	*	*	-	-
						Average	2.37	.177
						From Reference 63	2.45	.1715

*Sample lost due to leaking sample trap.

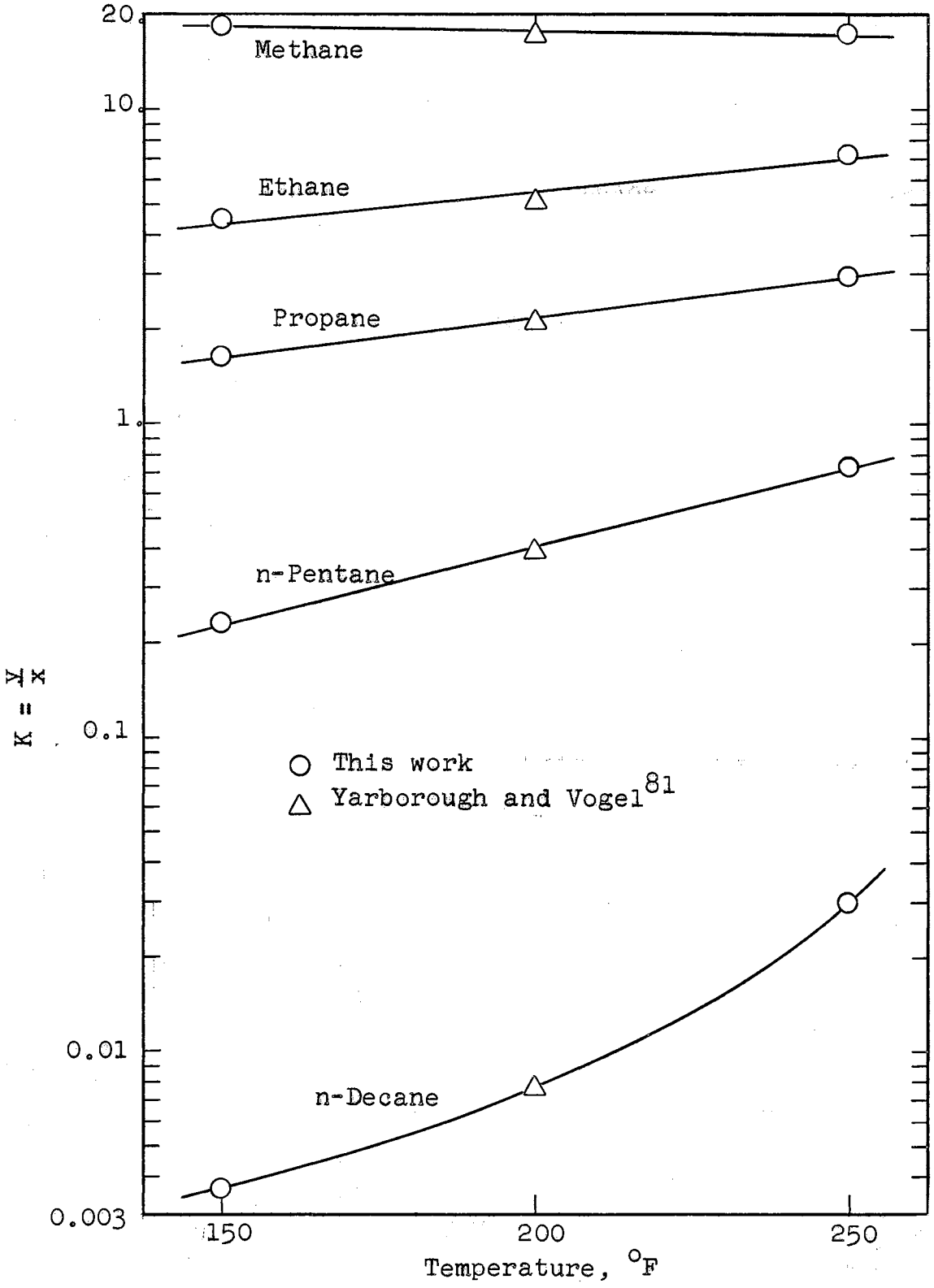

FIGURE 26

K-VALUE COMPARISON AT 200 PSIA - BASE SYSTEM

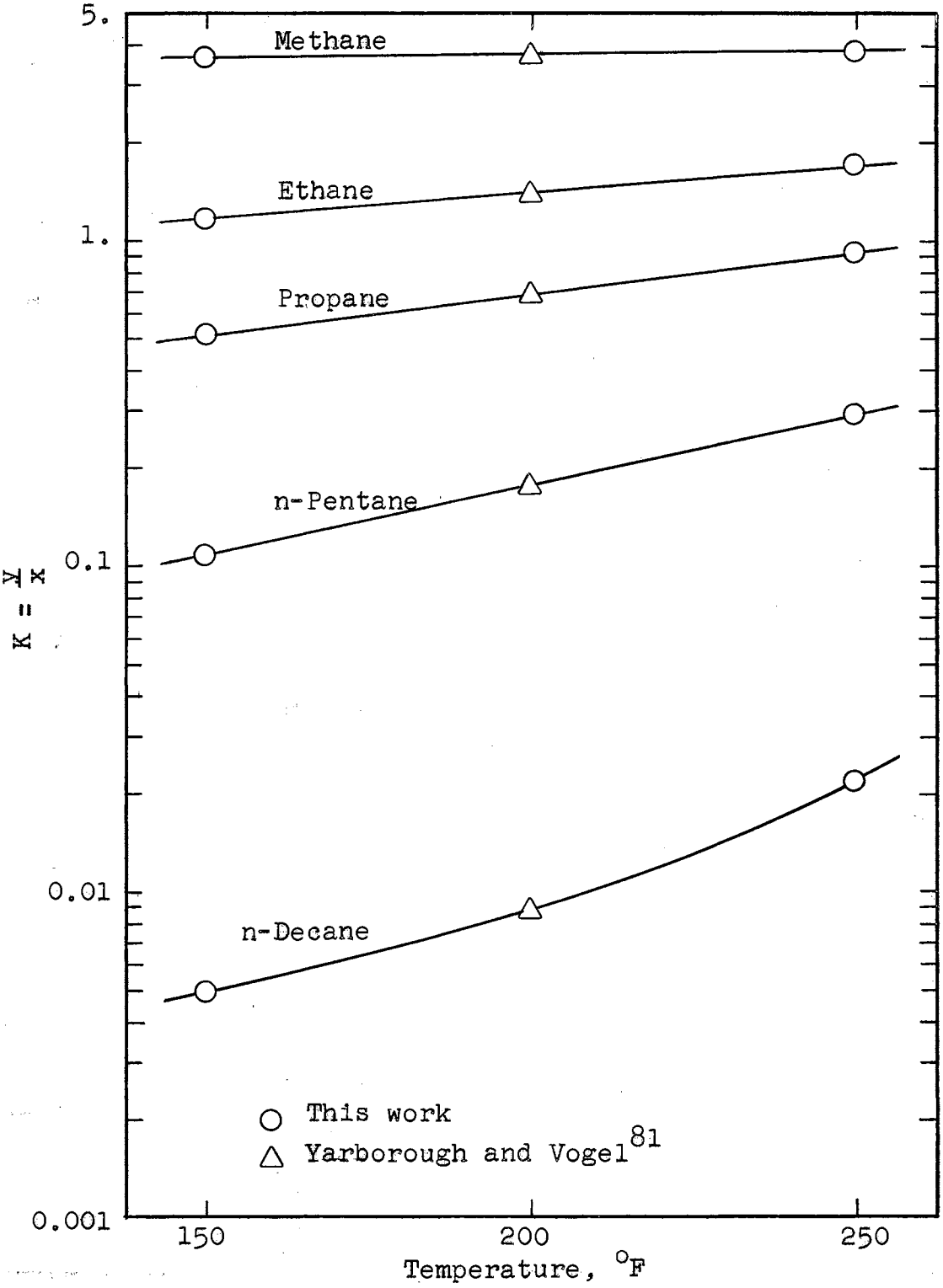

FIGURE 27

K-VALUE COMPARISON AT 1000 PSIA - BASE SYSTEM

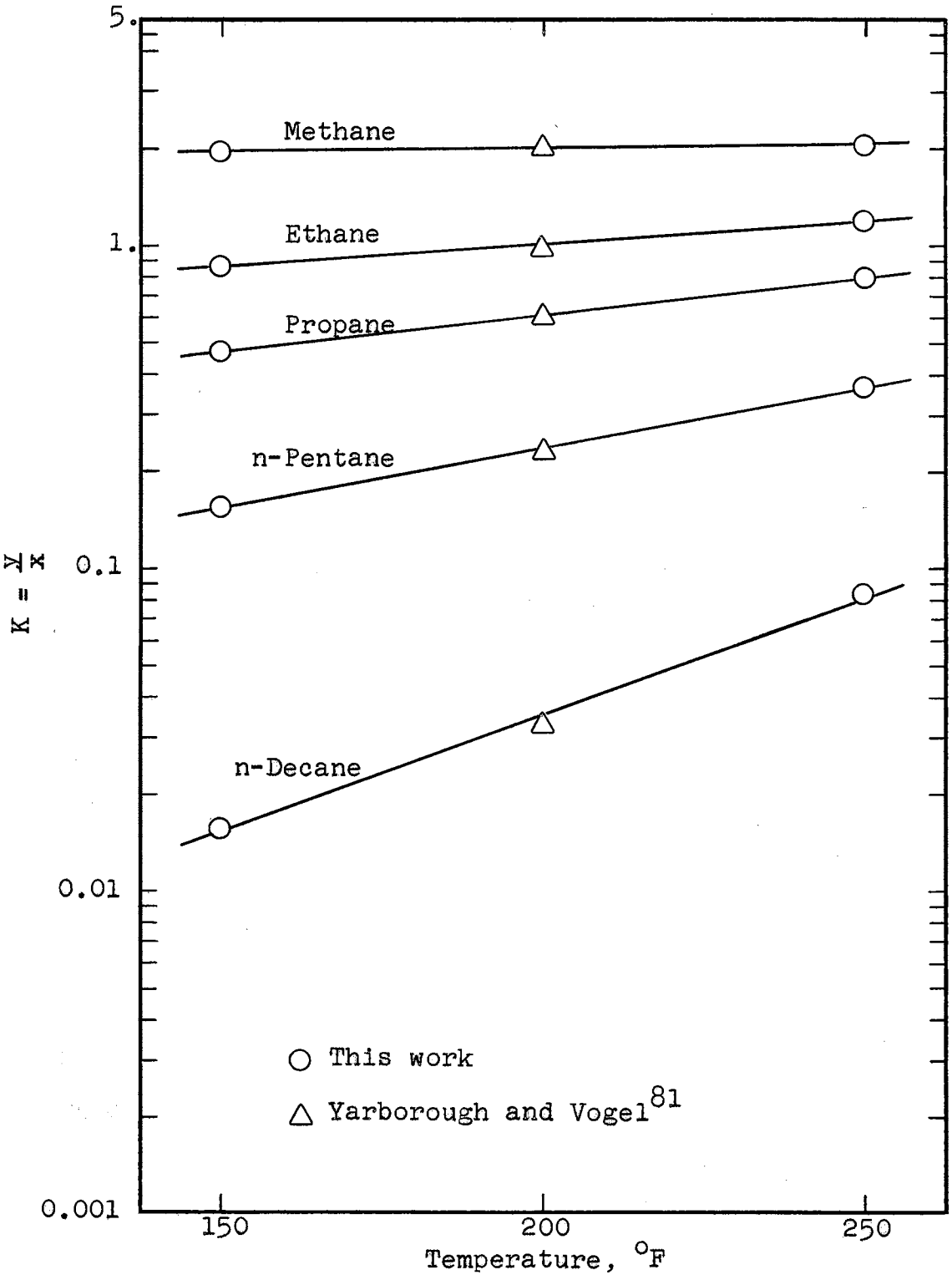

FIGURE 28

K-VALUE COMPARISON AT 2000 PSIA - BASE SYSTEM

a very slight concavity upwards. The only exception is n-decane which has a pronounced upward concavity. Jacoby and Rzasa[30] have obtained similar behavior for the lighter components. Although it is impossible to assign quantitatively a per cent deviation of the base system K-values from the Yarborough and Vogel values, Figures 26, 27 and 28 clearly show that the agreement between the two sets of data is good.

Directly comparable multicomponent systems with CO_2 have not been published and hence a similar comparison cannot be made for the CO_2 systems. In Table H-II the CO_2 data are compared with the CO_2-n-decane data at 150°F. They should tend to agree at the lower pressures. Included also are results from multicomponent systems although their compositions are not very similar to the compositions used here.

Examination of the CO_2 K-values shows that those obtained in this work as well as a few others are lower than the infinite dilution data. That is the expected behavior. The comparison of the systems with this type of CO_2 K-value behavior shows that the data obtained in this work are lower than those previously published. That may be due to composition differences and does not necessarily represent a disagreement of the data.

TABLE H-II

SMOOTHED K-VALUE COMPARISON FOR SYSTEMS WITH CO_2 AT 150°F

	From Fig. 8	From Fig. 10	Ref. 31	Ref. 41	Ref. 30	Ref. 43	Ref. 54	Infinite Dilution*
				Pressure = 200 psia				
CO_2	7.5	6.4					8.6	9.5
C_{10}	0.0049	0.0044					0.0036	
				Pressure = 400 psia				
C_1	7.3	6.6			10.5			
CO_2	3.9	3.5			5.0		4.5	4.8
C_2	2.2	2.25			2.5			
C_{10}	0.0036	0.0033					0.0030	
				Pressure = 600 psia				
C_1	4.8	4.6	7.0		7.0	6.9		
CO_2	2.75	2.55	4.0	3.7	3.6	3.0	3.1	3.27
C_2	1.55	1.60	1.95		1.8	1.7		
C_{10}	0.00315	0.00345					0.00305	
				Pressure = 800 psia				
C_1	3.65	3.65	5.3		5.5	5.2		
CO_2	2.15	2.08	3.0	2.9	3.0	2.4		2.57
C_2	1.22	1.28	1.5		1.5	1.4		
				Pressure = 1000 psia				
C_1	2.95	3.0	4.5		4.6	4.3		
CO_2	1.84	1.8	2.5	2.4	2.5	2.0		2.12
C_2	1.04	1.1	1.3		1.4	1.2		

*Yudovich, A., PhD Thesis, Oklahoma State University, Stillwater, Oklahoma (1969).

VITA

Juris Vairogs

Candidate for the Degree of

Doctor of Philosophy

Thesis: THE EFFECT OF CO_2 ON THE PHASE BEHAVIOR OF NORMAL PARAFFINS

Major Field: Chemical Engineering

Biographical:

Personal Data: Born at Jelgava, Latvia, May 14, 1937, the son of Verners and Karline E. Vairogs.

Education: Attended elementary school in Germany. Graduated from Stillwater High School, Stillwater, Oklahoma in 1954; received the Bachelor of Science degree in Chemical Engineering from the University of Nebraska in June, 1958; received the master of Science degree with a major in Chemical Engineering from Oklahoma State University in May, 1966; completed requirements for the Doctor of Philosophy degree in May, 1969.

Organizations: Omega Chi Epsilon, American Institute of Chemical Engineers, American Chemical Society.

Professional Experience: Employed as junior engineer with the Nebraska Department of Roads from May, 1959 to August, 1963. Employed as junior engineer with Sinclair Research, Inc. at Harvey in the summer of 1965. Employed by Cities Service Oil Company in Tulsa from January, 1968 to the present as Research Engineer.